Carnets Geol. 24 (13)

E-ISSN 1634-0744
DOI: 10.2110/carnets.2024.2413

Radiolarian and planktonic foraminiferal biochronology of the Soğukçam Limestone Group, Elmadağ Olistostrome, and Unaz Formation (Ankara region, central Türkiye): Insights into the Cretaceous evolution of the Sakarya Continent and overlying units

U. Kağan Tekin [1]
Bilal Sarı [2]
Alaettin Tuncer [1]
Kaan Sayıt [3]
Cengiz Okuyucu [4]
Çağrı Güzgün [1]

Abstract: The Ankara region (central Türkiye) comprises a part of the Sakarya Terrane and the accretionary remnants inherited from the Izmir-Ankara-Erzincan (IAE) branch of the Northern Neotethys. The Sakarya Terrane is characterized by a pre-Jurassic basement overlain by Jurassic-Cretaceous sedimentary assemblages, collectively known as the Sakarya Continent Cover. In this study, we aim to elucidate the Jurassic-Cretaceous evolution of the Sakarya Terrane through detailed geological mapping in the regions of Haymana, Yakacık, north of Alagöz and west of Memlik, located to the west and southwest of Ankara city, central Türkiye. By analyzing radiolarian and planktonic foraminiferal assemblages, we provide precise dating for three key lithological units: the Soğukçam Limestone Group (part of the Sakarya Continent Cover), the Elmadağ Olistostrome, and the Unaz Formation (from the overlying units). The oldest rock unit exposed in the Haymana region, south of Ankara city, is the Bilecik Limestone Group, consisting of Tithonian to lower Berriasian platform carbonates. A drowning unconformity separates the Bilecik Limestone Group from the overlying middle Berriasian-uppermost Albian Soğukçam Limestone Group, which has been elevated to "group" status in this study. The Soğukçam Limestone Group is subdivided into two formations -the Seyran Formation and the Akkaya Formation- separated by a disconformity surface. The Seyran Formation, at the base, consists of middle Berriasian limestone breccia in a micritic pelagic matrix, and upper Berriasian-lower Aptian micritic clayey, cherty pelagic limestones with abundant and diverse radiolarians in its upper part. The disconformity between the Seyran and Akkaya formations represents a small depositional gap corresponding to the middle to late Aptian. The lower part of the Akkaya Formation contains lower to middle Albian debris flow deposits while the upper part is composed of clayey pelagic limestones rich in glauconite and planktonic foraminifers, dating to the latest Albian. Overall, the Akkaya Formation is roughly assigned to the Albian stage.

[1] *Department of Geological Engineering, Hacettepe University, 06800, Beytepe, Ankara (Türkiye)*

[2] *Department of Geological Engineering, Dokuz Eylül University, Izmir (Türkiye)*

[3] *Department of Geological Engineering, Middle East Technical University, 06800, Ankara (Türkiye)*

[4] *Corresponding author;*
Department of Geological Engineering, Konya Technical University, Konya (Türkiye)
cokuyucu@ktun.edu.tr *cokuyucu@ktun.edu.tr*

Published online in final form (pdf) on December 15, 2024
[Editor: Bruno Granier; language editor: Stephen Eagar]

The Akkaya Formation within the Soğukçam Limestone Group is unconformably overlain by the Coniacian Elmadağ Olistostrome, which also covers the ophiolitic mélange of the IAE Ocean (containing Turonian radiolarian blocks) to the west of the Memlik region. The basal part of the Elmadağ Olistostrome is characterized by an unstratified, loosely-packed, gray- to beige-colored carbonate matrix, while its upper part features stratified, highly-sheared gray- to beige-colored clayey carbonate/marl matrix with embedded carbonate blocks. These blocks, dated through radiolarians and planktonic foraminifers, range from the early Callovian to Coniacian. These blocks, observed in the Haymana, north of Alagöz, and Yakacık regions, primarily originated from the underlying Soğukçam Limestone Group. The Elmadağ Olistostrome was likely deposited in a peripheral foreland flysch basin, resembling trench-like settings, in front of the southward-moving nappes derived from the Neotethys Intra-Pontide Ocean. This olistostrome is unconformably overlain by the Unaz Formation, which represents the lowermost unit of the fore-arc basin within the Galatean Arc and is present in all four studied regions. The Unaz Formation mainly consists of thin-bedded, gray- to red-colored clayey limestones with abundant planktonic foraminifers, along with red- to pink-colored marls. In the northern part (west of Memlik), the Unaz Formation also includes basal clastics. Based on its characteristic planktonic foraminiferal assemblages, the formation is dated to the late Santonian and correlates well with the type locality in the Pontides, northwestern Türkiye. Following this sequence, a brief period of continental arc magmatism occurred in the Santonian-Campanian, accompanied by the deposition of fore-arc sediments (the Haymana Formation, consisting of clastics) during the Campanian-Maastrichtian interval.

In this study, an abundant, well-preserved, and diverse radiolarian microfauna (146 taxa, including fourteen new species and four new subspecies from the early Hauterivian to early Aptian) were recovered from the clayey micritic limestones of the Seyran Formation in the Soğukçam Limestone Group. The vertical distributions of these radiolarians and their age correlations with previous studies are also documented.

Keywords:

• Ankara region;
• central Türkiye;
• biochronology;
• radiolarians;
• planktonic foraminifers;
• stratigraphy;
• Cretaceous geodynamic evolution

Citation: TEKIN U.K., SARI B., TUNCER A., SAYIT K., OKUYUCU C. & GÜZGÜN Ç. (2024).- Radiolarian and planktonic foraminiferal biochronology of the Soğukçam Limestone Group, Elmadağ Olistostrome, and Unaz Formation (Ankara region, central Türkiye): Insights into the Cretaceous evolution of the Sakarya Continent and overlying units.- *Carnets Geol.*, Madrid, vol. 24, no. 13, p. 187-263. DOI: 10.2110/carnets.2024.2413

Résumé : ***Biochronologie des radiolaires et des foraminifères planctoniques du Groupe des calcaires de Soğukçam, de l'Olistostrome d'Elmadağ et de la Formation d'Unaz (région d'Ankara, centre de la Turquie) : Perspectives sur l'évolution crétacée du Continent de Sakarya et des unités sus-jacentes.-*** La région d'Ankara, située au centre de la Turquie, englobe une partie du Terrane de Sakarya ainsi que des vestiges d'accrétion hérités de la branche Izmir-Ankara-Erzincan (IAE) de la Néotéthys septentrionale. Le Terrane de Sakarya est caractérisé par un socle pré-jurassique surmonté de séries sédimentaires jurassiques et crétacées, regroupées sous l'appellation collective de "Couverture du Continent de Sakarya". Cette étude vise à clarifier l'évolution jurassico-crétacée du Terrane de Sakarya en s'appuyant sur une cartographie géologique détaillée des régions d'Haymana, d'Yakacık, du nord d'Alagöz et de l'ouest de Memlik, situées à l'ouest et au sud-ouest de la ville d'Ankara. En analysant les associations de radiolaires et de foraminifères planctoniques, nous fournissons des datations précises pour trois unités lithologiques clés : le Groupe des Calcaires de Soğukçam (faisant partie de la Couverture du Continent de Sakarya), l'Olistostrome d'Elmadağ et la Formation d'Unaz (appartenant aux unités sus-jacentes). Dans la région d'Haymana, au sud de la ville d'Ankara, l'unité rocheuse la plus ancienne exposée est le Groupe des Calcaires de Bilecik, constitué de calcaires de plateforme datant du Tithonien au Berriasien inférieur. Une discordance d'ennoiement le sépare du Groupe des Calcaires de Soğukçam, qui lui succède et couvre l'intervalle Berriasien moyen à Albien terminal. Cette dernière unité, élevée au rang de "groupe" dans cette étude, est subdivisée en deux formations distinctes : la Formation de Seyran et celle d'Akkaya, séparées par une surface de discontinuité. La Formation de Seyran est composée, pour sa base datant du Berriasien moyen, de brèches calcaires avec une matrice micritique et, pour sa partie supérieure datant du Berriasien supérieur à l'Aptien inférieur, de calcaires micritiques argileux, à silex et riches en radiolaires. La discontinuité entre les formations de Seyran et d'Akkaya correspond à un court hiatus sédimentaire équivalent à l'intervalle Aptien moyen à supérieur. La partie inférieure de la Formation d'Akkaya est constituée de dépôts de coulées de débris, datant de l'Albien inférieur à moyen, alors que sa partie supérieure est composée de calcaires argileux et glauconieux, riches en foraminifères planctoniques, datant de l'Albien terminal. En généralisant, on peut dire que la Formation d'Akkaya correspond approximativement à l'étage Albien.

La Formation d'Akkaya, appartenant au Groupe des Calcaires de Soğukçam, est recouverte de manière discordante par l'Olistostrome d'Elmadağ d'âge Coniacien, qui recouvre également le mélange ophiolitique de l'océan IAE (contenant des blocs à radiolaires d'âge Turonien) à l'ouest de la région de Memlik. La partie basale de l'Olistostrome d'Elmadağ est caractérisée par une matrice carbonatée non stratifiée, faiblement compactée, de couleur grise à beige, alors que sa partie supérieure présente une ma-

trice stratifiée, fortement cisaillée, composée de calcaires argileux et de marnes, gris à beiges, emballant des blocs calcaires. Les radiolaires et les foraminifères planctoniques permettent d'attribuer ces blocs à l'intervalle Callovien inférieur à Coniacien. Observés dans les régions d'Haymana, de Yakacık et au nord d'Alagöz, ils proviennent principalement du Groupe des Calcaires de Soğukçam sous-jacent. L'Olistostrome d'Elmadağ s'est probablement déposé dans un bassin de flysch périphérique de type avant-pays, analogue à une fosse, en avant des nappes se déplaçant vers le sud et provenant de la branche Intra-Pontide de l'océan Néotéthys. Cet olistostrome est surmonté en discordance par la Formation d'Unaz qui représente l'unité la plus basse du bassin d'avant-arc au sein de l'Arc de Galatea et est présente dans les quatre régions étudiées. La Formation d'Unaz est composée principalement de calcaires argileux gris à rouge, finement lités, riches en foraminifères planctoniques, ainsi que de marnes rouges à roses. Dans la partie nord, à l'ouest de Memlik, la Formation d'Unaz comprend également des sédiments clastiques à sa base. Grâce aux associations caractéristiques de foraminifères planctoniques, cette formation est datée du Santonien supérieur et est bien corrélée avec sa localité-type dans les Pontides au nord-ouest de la Turquie. Par la suite, au Santonien-Campanien, une brève période de magmatisme d'arc continental est observée. Elle est suivie du dépôt de sédiments clastiques d'avant-arc regroupés dans la Formation d'Haymana datée du Campano-Maastrichtien.

Dans cette étude, une abondante microfaune de radiolaires bien préservés et très variés (avec 146 taxons, parmi lesquels quatorze nouvelles espèces et quatre nouvelles sous-espèces datant de l'Hauterivien inférieur à l'Aptien inférieur) a été identifiée dans les calcaires micritiques argileux de la Formation de Seyran du Groupe des Calcaires de Soğukçam. Les répartitions verticales de ces radiolaires ainsi que leurs calibrations stratigraphiques étayées par des études antérieures sont également renseignées.

Mots-clefs :

- région d'Ankara ;
- Anatolie centrale ;
- Turquie ;
- biochronologie ;
- radiolaires ;
- foraminifères planctoniques ;
- stratigraphie ;
- évolution géodynamique crétacée

1. Introduction

The present-day tectonic mosaic of Anatolia was established by the closure of the multi-branched Neotethys Ocean (Şengör & Yilmaz, 1981). Among these branches, the remnants of the northern oceanic domains are preserved in the Intra-Pontide and Izmir-Ankara-Erzincan (IAE) suture zones. From the Biga peninsula (NW Türkiye) to the Caucasus in the east, including the Ankara region (northern Türkiye), the terrane bounded by the Intra-Pontide and IAE suture zones is termed the Sakarya Zone by Okay (1989) or the Sakarya Composite Terrane by Göncüoğlu *et al.* (1997; Fig. 1.A). This zone is composed of two main components:
1) a pre-Jurassic rock assemblage comprising the Karakaya Complex and its pre-Permian basement. The Karakaya Complex developed due to the closure of the "Karakaya Marginal Sea" in the Late Triassic, together with the basement forming the "Sakarya Continent", and
2) Jurassic to Cretaceous sedimentary deposits overlying the Karakaya Complex, termed the "Sakarya Continent Cover" by Şengör and Yilmaz (1981) and Şengör *et al.* (1984).

In the Sakarya Zone, the Early Cretaceous saw the deposition of turbiditic sediments, known as the Çağlayan Formation, in the central Pontides (*e.g.*, Tüysüz, 2018). These turbidites were subsequently covered by a volcano-sedimentary sequence in the Late Cretaceous, represented by the Dereköy, Unaz, and Cambu formations (Tüysüz *et al.*, 2012). This volcano-sedimentary succession, representing a portion of the so-called Pontide magmatic arc, is considered to have developed in response to arc-rifting during the Turonian-Maastrichtian (Tüysüz *et al.*, 2012; Keskin & Tüysüz, 2018). The Late Cretaceous also marked the closure of the Intra-Pontide oceanic realm, which was possibly completed before the Turonian (*e.g.*, Tüysüz *et al.*, 2012; Marroni *et al.*, 2020). Remnants of the Pontide Arc magmatism are also suggested to occur further south, in the Ankara region (central Anatolia), situated in the southern part of the Sakarya Terrane (Fig. 1.A; *e.g.*, Koçyiğit, 1991; Okay *et al.*, 2019). The Campanian-Maastrichtian siliciclastic turbidites and overlying Paleocene-middle Eocene sediments of the Haymana Basin were suggested by Koçyiğit (1991) to have been deposited in the fore-arc basin of the Galatean Arc. This arc, representing the active margin of the Sakarya Terrane, is thought to have developed by the northward subduction of the IAE oceanic lithosphere.

With regard to the Ankara region, Koçyiğit (1991) proposed a long lifespan for the IAE oceanic lithosphere, which existed until the middle Eocene. In contrast, the youngest age obtained from the chert blocks within the Ankara Ophiolitic Mélange thus far is Turonian (Bragin & Tekin, 1999). Ages of the subophiolitic metamorphic soles from the western sector of the IAE (Orhaneli and Kınık ophiolites) are comparable, having Turonian-Coniacian ages (101 to 93 Ma; Harris *et al.*, 1994; Önen, 2003). Furthermore, ages obtained from continental and oceanic arc-related magmatism linked to the IAE events yield Cenomanian-Maastrichtian ages (Tüysüz *et al.*, 1995; Koçyiğit *et al.*, 2003; Ellero *et al.*, 2015; Beyazpi-

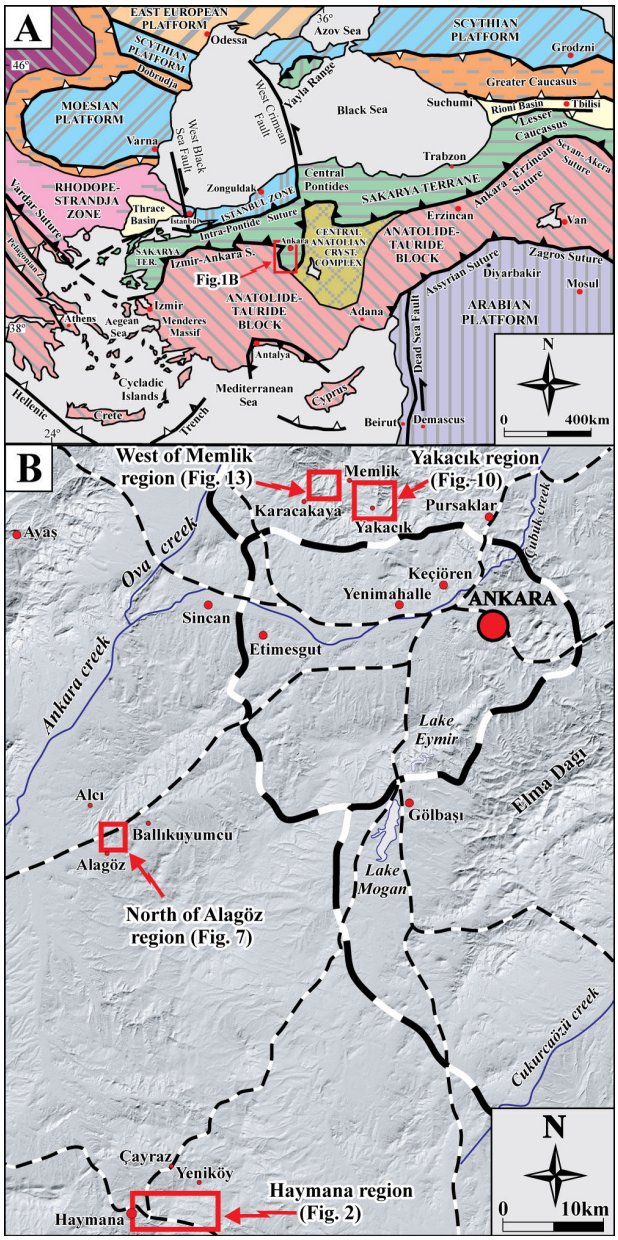

Figure 1: A: Tectonic map of Türkiye with major suture zones/terranes and location of the study area (slightly revised after Okay & Tüysüz, 1999; Okay & Göncüoğlu, 2004), **B.** Location map showing the distribution of studied regions (west of Ankara city).

rinç *et al.*, 2019). Thus, these data, reflecting the age of oceanic crust and associated magmatism, contrast with the notion of an in-situ oceanic crust of the IAE Ocean extending to the middle Eocene. Consequently, the lifetime of the IAE Ocean remains unclear, which also limits interpretations regarding the duration of the Sakarya active continental margin.

Another major issue concerns the relationship between the Sakarya Continent Cover sediments (*e.g.*, the Bilecik Limestone Group and the Soğukçam Limestone Group), the Elmadağ Olistostrome, and the overlying fore-arc deposits (Kocatepe Formation *sensu* Yüksel, 1970, and the Haymana Formation *sensu* Schmidt, 1960) in the Ankara region (*e.g.*, Koçyiğit, 1991; Okay & Altiner, 2016, 2017; Okay *et al.*, 2019; Sariaslan *et al.*, 2020, for a brief review). Regarding this, the origin of the Elmadağ Olistostrome (adopted from the "Elma Dağı Exotic-Block Serie" by Erol, 1956) also remains uncertain, as there is no consensus on its contact relationship with the Ankara Ophiolitic Mélange. Overall, the Jurassic-Cretaceous assemblages of the Ankara region present several critical issues for understanding the geological framework of the Ankara region and the Sakarya Continent. Therefore, in this study, we examine the lithological and biostratigraphical characteristics (using radiolarians and planktonic foraminifers) of several key units and their relationships in the Ankara region: i) the Soğukçam Limestone Group, which is the uppermost unit of the Sakarya Continent Cover, ii) a sedimentary mélange, for which the name "Elmadağ Olistostrome" is used here as proposed by Erol (1956), and iii) the "Unaz Formation" *sensu* Akyol *et al.* (1974), subsequently cited by Tüysüz *et al.* (1997, 2012) and Tüysüz (1999). Accordingly, we study four critical regions (the Haymana, north of Alagöz, Yakacık, and west of Memlik) southwest and northwest of Ankara city, central Türkiye (Fig. 1.B). Based on the characteristic features of these units, we interpret the Cretaceous geodynamic evolution of the Sakarya Continent Cover and overlying units.

2. Geological framework

The Ankara region, part of the Sakarya Terrane, is bordered by remnants of an accretionary complex tied to the Neotethys IAE Ocean (Şengör & Yilmaz, 1981; Şengör *et al.*, 1984; Fig. 1.A). In this region, the "Ankara Mélange", a term first introduced by Bailey and McCallien (1950), spans from the Ankara city center to the Kızılırmak River, covering a 50 km width from NNE to SSW (Çapan, 1981; Fig. 1.A). According to Bailey and McCallien (1950), the Ankara Mélange formed as a result of tectonic processes fragmentating a single nappe stack, known as the Anatolian Thrust, which comprises rock units from the Triassic and Jurassic periods. Since then, the Ankara Mélange has been extensively studied from 1919 through the early 1990s (*e.g.*, Philippson, 1919; Nowack, 1928; Chaput, 1931, 1936; Leuchs, 1939; Salamon-Calvi, 1940; Erol, 1956; Gannser, 1959; Boccaletti *et al.*, 1966; Sestini, 1971; Norman, 1975; Çapan & Buket, 1975; Batman *et al.*, 1978; Çapan, 1981; Erk, 1981; Ünalan, 1981; Çapan *et al.*, 1983; Koçyiğit *et al.*, 1988; Koçyiğit, 1991). These studies have identified two main types of mélanges:

1) Blocks of Carboniferous, Permian, and Triassic rocks are found within a highly deformed, sheared graywacke and shale matrix belonging to the Karakaya Complex (for a brief review, see Okay & Göncüoğlu, 2004; Sayit & Göncüoğlu, 2013; Okay & Altiner, 2017). The Karakaya Complex is characterized as a strongly deformed and variably metamorphosed Permo-Triassic orogenic

series in the Sakarya Continent (OKAY & GÖNCÜOĞLU, 2004). These lithologies were initially introduced by BINGÖL *et al.* (1975) under the name "the Karakaya Formation" to describe a pre-Jurassic low-grade metamorphic, blocky series widely distributed in the Biga peninsula, NW Türkiye. This formation was later renamed the "Karakaya Complex" by ŞENGÖR *et al.* (1984). The Karakaya Complex can be divided into two main tectonic units, *i.e.*, the "Lower Karakaya Complex" and the "Upper Karakaya Complex" (OKAY & GÖNCÜOĞLU, 2004).

In the east and southeast of the Ankara region, two primary lithological units equivalent to the Karakaya Complex were defined by EROL (1956) as the "Dikmen Graywacke Serie" at the base, and the "Elma Dağı Exotic-Block Series" at the top. A recent study conducted in this area (TEKIN & TUNCER, 2024) indicates that the Middle Triassic basal unit, *i.e.*, the Dikmen Graywacke, is primarily composed of very low-grade metaclastics (including graywacke, conglomerate, and slate), with rare interlayers of carbonate and chert, along with basic volcanics at the top. While the Dikmen Graywacke is correlated with part of the Karakaya Complex in the Biga peninsula (for a brief review, see OKAY & GÖNCÜOĞLU, 2004; SAYIT & GÖNCÜOĞLU, 2013; OKAY & ALTINER, 2017), the Orhanlar Graywacke, as defined by OKAY *et al.* (1990, 1991), within the Upper Karakaya Complex, is the local equivalent of the Dikmen Graywacke. Contrary to the original definition, the Dikmen Greywacke does not contain blocks, as clarified in previous studies (OKAY *et al.*, 1990, 1991). However, isolated patches of the Elmadağ Olistostrome can be observed over the Dikmen Graywacke. This unit dates to the Middle Triassic and forms the rift-related basement of the Sakarya Continent *sensu* ŞENGÖR and YILMAZ (1981) and ŞENGÖR *et al.* (1984).

The overlying olistostromal unit, which contains various blocks within the matrix, was named the "Elma Dağı Exotic-Block Series (=Boulder Bed Series)" by EROL (1956) based on outcrops exposed in the Elma Dağı region to the southeast of Ankara city center (Fig. 1.B). In this study, we adopted the name "Elmadağ Olistostrome", following the nomenclature by EROL (1956). This unit was previously correlated with a part of the Karakaya Complex in the Biga peninsula (for a brief review, see OKAY & GÖNCÜOĞLU, 2004; SAYIT & GÖNCÜOĞLU, 2013; OKAY & ALTINER, 2017). However, the Nilüfer Unit, as identified by OKAY *et al.* (1990, 1991), which characterizes the Lower Karakaya Complex, the "Arkosic Sandstone Series" by OKAY and GÖNCÜOĞLU (2004) - corresponding to the Hodul Unit by OKAY *et al.* (1990, 1991) -, and the "Basalt, Limestone, Grain Flows, Debris Flows and Olistostrome Series" by OKAY and GÖNCÜOĞLU (2004) - corresponding to the Çal Unit by OKAY *et al.* (1990, 1991) -, both included in the Upper Karakaya Complex (OKAY & GÖNCÜOĞLU, 2004), are parts of the Coniacian (Upper Cretaceous) Elmadağ Olistostrome (*sensu* EROL, 1956), according to TEKIN and TUNCER (2024).

To the south of the Ankara city center, similar olistostromal units occur, which include pelagic blocks ranging from Callovian (Middle Jurassic) to Coniacian (Late Cretaceous) age, embedded within a Coniacian (Late Cretaceous) silt, clay, and marl matrix (BATMAN *et al.*, 1978; ÜNALAN, 1981; KOÇYIĞIT, 1991; DELI & ORHAN, 2007; ROJAY, 2013; OKAY & ALTINER, 2017; OKAY *et al.*, 2019; SARIASLAN *et al.*, 2020). According to our new findings, these units are the local equivalents of the Elmadağ Olistostrome (TEKIN & TUNCER, 2024). The Elmadağ Olistostrome was previously termed the "Akkayatepe Mélange" by BATMAN *et al.* (1978), the "Mélange with limestone blocks" by ÜNALAN (1981), the "Damlaağaçderesi Formation" by KOÇYIĞIT (1991), and the "Alacaatlı Olistostrome" by OKAY and ALTINER (2017). Also, all these olistostromal units appear to have originated from the Intra-Pontide Ocean, which was located north of the Sakarya Continent *sensu* ŞENGÖR and YILMAZ (1981) and ŞENGÖR *et al.* (1984) (TEKIN & TUNCER, 2024).

2) Ophiolitic mélange as a part of the accretionary prism of the Neotethys IAE Ocean (ÇAPAN & BUKET, 1975; BRAGIN & TEKIN, 1996; DANGERFIELD *et al.*, 2011; ROJAY, 2013; SARIFAKIOĞLU *et al.*, 2014; OKAY *et al.*, 2022; ROBERTSON *et al.*, 2023), comprising slices and blocks of basalt, radiolarian chert, serpentinite, limestone, gabbro, diabase, shale, and sandstone from the Ladinian (Middle Triassic) to Turonian (Late Cretaceous) interval (ages were obtained from different parts of the Izmir-Ankara Suture Belt: MOIX & GORICAN, 2013, from the Izmir Flysch; TEKIN *et al.*, 2006; GÖNCÜOĞLU *et al.*, 2006a, 2006b; TEKIN & GÖNCÜOĞLU, 2007, 2009; TEKIN *et al.*, 2012a, from the Bornova Flysch Zone; SERVAIS, 1982; GÖNCÜOĞLU *et al.*, 2000, 2006a, 2006b, 2010; TEKIN *et al.*, 2002, from the Central Sakarya Ophiolitic Complex/Dağküplü Mélange; BRAGIN & TEKIN, 1996; TEKIN *et al.*, 2002; ROJAY *et al.*, 2004; BORTOLOTTI *et al.*, 2013, 2018, from the Ankara Ophiolitic Mélange; TÜYSÜZ & TEKIN, 2007; BOZKURT *et al.*, 1997, from the central part of this zone; for the block ages, see brief review of ROBERTSON *et al.*, 2023). It is noteworthy that the Mersin Mélange and the mélange cropping out near the Taşkent town (southern Türkiye) were recently revealed to represent transported foreland deposits in front of the southwardly advancing nappes that originated from the IAE Ocean. This finding is critical since these mélange units suggest a latest Carboniferous-early Permian rifting of the Northern Neo-Tethys, which subsequently gave way to the opening of this ocean (TEKIN *et al.*, 2016, 2019; SAYIT *et al.*, 2017, 2020; OKUYUCU *et al.*, 2024).

Within the scope of this study, four target areas were chosen to check the upper and lower stratigraphical boundaries of the Elmadağ Olistostrome. For dating, samples were collected from

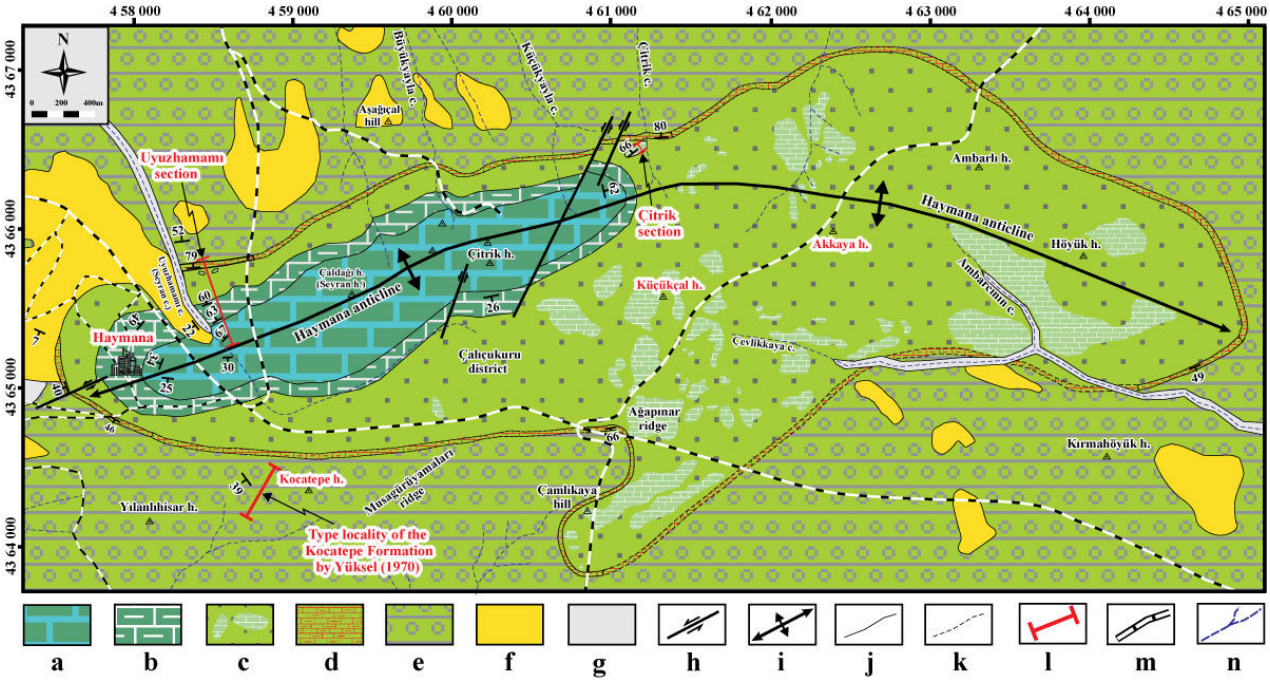

Figure 2: Geological map showing the distribution of stratigraphical/structural units around the Haymana anticline and locality of the Uyuzhamamı and the Çitrik sections. **Key: a.** The Tithonian-early Berriasian Bilecik Limestone Group, **b.** The middle Berriasian-latest Albian Soğukçam Limestone Group, **c.** The Coniacian Elmadağ Olistostrome with different types of blocks, **d.** The Santonian Unaz Formation, **e.** The Campanian-Maastrichtian Haymana Formation, **f.** Neogene deposits, **g.** Recent deposits, **h.** Strike-slip fault, **i.** Plunged anticline, **j.** Stratigraphic contact, **k.** Probable stratigraphic contact, **l.** Section locations, **m.** Main roads, **n.** Drainage system (redrawn and mainly revised after YÜKSEL, 1970).

a) the underlying Soğukçam Limestone Group (the Seyran and Akkaya formations) belonging to the Sakarya Continent Cover, b) the blocks of the Elmadağ Olistostrome, and c) the overlying Unaz Formation. Based on the age findings extracted from these units, we evaluate the stratigraphy of the upper part of the Sakarya Continent Cover (the Soğukçam Limestone Group consisting of the Seyran and Akkaya formations), the formation mechanism of the Elmadağ Olistostrome, and the depositional age of the Unaz Formation.

3. Lithological characteristics of sections and spot samples

Detailed studies were performed in four different regions: Haymana and north of Alagöz regions to the southwest Ankara city center, Yakacık and east of Memlik regions to the northwest of Ankara city center (Fig. 1.B) as follows.

3.1. HAYMANA REGION

To the east of Haymana town, located at the southwest of Ankara city, stratigraphically older rock units belonging to the cover of Sakarya Continent are exposed along the well-known Haymana anticline (Fig. 2). The Haymana region has been subject of many studies since the 1940s (LOKMAN & LAHN, 1946; SCHMIDT, 1960; YÜKSEL, 1970, 1973; ÜNALAN *et al.*, 1976; BATMAN, 1978; ÜNALAN & YÜKSEL, 1978; ŞENALP & GÖKÇEN, 1978; TOKER, 1979, 1980; GÖKÇEN & KELLING, 1983; SIREL *et al.*, 1986; ÖZCAN & ÖZKAN-ALTINER, 1997; ESMERAY-ŞENLET *et al.*, 2015; OKAY & ALTINER, 2016; GÜLYÜZ *et al.*, 2019; KARABEYOĞLU *et al.*, 2019). The Haymana anticline was mapped and studied in detail by YÜKSEL (1970), ÜNALAN *et al.* (1976), and OKAY and ALTINER (2016). To clarify the stratigraphical features of the units exposed in the Haymana anticline, samples from the Uyuzhamamı section were collected along the Uyuzhamamı creek in the northern flank of the Haymana anticline (Figs. 2-3, 4.a). In addition, one of the megablocks in the Elmadağ Olistostrome along the Çitrik creek was studied in the Çitrik section (Figs. 2, 5, 6.a-c).

3.1.1. The Uyuzhamamı section (US)

This section, named after the Uyuzhamamı creek (Figs. 2, 4.a), is located approximately 900 meters northeast of the Haymana city center on the northeast side of Uyuzhamamı creek, within the Ankara J29-a1 quadrangle sheet (between 4365250N/0458650E and 4365787N/0458498E, UTM Zone 36S; GPS coordinates 39°26'3.14"N 32°31'8.83"E and 39°26'20.55"N 32°31'02.37"E; Figs. 2, 4.a). The total thickness of the section is about 402 meters, and forty-one samples were collected (Fig. 3). The basal part corresponds to the base of the northern flank of the Haymana anticline to the southwest (Figs. 2, 4.b), while the top lies at the boundary between the Unaz and Haymana formations to the northwest (Fig. 2).

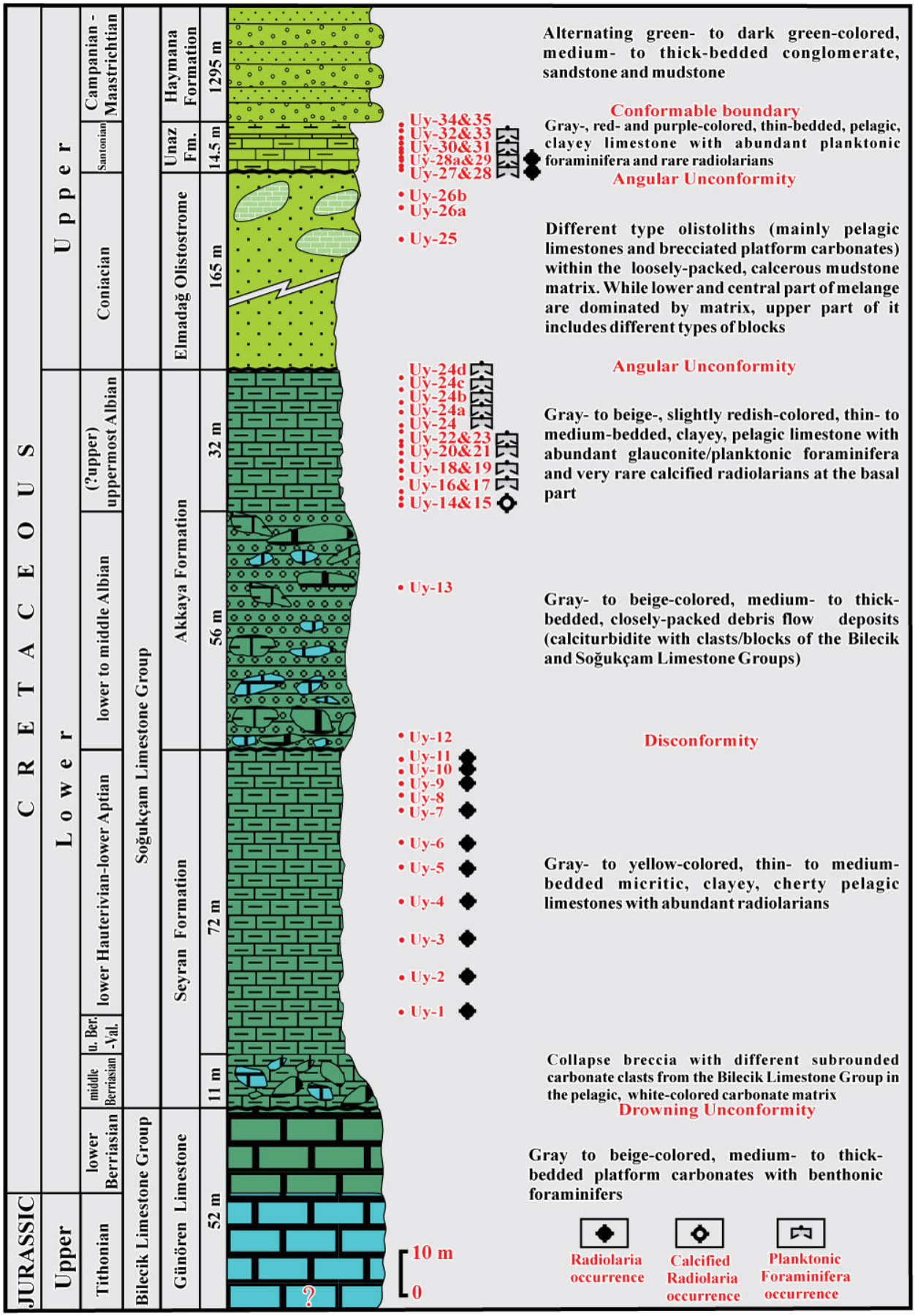

Figure 3: Log of the Uyuzhamamı section and sampling levels. Abbreviation: U. Ber.- Val.: Upper Berriasian-Valanginian.

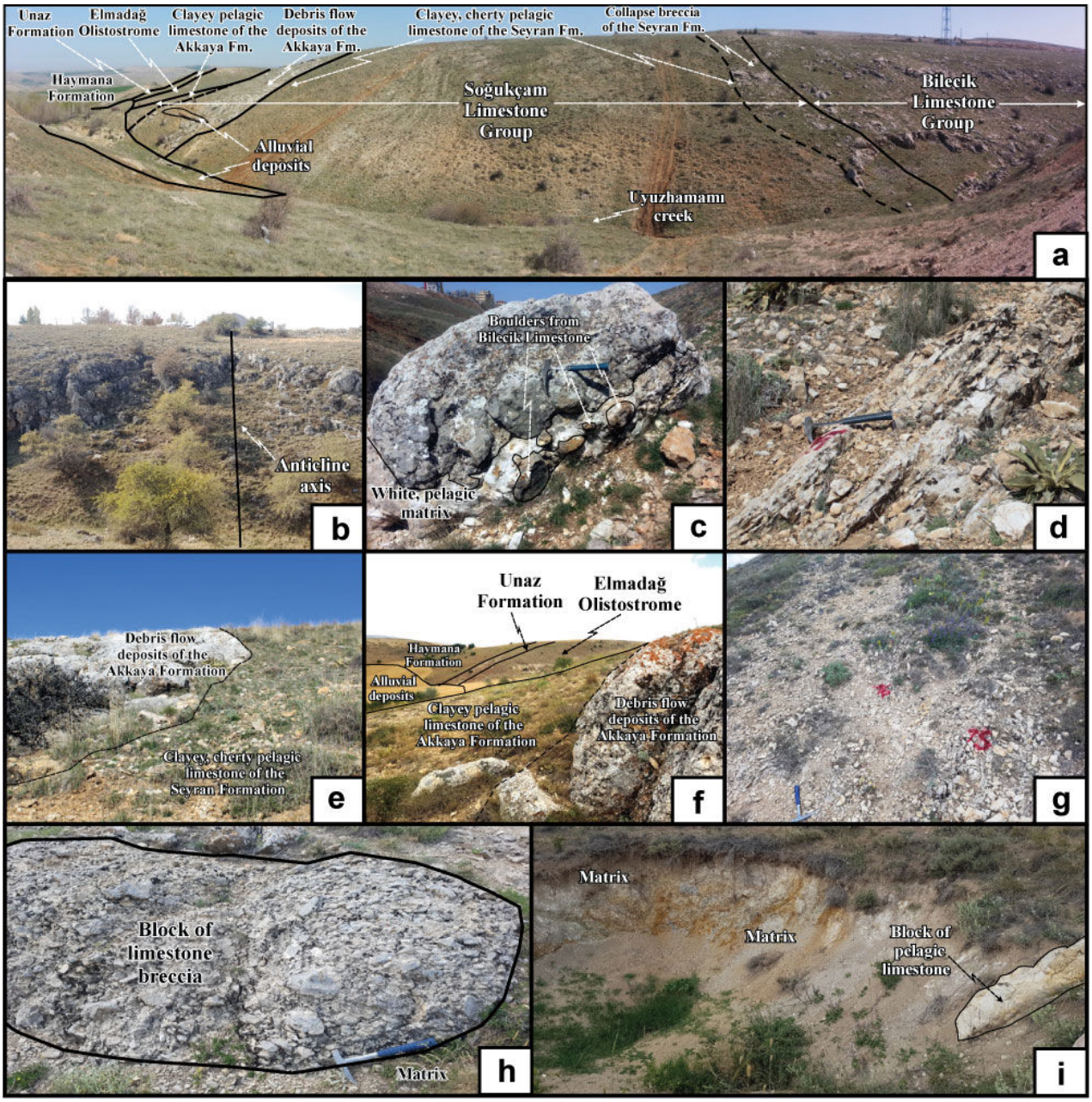

Figure 4: Field photographs from the Uyuzhamamı section in the Haymana region; **a.** Panoramic view showing all the lithostratigraphic units along the section, view from southwest to northeast. **b**. The basal part of the Uyuzhamamı section, composed of gray to beige-colored, medium to thick-bedded platform carbonates of the Bilecik Limestone Group at the center of the Haymana anticline, **c.** View from the lowermost part of the Seyran Formation within the Soğukçam Limestone Group, including collapse breccia with the platform carbonate pebbles and blocks in a white-colored pelagic matrix of the middle Berriasian age, **d**. View from the upper part of the Seyran Formation within the Soğukçam Limestone Group consisting of gray- to yellow-colored, thin- to medium-bedded micritic, clayey radiolarian-rich pelagic limestones from which sample Uy-5 of early Barremian age was collected, **e.** View from the Seyran Formation within the Soğukçam Limestone Group, made up of radiolarian-rich clayey limestones of early Aptian age, and the overlying Akkaya Formation within the Soğukçam Limestone Group composed of gray- to beige-colored, medium- to thick-bedded, closely-packed debris flow deposits of the ? middle to late Aptian-Albian age, **f.** Photograph showing the boundary between underlying debris flow deposits of early to middle Albian age belonging to Akkaya Formation within the Soğukçam Limestone Group and overlying clayey pelagic limestone part belonging to Akkaya Formation within the Soğukçam Limestone Group of the ? late (latest) Albian age and overlying units, **g.** Detailed view from the upper part of the Akkaya Formation within the Soğukçam Limestone Group consisting of gray- to beige-, slightly reddish-colored, thin- to medium-bedded, clayey pelagic limestone with abundant glauconite and planktonic foraminiferal assemblages of the latest Albian age, **h.** Close-up view from the Elmadağ Olistostrome, showing the block of carbonate breccia within a loosely packed, calcareous mudstone matrix of Coniacian age, **i.** Detailed view from a pelagic block within a loosely packed, calcareous mudstone matrix of the Coniacian Elmadağ Olistostrome.

3.1.1.1. The Bilecik Limestone Group in the US

Although the central part of the Haymana anticline, composed of platform carbonates, was called the "Çaltepe Formation" of the Barremian-Aptian age by YÜKSEL (1970, 1973), the recent study by OKAY and ALTINER (2016) named this unit the Bilecik Limestone Group (*sensu* GRANIT & TINTANT, 1960, and subsequently ALTINLI, 1965; EROSKAY, 1965; ALTINLI *et al.*, 1970; ALTINLI, 1975a, 1975b; *etc.*; see ALTINER *et al.*, 1991, for a comprehensive list on the studies related to the Bilecik Limestone) with correlation to the sequences exposed at the NW Pontides. In their study (OKAY & ALTINER, 2016), the Bilecik Limestone was raised to the Bilecik Limestone Group, including Callovian-Kimmeridgian Taşcıbayırı Formation and Kimmeridgian-Hauterivian Günören Limestone studied in the NW Pontides (ALTINER *et al.*, 1991). In the same study, it was also mentioned that the lithologies examined in the Uyuzhamamı region correspond to the Günören Limestone (ALTINER *et al.*, 1991).

Following the study of OKAY and ALTINER (2016), we applied the same terminology for this part of the section. The Bilecik Limestone Group corresponding to the Günören Limestone (ALTINER *et al.*, 1991) at the base of the section is about 52 meters thick and covers the central part of the Haymana anticline (Figs. 2-3, 4.b). It comprises gray- to beige-colored, medium- to thick-bedded platform limestones rich in benthonic foraminiferal assemblages (Figs. 3, 4.b). The age of the Bilecik Limestone Group was reported by OKAY and ALTINER (2016) as the latest Jurassic (Tithonian) to earliest Cretaceous (Berriasian), based on the comprehensive studies of benthonic foraminiferal assemblages. This age assignment was also applied to this study (Fig. 3).

3.1.1.2. The Soğukçam Limestone Group in the US

The name "Seyran Formation" was attributed by YÜKSEL (1970) to the units overlying the Bilecik Limestone Group in the US, with the contact relationship with the underlying unit defined as an unconformity (YÜKSEL, 1970, 1973). The Seyran Formation was originally subdivided into three subunits, from bottom to top: "Brèches calcaires polygéniques" (polygenic limestone breccias), "calcaires sublithographiques" (fine-grained limestone), and "marnes plus ou moins calcaires et plus ou moins détriques" (marls more or less calcareous and detrital)" of the early Late Cretaceous (Cenomanian-Turonian) age (YÜKSEL, 1970, 1973). Based on our field studies, since a clear disconformity surface is observed between the second unit (fine-grained limestone) and third unit (marls, more or less calcareous and detrital), we have revised the definition of this formation: only the lower two units were retained in the Seyran Formation, while the third unit (marls, more or less calcareous and detrital) was reassigned to the Akkaya Formation, following the revision by OKAY and ALTINER (2016). The rank of Soğukçam Limestone, which contains a pelagic rock suite from the middle Berriasian to latest Albian, was raised to the group status in this study, now comprising two formations: Seyran and Akkaya (Fig. 3).

3.1.1.2.1. The Seyran Formation within the Soğukçam Limestone Group

Based on new observations from this study, the Seyran Formation within the Soğukçam Limestone Group is now interpreted as comprising two parts instead of three, as follows (Fig. 3):

1) The basal part of this formation consists of limestone breccia with various subrounded clasts from the Bilecik Limestone Group embedded in a white-colored pelagic carbonate matrix (Figs. 3, 4.c). The total thickness of this typical collapse breccia is about 11 meters and OKAY and ALTINER (2016) identified Calpionellids [specifically, *Calpionella alpina* LORENZ and *Remaniella cadischiana* (COLOM)] in the pelagic matrix of this "collapse" breccia, suggesting a middle Berriasian age (based on sample 9595E from their study) through comparison with the study of GALE *et al.* (2020);

2) The basal part of the Seyran Formation is overlain by gray- to yellow-colored, thin- to medium-bedded micritic, clayey, cherty pelagic limestone, which is rich in radiolarians (Fig. 3). With a total thickness of 72 meters, this section also contains rare thin calciturbidite levels. Eleven samples (Uy-1 to Uy-11) were collected from this part of the section (Figs. 3, 4.d-e), which yielded abundant and diverse radiolarians, with the exception of sample Uy-8 (Fig. 3). In total, 146 radiolarian taxa from the lower Hauterivian to lower Aptian were identified in these limestones, including fourteen new species and four new subspecies. The first radiolarian-bearing sample (Uy-1) was taken nine meters above the breccia unit, indicating an early Hauterivian age (Fig. 3). Accordingly, the age interval between the collapse breccia and the basal nine meters of the micritic, clayey, pelagic limestone is assigned to the late Berriasian-Valanginian, marking the gradual platform drowning. Towards the upper part of the Seyran Formation, from sample Uy-1 to Uy-11, stepwise younger radiolarian assemblages were identified, with the last sample Uy-11 ascribed to the early Aptian (Fig. 3). Based on this observation, the late Berriasian age previously assigned to the calciturbidite level within pelagic limestone by OKAY and ALTINER (2016) should be reconsidered, as it was possibly derived from reworked material.

3.1.1.2.2. The Akkaya Formation within the Soğukçam Limestone Group

This formation was first proposed by OKAY and ALTINER (2016) and corresponds to the upper unit of the Seyran Formation as defined by YÜKSEL (1970, 1973). Although the type locality (Akkaya hill and surroundings, Fig. 2) for this formation corresponds to the Elmadağ Olistostrome *sensu* EROL (1956), which includes pelagic limestone blocks in the matrix, the definition of OKAY and

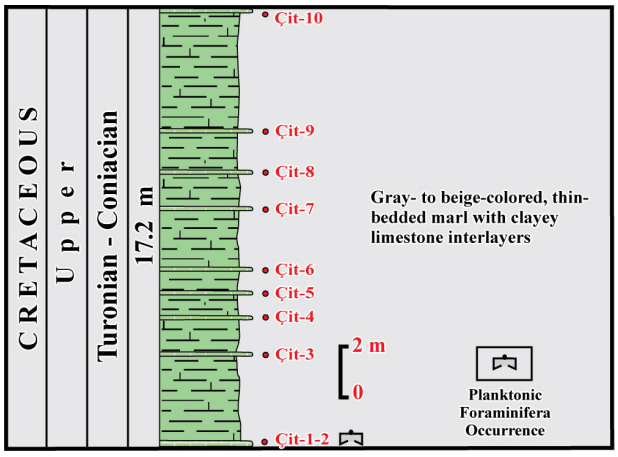

Figure 5: Log of the Çitrik section from the Çitrik block within the Elmadağ Olistostrome around the Haymana region and sampling levels.

Altiner (2016) was based on observations from the Uyuzhamamı region. Because of this, the term Akkaya Formation is accepted here, but with some revisions. Since age findings from the blocks in the Elmadağ Olistostrome were also factored in the age assignment to this formation by Okay and Altiner (2016), this aspect has been revised in this study.

The basal part of the formation consists of debris flow deposits (Figs. 3, 4.e-f). The contact of the debris flow deposits of the Akkaya Formation over the radiolarian-rich fine-grained clayey limestone of the Seyran Formation is not gradual, suggesting a sedimentation gap between these two units (Fig. 4e). Since the layer positioning does not change drastically across the contact, a disconformable relationship with a minor sedimentation gap is inferred for this boundary (Fig. 4e).

Debris flow deposits of the Akkaya Formation consist of gray- to beige-colored, medium- to thick-bedded, closely-packed calciturbidites with clasts and blocks derived from both the Bilecik Limestone Group and the Seyran Formation within the Soğukçam Limestone Group. The 56-meter-thick sequence shows larger blocks concentrated in the lower and upper sections, with smaller clasts in the central part. Two samples (Uy-12 and Uy-13) were retrieved from this unit (Fig. 3). The age of the matrix of this sequence was determined to be Albian (sample 9598) by Okay and Altiner (2016). Given the early Aptian age findings from the underlying Seyran Formation and the Albian age assigned to the matrix of the debris flow deposits from the Akkaya Formation, the interval from middle to late Aptian may represent the sedimentation gap (Fig. 3).

The upper part of the Akkaya Formation is approximately 32 meters thick. Fifteen samples (Uy-14 to Uy-24d, Fig. 3) were collected from gray- to beige-colored, slightly reddish-colored, thin- to medium-bedded, clayey, pelagic limestone rich in glauconite and planktonic foraminifers (Figs. 3, 4.f-g). The lowermost sample (Uy-14) contained limited remnants of radiolarians, which could not be extracted due to low silica content and extensive calcification of the radiolarian skeletons. While calcified radiolarians are rarely found, samples Uy-17 to Uy-24d contain abundant and diverse planktonic foraminifers, providing a latest Albian age (Fig. 3).

The depositional age of the Akkaya Formation is approximated as Albian based on both planktonic foraminiferal dating from the matrix of the basal debris flow deposits (Okay & Altiner, 2016) and the upper clayey pelagic limestone dated in this study. The Cenomanian pelagic limestone block within the Elmadağ Olistostrome at Çitrik creek (see locality in Fig. 2) was mistakenly included in the age dating of the Akkaya Formation by Okay and Altiner (2016). Thus, the age of the Akkaya Formation is revised to roughly Albian, rather than Albian-Cenomanian as previously suggested by Okay and Altiner (2016). The uppermost part of this unit exhibits a typical unconformity surface and forms the final stratigraphic unit of the Sakarya Continent Cover (Fig. 3).

3.1.1.3. The Elmadağ Olistostrome in the US

In the US, the upper clayey limestone unit of the Akkaya Formation within the Soğukçam Limestone Group is unconformably overlain by a sedimentary mélange unit (Figs. 3, 4.h-i), which we have named the "Elmadağ Olistostrome" in this study, following the definition by Erol (1956). Our recent study on the Elmadağ Olistostrome (Tekin & Tuncer, 2024) reveals block ages from Artinskian (late Early Permian) to late Hauterivian (Early Cretaceous), obtained from both platform and pelagic facies embedded into either a calcareous clayey or clayey calcareous matrix. While this sedimentary mélange has been defined by various authors at different localities [*e.g.*, "Akkayatepe Mélange" by Batman *et al.* (1978) near Alacaatlı village, close to Ankara city; "Unit with limestone blocks" by Ünalan (1981) around Yakacık region, NW Ankara; "Damlaağaçderesi Formation" by Koçyiğit (1991) near Bağlum and Yakacık villages, NW Ankara; and "Alacaatlı Olistostrome" by Okay and Altiner (2017) and Okay *et al.* (2019) in the Alacaatlı region, SW Ankara], all of these are considered junior synonyms of the "Elmadağ Olistostrome" *sensu* Erol (1956).

The Elmadağ Olistostrome has a total thickness of 165 meters in the US (Fig. 3). The thickness and lithological characteristics of the olistostrome vary in different locations; with wider outcrops mostly observed on the southern flank of the Haymana anticline, where it was erroneously mapped as the Akkaya Formation by Okay and Altiner (2016; Fig. 2). The lower part of the Elmadağ Olistostrome is dominated by gray- to beige-colored, loosely-packed carbonate matrix without stratification. In contrast, the upper part of the olistostrome (with 10 meters thick) contains larger

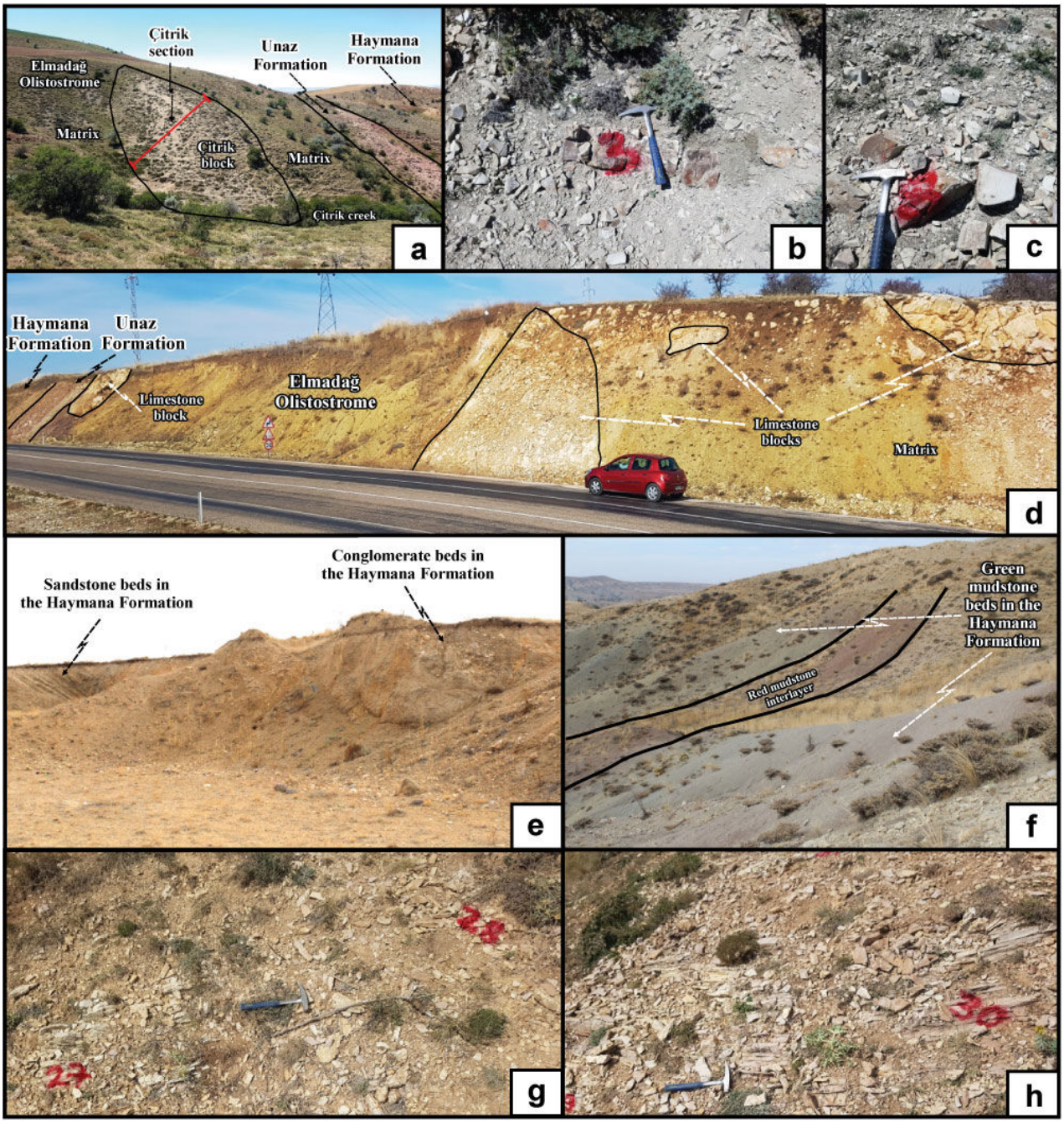

Figure 6: Field photographs from different parts of the Haymana anticline; **a.** Detailed photographs from the basal part of the Çitrik section, including the Çitrik block composed of gray- to beige-colored, thin- to medium-bedded marl with clayey limestone interlayers where the sample Çit-3 was collected, **b.** Detailed view from the gray to beige-colored clayey limestone bed, which is also the locality of sample Çit-3, **c.** Detailed photograph from the upper part of the Çitrik section, including the Çitrik block composed of the same lithology as the lower part where the sample Çit-8 was retrieved, **d.** General view from the southern flank of anticline (around the Ağapınar ridge in Fig. 2) showing the pelagic limestone blocks within the Elmadağ Olistostrome overlain by the Unaz and Haymana formations, respectively, **e.** View from the type locality of the "Kocatepe Formation" by YÜKSEL (1970); Sandstone beds overlain by conglomerates are situated at the base of the Haymana Formation, **f.** Green mudstone beds with red mudstone interlayer over the conglomerate beds in the Haymana Formation from the type locality. Red mudstone break was erroneously mapped and illustrated as red pelagic limestones of the Kocatepe Formation by YÜKSEL (1970), **g.** View from the basal part of the Unaz Formation in the US, made up of gray-, red- and purple-colored, thin-bedded, pelagic clayey planktonic foraminifer-rich limestones, **h.** Detailed view of the medial part of the Unaz Formation in the US, where sample Uy-30 was collected.

carbonate blocks (approximately 50x100 cm, 50x200 cm, 200x400 cm, some even pebble-sized) within gray- to beige-colored, stratified, highly-sheared, clayey carbonate and marl matrix (Figs. 3, 4.h-i).

The sedimentary mélange mainly includes two types of blocks and pebbles, *i.e.*, pelagic and platform carbonates (Fig. 4h-i). Gray- to beige-colored, micritic pelagic limestone blocks and pebbles

are widespread (Fig. 4i). Three samples (Uy-25, Uy-26a, and Uy-26b) were collected from these limestone blocks in the section; however, no radiolarian assemblages were extracted due to extensive calcification (Fig. 3).

It must be noted that to the northwest of the Haymana anticline, two pelagic limestone blocks (Küçükyayla and Çaldağ blocks), dated by OKAY and ALTINER (2016) as Turonian to Coniacian based on planktonic foraminifers, were mistakenly assigned to the basal part of the Kocatepe Formation by these authors. Our detailed mapping in this locality indicates that these pelagic fragments are actually blocks within the Elmadağ Olistostrome (Fig. 2). Although the third section (Çitrik section) was shown in the geological map by OKAY and ALTINER (2016) at the western bank of the Çitrik creek, three kilometers northwest of the Uyuzhamamı creek locality (Fig. 2), no age determination was provided in their study. Therefore, we measured the Çitrik section for paleontological dating, which included gray- to beige-colored clayey marl with interlayers of clayey marl and planktonic foraminifers that indicate a Turonian to Coniacian age (Figs. 2, 5, 6.a-c). Based on our new observations, the Turonian-Santonian age assigned to the Unaz Formation (formerly Kocatepe Formation *sensu* YÜKSEL, 1970) should be revised. We now propose a Santonian (more precisely, the late Santonian, although an early Santonian age cannot be excluded), based on the foraminiferal datings from four localities (*e.g.*, the US in Haymana, the Güdük section to the north of Alagöz, and the Çetinyatak section to the west of the Memlik region). Detailed characteristics of the Çitrik section will be discussed in the next section (Chapter 3.1.2).

Outcrops of larger blocks are primarily found on the southern flank of the Haymana anticline, between the Küçükçal hill and the Ağapınar ridge (Figs. 2, 6.d). The presence of these large olistoliths was first noted by YÜKSEL (1970, p. 20-22) as the "Le problème des olistolithes du Crétacé inférieur" (Problem of Lower Cretaceous Olistoliths). According to YÜKSEL (1970), these olistoliths likely formed due to the gravity sliding of Early Cretaceous blocks into younger sediments (possibly Late Cretaceous). However, this unit was not defined as a separate formation in YÜKSEL's studies (1970, 1973), nor was it addressed in the study of OKAY and ALTINER (2016). The age of the Elmadağ Olistostrome could be Cenomanian to Coniacian, based on the unconformable relationship between the underlying middle Berriasian to latest Albian Soğukçam Limestone Group and the overlying Santonian Unaz Formation. However, considering the overlying position of the Elmadağ Olistostrome above the previously-formed ophiolitic mélange of the IAE Ocean (with Turonian radiolarian blocks, *e.g.*, BRAGIN and TEKIN, 1996, in the north of the Ankara city close to the Memlik region, and TEKIN *et al.*, 2006, in the Mersin Mélange, southern Türkiye), it is apparent that the depositional age of Elmadağ Olistostrome is younger than Turonian and should be confined to the Coniacian (Fig. 3). The presence of a younger block (Çitrik block, dated Turonian-Coniacian) within the matrix of the Elmadağ Olistostrome further supports the Coniacian age for its formation. In previous studies, the Coniacian age was also assigned by OKAY and ALTINER (2017) and OKAY *et al.* (2019) to an equivalent unit (the Alacaatlı Olistostrome by OKAY and ALTINER, 2017) in their study conducted south of Ankara city. Additionally, radiolarian datings from the blocks within the Elmadağ Olistostrome have been performed in two other localities (north of Alagöz and Yakacık regions), and the results will be discussed in the following subchapters.

3.1.1.4. The Unaz Formation in the US

According to YÜKSEL (1970, 1973), the upper part of the US consists of lithological units attributed to the Kocatepe Formation *sensu* YÜKSEL (1970) in the Haymana region. YÜKSEL (1970, 1973) identified two distinct rock units in this formation: 1) a basal unit, 20-50 meter-thick, consisting of breccia, wild flysch, conglomerate, and sandstone; and 2) an upper unit, 15-50 meter-thick, composed of purple-colored limestones dated to the Coniacian. However, detailed studies conducted at the type locality (the Kocatepe hill, southeast of Haymana town) and in the US indicate that the basal unit, previously mapped as part of the Kocatepe Formation *sensu* YÜKSEL (1970), does not represent basal conglomerates associated with this formation but instead belongs to the overlying Haymana Formation (Figs. 2, 6.e). Additionally, green mudstone beds with red mudstone interlayers above the conglomerate beds in the Haymana Formation (Fig. 6.f) were incorrectly mapped as red pelagic limestones of the Kocatepe Formation by YÜKSEL (1970). Therefore, the so-called Kocatepe Formation, as applied to the Upper Cretaceous pelagic limestones, requires revision. In previous studies, similar pelagic limestones in the Pontide region were mapped as the "Unaz Clayey Limestone Unit" of the "Kurucaşile Formation" near the Amasra region, NW Türkiye, by AKYOL *et al.* (1974). These were later defined as the "Unaz Formation" by TÜYSÜZ *et al.* (1997, 2012). In its type locality, the pelagic clayey limestones of this formation vary in thickness from 5 to 20 meters and were dated to the late Santonian by TÜYSÜZ *et al.* (2012). These same lithological characteristics are also found in the red pelagic limestones around the Ankara region (Haymana, north of Alagöz, and west of Memlik, as observed in this study). Due to their close resemblance with the Unaz Formation, we have assigned the name "Unaz Formation" to the Upper Cretaceous pelagic limestones in the Ankara area (Figs. 2-3).

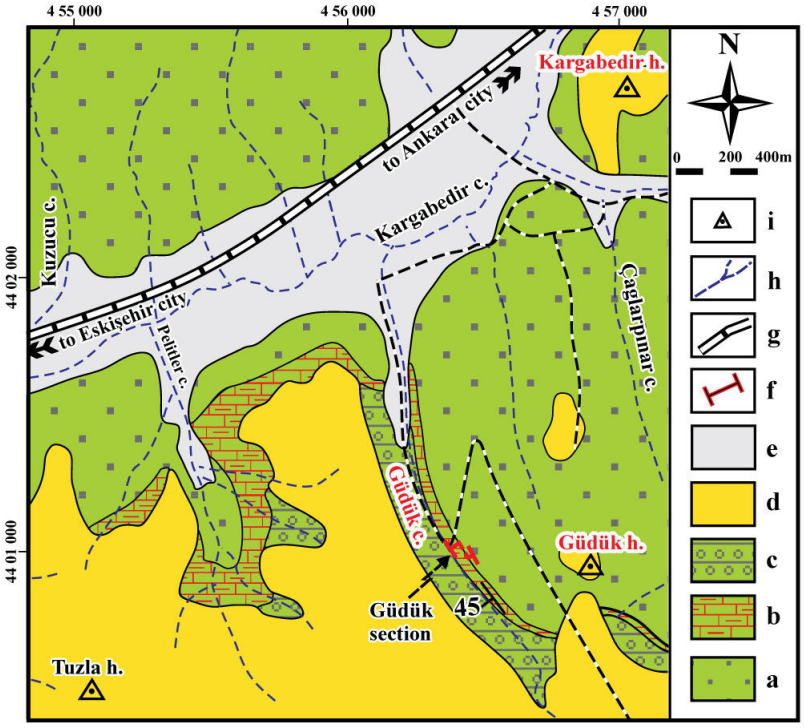

Figure 7: Geological map showing the distribution of stratigraphical/structural units around the north of Alagöz region and locality of the Güdük section. **Key: a.** The Coniacian Elmadağ Olistostrome, **b.** The Santonian Unaz Formation, **c.** The Campanian-Maastrichtian Haymana Formation, **d.** Neogene deposits, **e.** Quaternary deposits, **f.** Section locality, **g.** Main roads, **h.** Drainage system, **i.** Main peaks (slightly revised after OKAY & ALTINER, 2017; OKAY *et al.*, 2019).

The Unaz Formation in the US begins with gray- to beige-colored, thin-bedded, clayey limestone, followed by red- to purple-colored, thin-bedded clayey limestones (Figs. 3, 6.g-h). The upper part of the formation consists of red marl (Fig. 3). These two sections contain abundant planktonic foraminifers, and nine samples (Uy-27 to Uy-35) were taken from this formation. Planktonic foraminiferal assemblages primarily suggest a late Santonian age, though an early Santonian age could not be ruled out for the lower part of the formation. Additionally, samples Uy-28 and Uy-28a from the Unaz Formation in the US yielded abundant and moderately preserved radiolarians (Fig. 3). Based on data collected from the US, the Güdük section from the north of Alagöz, and the Çetinyatak section from the west of Memlik, it is shown that the carbonate portion of the formation does not exceed 14.5 meters in thickness, and its age is limited to the Santonian (mainly late Santonian). This contrasts with YÜKSEL (1970), who reported a Coniacian age, and with the Turonian-early Campanian age suggested by OKAY and ALTINER (2016).

3.1.1.5. The Haymana Formation in the US

Near the section locality, the pelagic limestones of the Unaz Formation gradually transition into the well-known, clastic-dominated lithologies of the Haymana Formation, first described by SCHMIDT (1960; Fig. 3). Although the Yılanlıhisar Formation, composed of alternating sandstone and marl layers, was proposed by YÜKSEL (1970, 1973) to overlie the Kocatepe Formation, subsequent studies (*e.g.*, ÜNALAN, 1976; TOKER, 1979, 1980; SIREL *et al.*, 1987; ÖZCAN & ÖZKAN-ALTINER, 1997; OKAY & ALTINER, 2016; GÜLYÜZ *et al.*, 2019; KARABEYOĞLU *et al.*, 2019) have generally included this unit within the Haymana Formation. The Haymana Formation is characterized by turbiditic sequences of green- to dark green-colored, medium- to thick-bedded conglomerates, sandstones, and mudstones. The total thickness of this formation was reported as 1295 meters by SCHMIDT (1960), while ÜNALAN *et al.* (1976) measured up to 1842 meters in different areas. Although this formation was first described as ranging from early Coniacian to early Maastrichtian by YÜKSEL (1970, 1973), more recent studies (*e.g.*, TOKER, 1979, 1980; ÖZCAN & ÖZKAN-ALTINER, 1997; OKAY & ALTINER, 2016) indicate a Campanian-Maastrichtian age based on planktonic foraminifers and nannoplankton assemblages.

3.1.2. The Çitrik section (ÇS) from the Çitrik block within the Elmadağ Olistostrome on the NW flank of the Haymana anticline

The Elmadağ Olistostrome contains numerous limestone blocks, especially in the upper sections, which are prominently exposed along the southern and southeastern flanks of the Haymana anticline (Fig. 2). One significant block, located along the western bank of Çitrik creek on the northern flank of the Haymana anticline (situated within the Ankara J29-a1 quadrangle sheet, coordinates 4366495N/0461201E and 4366522N/0461177E, UTM Zone 36S; GPS coordinates 39°26'43.95"N 32°32'55.27"E to 39°26'44.84"N 32°32'54.26"E; Figs. 2, 5, 6.a), is known as the Çitrik block. Ten samples (Çit-1 to Çit-10) were collected from the ÇS, which has a total thickness of 17.2 meters and a length of approximately 60 meters (Figs. 5, 6.a). This block consists of gray- to beige-colored, thin-bedded marl with interlayered clayey limestone (Fig. 5). Although numerous samples were taken, mainly from the clayey limestone interlayers, only sample Çit-2 from the basal part contained a planktonic foraminiferal assemblage

(Fig. 5). Based on the long-ranging planktonic foraminiferal species present, a Turonian to Coniacian age has been assigned to this block (Fig. 5). Although OKAY and ALTINER (2016) showed the ÇS on their map, they did not provide detailed section information. Also, lacking specific age data, the lithologies of the Çitrik block were assumed to be the lower levels of the Kocatepe Formation (Fig. 11 in OKAY & ALTINER, 2016). By combining data from these discrete units, these authors assigned a Turonian to Santonian age to the Kocatepe Formation *sensu* YÜKSEL (1970). Our detailed studies in this region indicate that the Santonian Unaz Formation (gray- to beige-colored, thin-bedded clayey limestone with clear stratification) overlies the Elmadağ Olistostrome (soft and clayey carbonate matrix without clear stratification) in an unconformable contact. Blocks within this olistostrome do not have direct contact with the overlying Unaz Formation (Fig. 6.a).

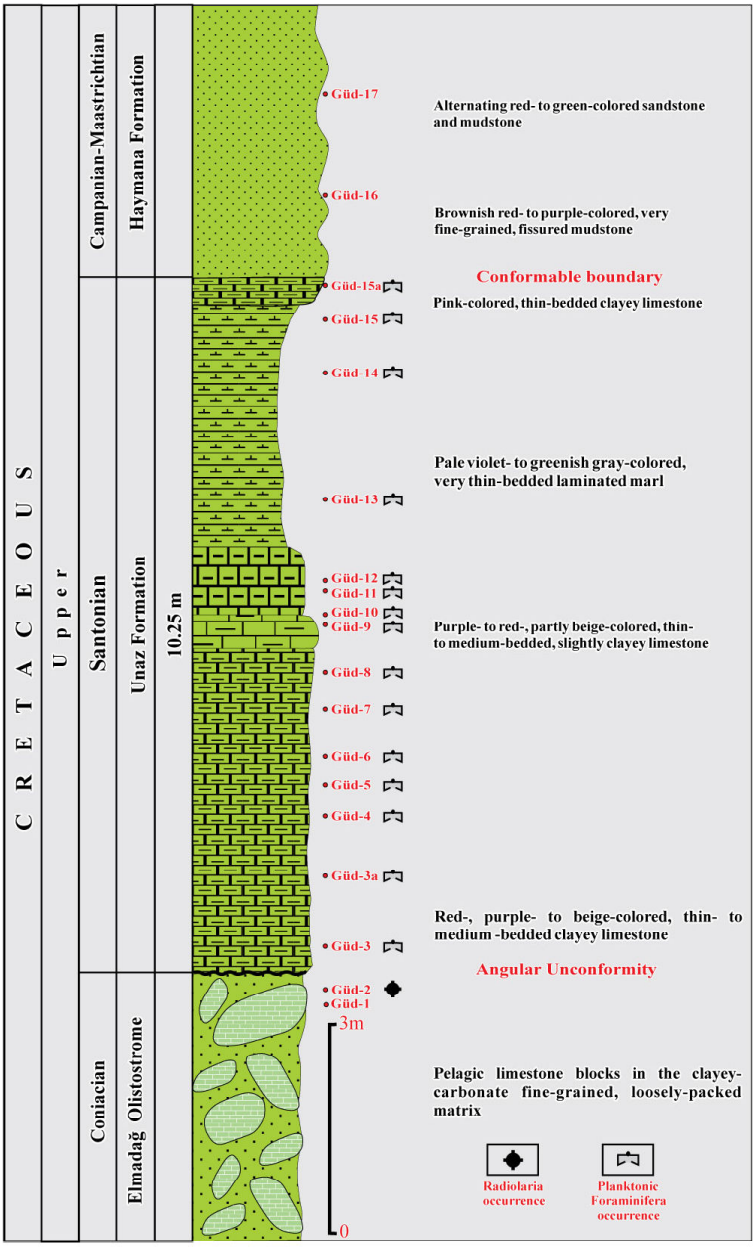

3.2. NORTH OF ALAGÖZ REGION

This region is situated approximately 40 km southwest of Ankara city center and very close to the highway between Ankara and Eskişehir (Figs. 1.B, 7). Three main units (Elmadağ Olistostrome, Unaz, and Haymana formations) are exposed here and exhibit similar lithological characteristics to those observed in the Haymana region. Recently, BILGIN (2014) provided a detailed study of this region. Basic stratigraphical features were presented by OKAY and ALTINER (2017), and OKAY *et al.* (2019), and subsequent dating for the stratigraphical units was performed by SARIASLAN *et al.* (2020). To analyze the stratigraphical sequence here and correlate them with those in the Haymana region, the Güdük section was measured (Figs. 7-8).

3.2.1. The Güdük section (GS)

This section is situated 1300 meters southwest of Kargabedir hill and northwest of Alagöz village (Ankara I28b3 quadrangle sheet between 4400944N/0456443E and 4400943N/0456442E, UTM Zone 36S; GPS coordinates 39°45'20.53"N 32°29'28.07"E and 39°45'20.51"N 32°29'28.03"E in the first part and shifted approximately 50 meters along the baseline of the Unaz Formation, then continues in the second part located between 4401057N/0456372E and 4401048N/0456355E, UTM Zone 36S; GPS coordinates 39°45'24.17"N 32°29'25.06"E and 39°45'23.88"N 32°29'24.36"E; Figs. 7-8). Seventeen samples (Güd-1 to Güd-17) were retrieved from the GS over a total of 15.75-meter-thick sequence (Fig. 8).

The Elmadağ Olistostrome constitutes the basal part of the GS (Figs. 7-8, 9.a-c). Different types of blocks (mainly pelagic, sometimes platform-type carbonates, sandstones, claystones, breccia, and cherts) of poorly-sorted, subrounded materials with varying sizes up to 100 meters occur in this region within a carbonate-marl-dominated matrix. A small pelagic block measuring 1.5 meters by 1.6 meters and composed of gray- to beige-colored, thin-bedded limestone with black chert lenses is present in the upper part of the Elmadağ Olistostrome (Figs. 8, 9.a-c). Although two samples were retrieved (Güd-1 and Güd-2) from chert lenses in this

◀ **Figure 8:** Log of the Güdük section and sampling levels.

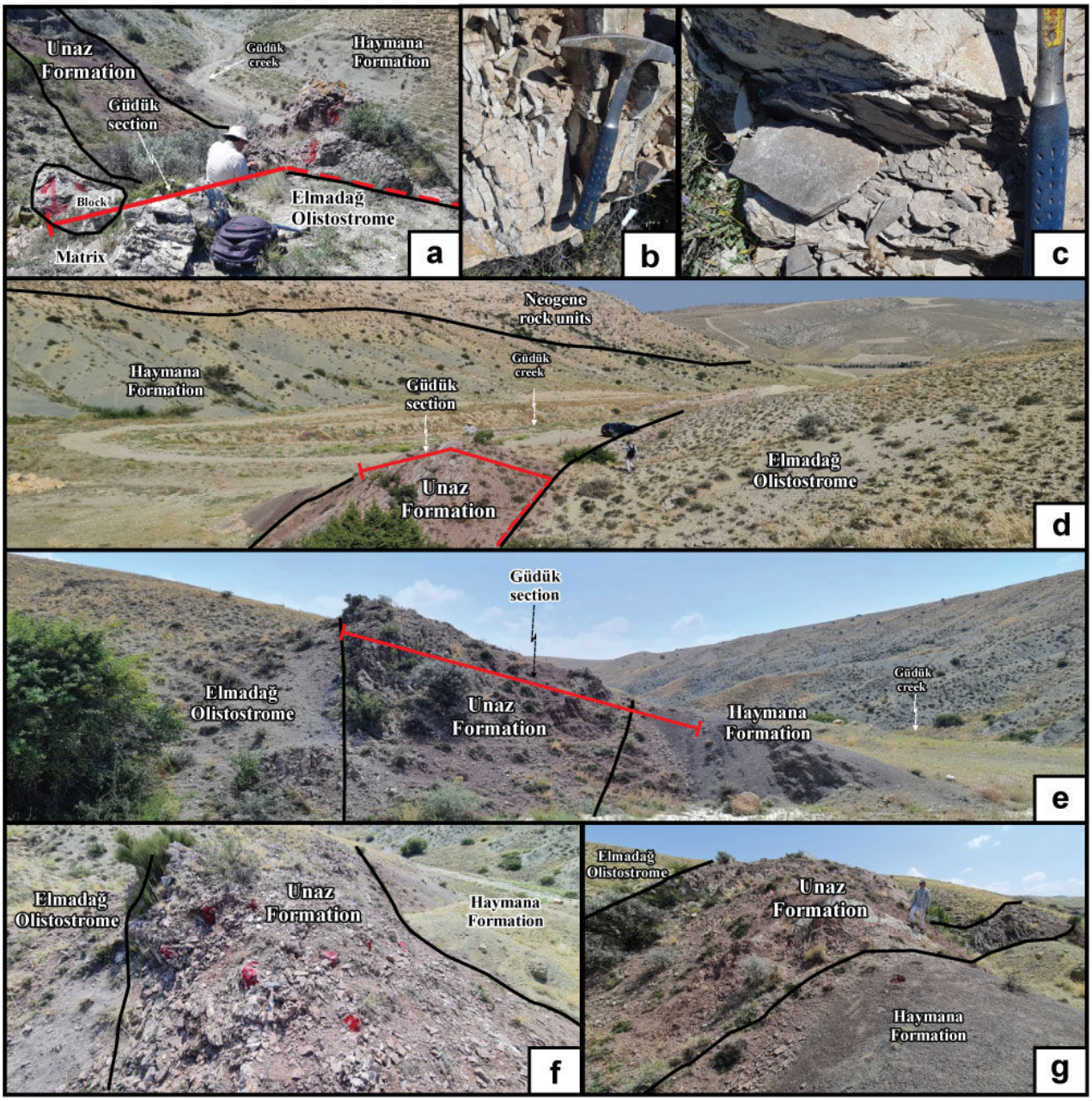

Figure 9: Field photographs from the Güdük section in the north of Alagöz region, **a.** General view showing the basal part of the Güdük section, including small pelagic limestone blocks of the Early Cretaceous age within the matrix of the Elmadağ Olistostrome, **b-c**. Detailed view of radiolarian-rich cherty limestone block of the latest Valanginian-early late Hauterivian age where sample Güd-2 was retrieved, **d.** Panoramic view from SE to NW showing the distribution of rock units (the Elmadağ Olistostrome, Unaz, and Haymana formations) on the deviation of section locality of the Güdük section, **e.** Another panoramic view from NW to SE showing the lithostratigraphic units in the Güdük section, **f.** Detailed view of sampling levels (Güd-3 to Güd-15a) from the red pelagic limestones of the Santonian Unaz Formation, **g.** View from the top of the Güdük section, showing the red pelagic limestone of the Santonian Unaz Formation passing to the alternating red- to green-colored sandstone and mudstone of the Campanian-Maastrichtian Haymana Formation.

cherty limestone block, only sample Güd-2 yielded a radiolarian assemblage dating to the late Valanginian-early middle Hauterivian (Early Cretaceous) (Fig. 8). Higher in the section, loosely packed, gray- to beige-colored marl matrix constitutes the dominant lithology in the Elmadağ Olistostrome (Figs. 8, 9.a).

The Elmadağ Olistostrome lies unconformably beneath the pelagic limestones of the Unaz Formation with a sharp contact (Figs. 8, 9.d-f). No clastic sediment appears at the base of this formation. Beige-, red- to violet-colored, thin- to medium-bedded clayey limestone with abundant planktonic foraminifers and 6.25 meters in thickness occurs at the base of this formation (Figs. 8, 9.e-f). This part is followed by a 4.5 meters-thick, pale violet- to purple-colored, very fine-grained, thin-bedded marl level (Figs. 8, 9.e-g). The uppermost part of this formation is represented by a 0.5 meter-thick, pink-colored pelagic clayey lime-

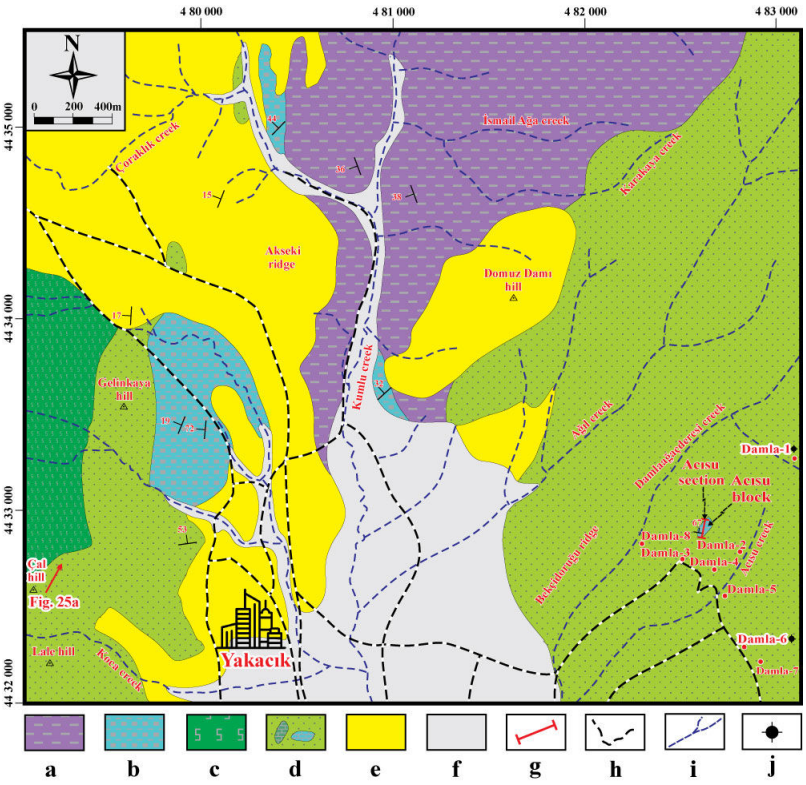

◀ **Figure 10:** Geological map of the Yakacık region showing the stratigraphical/structural units and locations of the samples collected in this study. **Key: a**. The Dikmen Graywacke consisting of Middle Triassic metaclastics belonging to the basement of Sakarya Continent, **b.** The Early Jurassic Bayırköy Formation (clastics and limestones of *rosso ammonitico* facies) overlying the basement of the Sakarya Continent (the Dikmen Graywacke), **c.** Ankara Ophiolitic Mélange with dismembered oceanic suit belonging to the Izmir-Ankara Ocean, **d.** The Coniacian Elmadağ Olistostrome with platform and pelagic carbonate blocks, **e.** The Neogene deposits, **f.** The Quaternary deposits, **g.** Location of the Acısu section, **h.** Main roads, **i.** Drainage system, **j.** Radiolaria occurrence in spot samples from blocks in the Elmadağ Olistostrome (redrawn, mainly revised after Duru & Aksay, 2002; Okay & Altiner, 2017; Okay *et al.*, 2019). The red arrow indicates the direction of the photograph in Fig. 25.a.

stone, with characteristics similar to the basal part of the Unaz Formation (Figs. 8, 9.g). The total thickness of the Unaz Formation is 10.25 meters, and fifteen samples (Güd-3 to Güd-15a) were collected for dating (Fig. 8). These samples yielded abundant Santonian planktonic foraminifers matching well with those determined by Sariaslan *et al.* (2020).

The Unaz Formation transitions to the overlying Haymana Formation, characterized by alternating shales and sandstones (Figs. 8, 9.e-g). While the lower part of the Unaz Formation is mainly composed of red-colored clastics, the color transitions to green towards the upper part. The age of the basal part of the Haymana Formation is precisely dated to the Campanian stage, based on planktonic foraminiferal assemblages by Sariaslan *et al.* (2020), an age assignment that has also been adopted in this study (Fig. 8).

3.3. Yakacık region

The third locality in this study is located approximately 17 km northwest of Ankara city, near the Yakacık village and its surroundings (Fig. 1.B). Detailed studies on the lithostratigraphic units of this area were conducted by Duru and Aksay (2002), Okay and Altiner (2017), and Okay *et al.* (2019).

In this locality, the oldest rock unit in the Ankara region, the Middle Triassic Dikmen Graywacke by Erol (1956), is exposed (Fig. 10). Rock units belonging to the Dikmen Graywacke in the Yakacık region are represented by deformed clastics, consisting mainly of shale and sandstone. This unit is unconformably overlain by a clastic-dominated sequence (sandstone, mudstone, conglomerate, shale, and *rosso ammonitico* limestone). This unit was first introduced as "Bayırköy Sandstone" by Granit and Tintant (1960), and subsequently named Bayırköy Formation by Altınlı (1975a) in the Bilecik region, NW Türkiye. Its age is assigned to the Early Jurassic by many authors (*e.g.*, Altınlı, 1975a; Altiner *et al.*, 1991; Alkaya & Meister, 1995; Vörös, 2014; Delikan & Orhan, 2020). To the west of Yakacık, the "Ankara Ophiolitic Mélange" (the Anatolian Complex *sensu* Koçyiğit, 1991), which is a part of Ankara Mélange, is exposed. This unit represents the remnants of the Izmir-Ankara Ocean *sensu* Şengör and Yılmaz (1981) and Şengör *et al.* (1984) with hundreds of meters in thickness (Fig. 10).

In this region, all these older units are unconformably overlain by the Coniacian Elmadağ Olistostrome, which is made up of carbonate blocks of different origins (*e.g.*, platform and pelagic carbonates) with irregular contacts (Fig. 10). Although this olistostromal unit is also exposed in other parts of the region, a major part of it crops out east of the Yakacık region around Damlaağaçderesi creek. The Elmadağ Olistostrome is composed of carbonate blocks of various sizes and origins (mainly pelagic) within a gray- to beige-colored, loosely- to slightly-stratified marl matrix (Figs. 10, 11.a). Koçyiğit (1991) designed this unit "Damlaağaçderesi Formation", which is considered a junior synonym of Elmadağ Olistostrome *sensu* Erol (1956). To determine the ages of the pelagic blocks in this olistostrome, eight spot samples (Damla-1 to Damla-8) were collected on the southeast bank of Damlaağaçderesi creek (Figs. 10, 11.a-d). In addition to these single-point samples, five samples (Acı-1 to Acı-5) were retrieved from a large block (the Acısu block) in the Acısu section within the Elmadağ

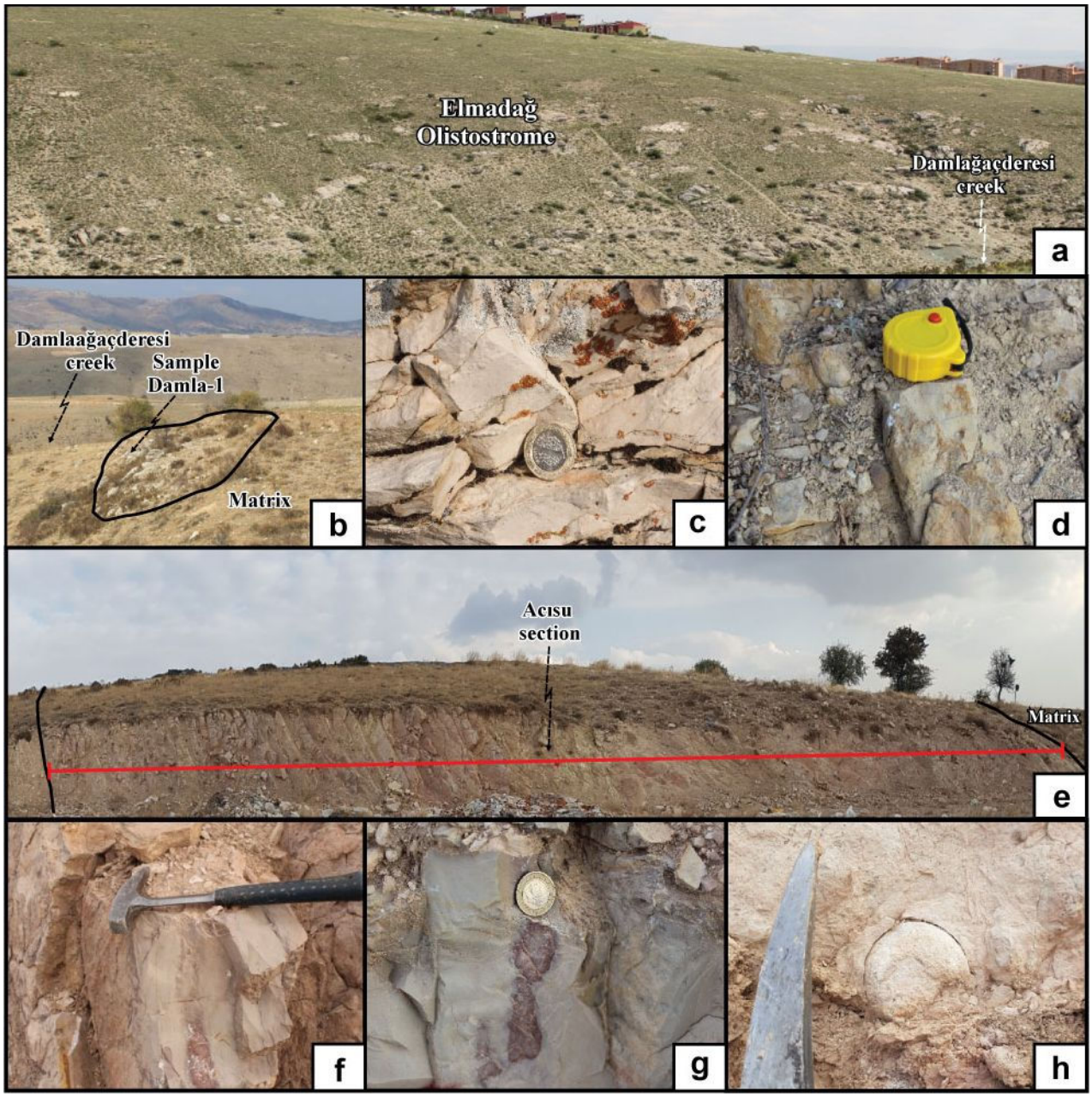

Figure 11: View from the Elmadağ Olistostrome in the Yakacık region; **a.** General view of the eastern bank of Damlaağaçderesi creek, showing the gray- to beige-colored pelagic cherty limestone and rare green-colored tuffite blocks in the Elmadağ Olistostrome, **b.** General view of the beige- to gray-colored cherty limestone block within the calcareous fine-grained matrix at the southeastern bank of the Damlaağaçderesi creek, **c.** Detailed view of the same block shown in Fig. 11.b, where sample Damla-1 with radiolarians of Hauterivian age was retrieved, **d.** Detailed view from the small block (sample Damla-6) made up of alternating gray- to red-colored cherty limestone and mudstone with abundant early Callovian-early Kimmeridgian radiolarians in the Elmadağ Olistostrome, **e.** General view of the Acısu section measured on the Acısu mega-block at the southeastern bank of Damlaağaçderesi creek; **f.** Detailed view from the central part corresponding to sample Acı-3 of the Acısu section, highlighting the alternating gray- to red-colored cherty limestone with abundant ammonoids and radiolarians and red mudstone of the early Callovian-early Kimmeridgian age, **g.** View from the overlying level (sample Acı-4), showing the red chert drops within the gray- to green-colored limestone beds with the early Callovian-middle to late Tithonian radiolarians, **h.** Ammonoid from the upper part of the Acısu section where the sample Acı-5 was collected.

Olistostrome (Figs. 10, 11.e-h, 12). Determinable radiolarian assemblages were obtained from two single-point samples (Damla-1 and Damla-6) and two additional samples (Acı-3 and Acı-4) from the Acısu section (Figs. 10-12). The locality and lithological descriptions of these samples are as follows.

3.3.1. Sample Damla-1

This sample was retrieved from a limestone block within a loosely-packed marl matrix in the Elmadağ Olistostrome (H29c4 quadrangle sheet, 4433277N/0483091E, UTM Zone 36S; GPS coordinates 40°02'52.67"N 32°48'04.91"E; Figs. 10, 11.b-c). This block is medium-sized (3 meters in

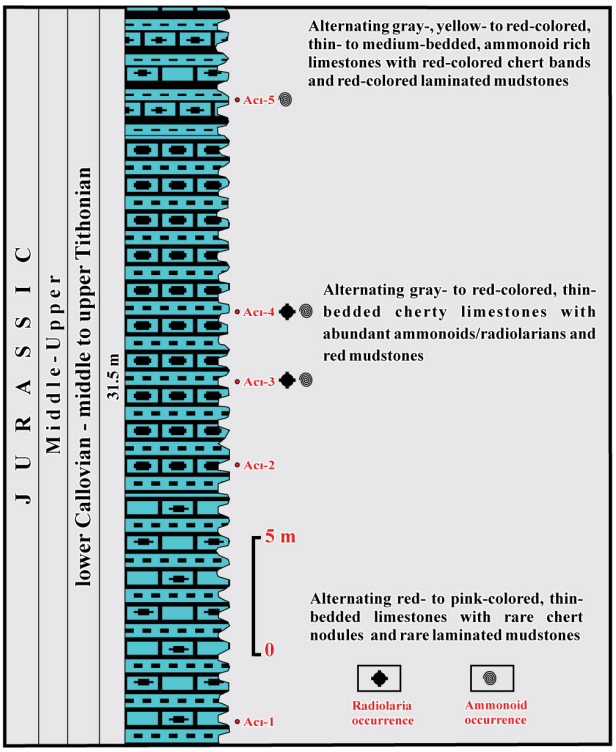

Figure 12: Log of the Acısu section from the Acısu block within the Elmadağ Olistostrome in the Yakacık region and sampling levels.

width and 25 meters in length) and is located on the southeast bank of Damlaağaçderesi creek (Figs. 10, 11.b). It consists of gray- to beige-colored, thin-bedded pelagic limestones with gray-colored chert nodules and drops (Fig. 11.c). The radiolarian assemblage obtained from this block reveals a Hauterivian (Early Cretaceous) age.

3.3.2. Sample Damla-6

A small block (1 meter in width and 3 meters in length) within the same type of matrix is situated on the southeast bank of Acısu creek (H29c4 quadrangle sheet, 4432260N/0482906E, UTM Zone 36S; GPS coordinates 40°02'19.69"N 32°47'57.21"E; Figs. 10, 11.d). It consists of red- to green-colored, thin- to medium-bedded silicified mudstone alternating with brown-colored limestone with chert nodules (Fig. 11.d). Early Callovian (late Middle Jurassic) to early Kimmeridgian (middle Late Jurassic) radiolarian assemblage was obtained from this block (Fig. 10).

3.3.3. The Acısu section (AS)

Although the blocks in the Elmadağ Olistostrome are generally small- to medium-sized to the east of the Yakacık region (Fig. 11.a), one mega-block with 31.5 meters thickness is exposed on the ridge between Damlaağaçderesi and Acısu creeks (H29-c4 quadrangle sheet, between 4432930N/0482625E and 4432880N/0482597E, UTM Zone 36S; GPS coordinates 40°02'41.39"N 32°47'45.28"E and 40°02'39.77"N 32°47'44.10"E; Figs. 10, 11.e). This block was called "the Acısu block" based on its location close to the Acısu creek (Fig. 10). The Acısu section (AS) measured on the Acısu block was subdivided into three parts (Fig. 12). The lower part is composed of red- to pink-colored, thin-bedded limestones with rare chert nodules and laminated mudstones. Two samples (Acı-1 and Acı-2) were taken from this part. This is followed by gray- to red-colored cherty limestones with abundant ammonoids and radiolarians interbedded with red mudstones (Figs. 11.f-g, 12). Two samples (Acı-3 and Acı-4) obtained from the central part of this section yielded abundant radiolarians revealing an early Callovian-middle to late Tithonian age (Fig. 12). The upper part of the section includes an alternation of gray-, yellow- to red-colored, thin- to medium-bedded ammonoid-rich limestones with chert bands and red-colored laminated mudstones (Figs. 11.h, 12). No radiolarian assemblage was recovered from the upper part of the sequence due to the extensive calcification of radiolarian tests.

3.4. West of Memlik region

To the 25 km northwest of Ankara city, the west of Memlik village (Fig. 1.B), extensive outcrops of ophiolitic mélange and overlying units are exposed (Fig. 13). This region was studied and mapped in detail by Koçyiğit (1991), Okay and Altiner (2017), and Okay *et al.* (2019). To understand the relationship between the ophiolitic mélange and the overlying units, the Çetinyatak section was measured in this region (Fig. 14).

3.4.1. Çetinyatak section (ÇS)

Well-exposed outcrops of the Upper Cretaceous sequence are located near Çetinyatak creek (Ankara H29-d3 quadrangle sheet, between 4436043N/0476500E and 4436195N/ 0476680E, UTM Zone 36S; GPS coordinates 40°04'21.81"N 32°43'26.37"E and 40°04'26.76"N 32°43'33.95"E; Fig. 13). The section derives its name from this creek (Fig. 13). The total thickness of the section is 94.5 meters, and five samples (Çet-1 to Çet-5) were collected from the Unaz Formation (Figs. 13-14) for dating using planktonic foraminifers.

The basal part of the ÇS is represented by the ophiolitic mélange, a chaotic mixture of various blocks and slices, mainly originating from an ophiolitic suite and its cover (*e.g.*, serpentinite, spilitic basalt, spilitic olistostrome, tectonic breccia, radiolarite, *etc.*). This basal part comprises two slices (Figs. 13-14): 1) Spilitic basalt: This unit exhibits green to dark green alteration and occasionally displays pillow structures (Figs. 14, 15.a); 2) Spilitic olistostrome: This slice contains semi-rounded spilitic basalt pebbles and blocks within a volcaniclastic matrix (Figs. 14, 15.b).

A 12-meter-thick sedimentary chaotic sequence (the Elmadağ Olistostrome) unconformably overlies the ophiolitic mélange with an abrupt contact (Figs. 14, 15.c). The olistostrome primarily consists of pelagic, clayey limestone with dark gray-colored chert lenses, set within a gray to beige-colored, loosely-packed clayey carbonate matrix (Figs. 14, 15.d). Although Koçyiğit *et al.* (1988) and Koçyiğit (1991) suggested that the pelagic limestone-bearing olistostromal unit occurs as tectonic slices within the ophiolitic mélange, our detailed mapping in this area dem-

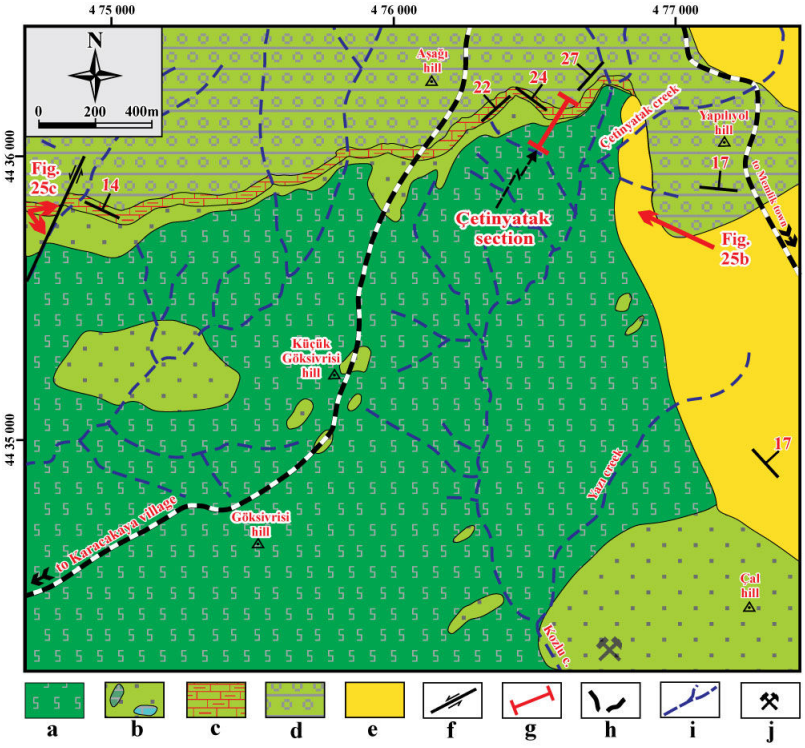

◀ **Figure 13:** Geological map of the west of Memlik region, showing the stratigraphical/structural units and location of the Çetinyatak section. **Key: a.** Ophiolitic mélange with dismembered oceanic suite belonging to the Neotethys Izmir-Ankara-Erzincan Ocean, **b.** The Coniacian Elmadağ Olistostrome with mainly pelagic carbonate blocks, **c.** The Santonian Unaz Formation with basal clastics, **d.** The Campanian-Maastrichtian Haymana Formation, **e.** Neogene deposits, **f.** Strike-slip fault, **g.** Location of the Çetinyatak section, **h.** Main roads, **i.** Drainage system, **j.** Limestone quarry (redrawn and mainly revised after KAZANCI & GÖKTEN, 1986; GÖKTEN *et al.*, 1988; KOÇYIĞIT *et al.*, 1988; KOÇYIĞIT, 1991). Red arrows indicate the directions of the photographs in Fig. 25.b-c.

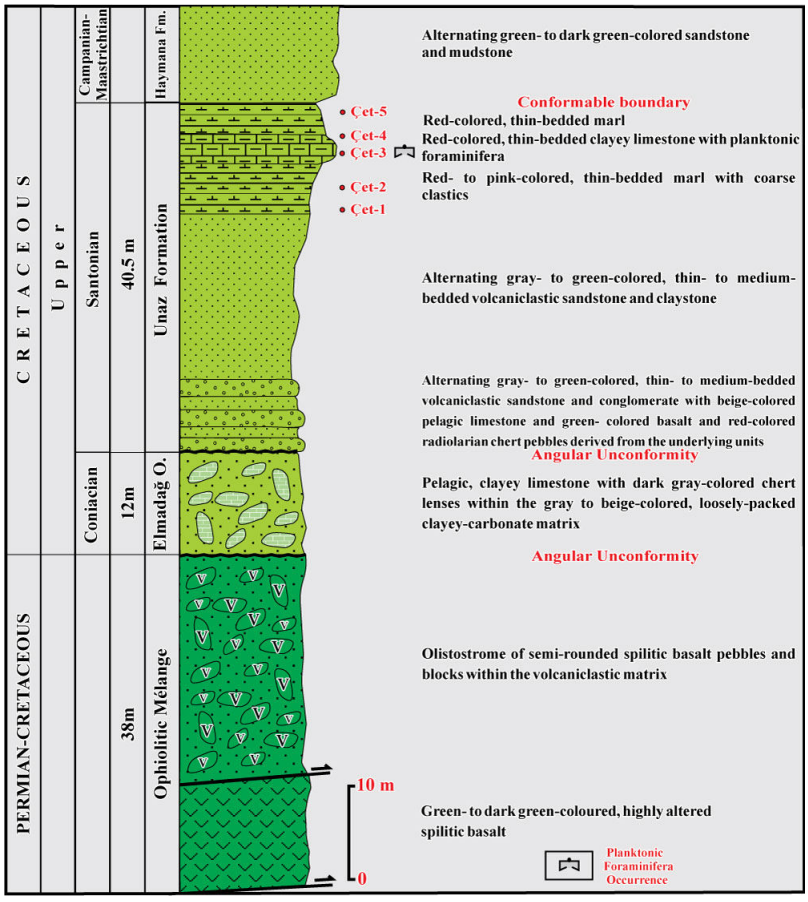

◀ **Figure 14:** Log of the Çetinyatak section and sampling levels.

onstrates that this unit (the Elmadağ Olistostrome) unconformably overlies the ophiolitic mélange (Fig. 13). Small remnants of this olistostromal unit are also observed resting atop of the ophiolitic mélange in various localities west of the Memlik region, including Çal hill to the east and Küçükgöksivrisi hill in the central part of the area (Fig. 13).

Towards the upper part of the sequence, the overlying units (Figs. 13-14, 15.e) consist of clastics, marl, and clayey carbonates, which transition upwards into clastic units. These were collectively

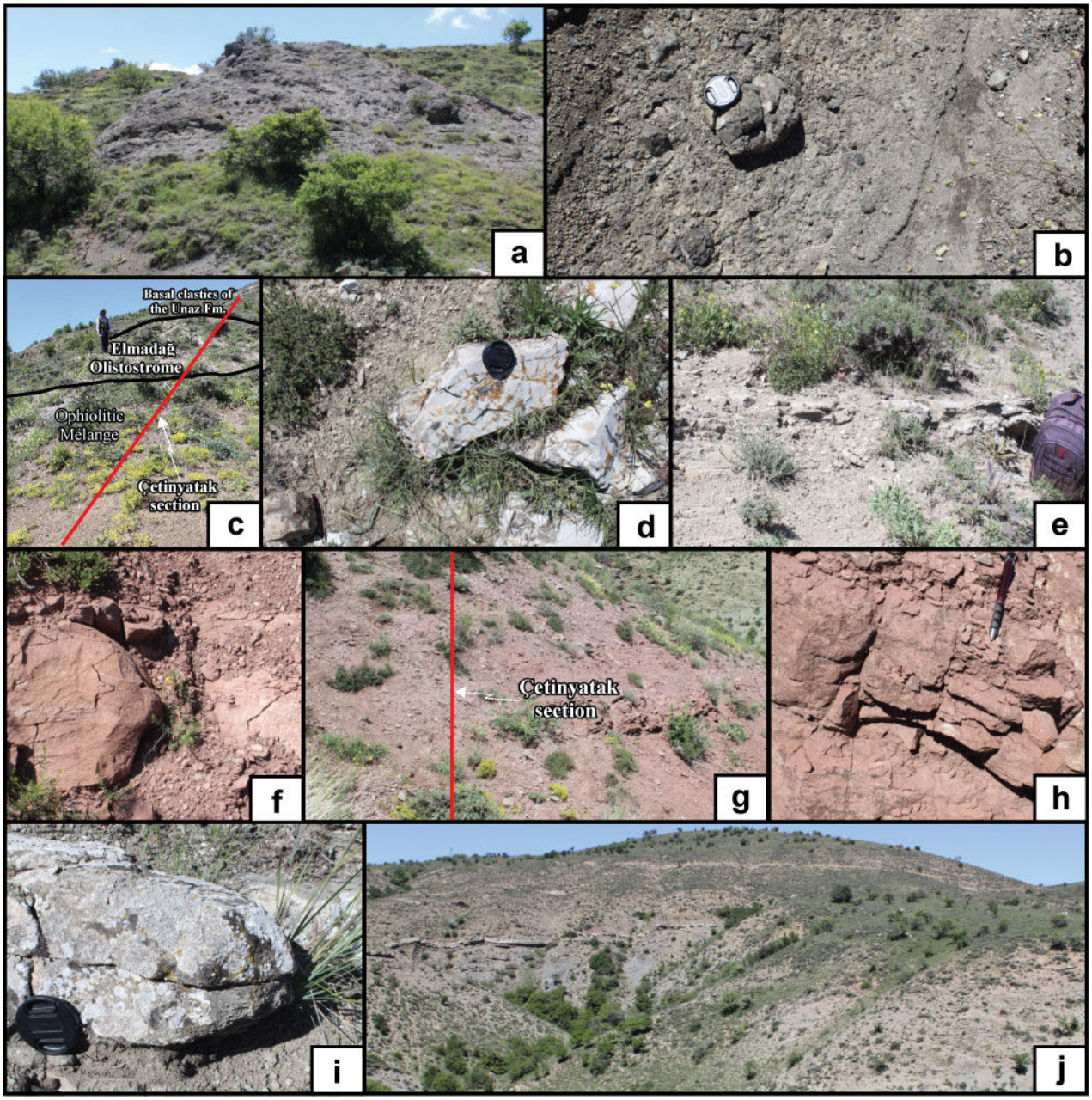

Figure 15: Field photographs from the Çetinyatak section (ÇS) in the west of the Memlik region, **a.** View from the basal part of the section, including spilitic basalt slice of the ophiolitic mélange, **b.** Detailed view of the second slice in the ophiolitic mélange composed of an olistostrome of semi-rounded spilitic basalt pebbles and blocks within a volcaniclastic matrix, **c.** Unconformable relations between the ophiolitic mélange, the Elmadağ Olistostrome, and the basal clastics of Unaz Formation, respectively, **d.** Detailed view from the Elmadağ Olistostrome composed of mainly pelagic, clayey limestone with dark gray-colored chert lenses within a gray- to beige-colored, loosely packed clayey-carbonate matrix, **e.** View from the basal clastics of the Unaz Formation consists of alternating gray- to green-colored, thin- to medium-bedded conglomerate and sandstone, **f-h.** Views from the upper limestone part of the Santonian Unaz Formation, **f.** View from the lower part of the clayey limestone in the Unaz Formation showing red- to pink-colored, thin-bedded marl with coarse volcaniclastics, **g.** General view from the upper limestone part of the Santonian Unaz Formation, displaying the lower red-colored marl, central red-colored, thin-bedded pelagic limestone with planktonic foraminifers, and upper red-colored marl, **h**. Detail view from the central red-colored, thin-bedded clayey limestone of the Unaz Formation from which planktonic foraminifer-bearing sample Çet-3 was retrieved**, i-j.** Views from the Campanian-Maastrichtian Haymana Formation; **i.** Detailed view from the uppermost part of the ÇS, showing alternating green- to dark green-colored, medium- to thick-bedded claystone and sandstone, **j.** View from the uppermost part of the section to the northeast direction, highlighting the general outline of the Haymana Formation; thick interlayers in this unit with gravel and coarse sandstone constitute the distributary channels within the turbiditic facies formed in the fore-arc basin.

referred to as the "Kızılyaka Formation" in this locality by Koçyiğit *et al.* (1988) and Koçyiğit (1991). However, this unit can be subdivided into two parts: 1) a lower unit of clastic and marl, and 2) an upper unit of clayey limestone, both equivalent to the "Unaz Formation" (Akyol *et al.*, 1974; Tüysüz *et al.*, 1997, 2012). We have adopted the name "Haymana Formation" *sensu* Schmidt (1960)

for the upper clastic sequence, correlating it with the Haymana Basin.

The Elmadağ Olistostrome is unconformably overlain by the 40.5-meter-thick Unaz Formation (Figs. 14, 15.f-h), which begins with an alternation of gray- to green-colored, thin- to medium-bedded conglomerate and sandstone. The conglomerate pebbles include pelagic limestone, green-colored basalt, and red-colored radiolarian chert, indicating derivation from both the Elmadağ Olistostrome and ophiolitic material from the underlying units. These lithologies transition into gray- to green-colored, thin- to medium-bedded volcaniclastic sandstone and claystone (Figs. 14, 15.e). Overlying these is a carbonate-bearing sequence composed of three distinct parts. The basal portion consists of red- to pink-colored, thin-bedded marl interspersed with coarse clastics derived from volcanic material (Figs. 14, 15.f). The central portion, approximately two meters thick is composed of red-colored, thin-bedded clayey limestone containing planktonic foraminifers (Figs. 14, 15.g-h). The uppermost portion closely resembles the basal part and is characterized by red-colored marl. Five samples (Çet-1 to Çet-5) were collected from the clayey limestone section of the Unaz Formation to analyze planktonic foraminiferal content. However, only one sample (Çet-3) yielded a discernible planktonic foraminiferal assemblage (Fig. 14). While Koçyiğit *et al.* (1988) and Koçyiğit (1991) originally assigned an early-middle Campanian (Late Cretaceous) age to this limestone, the planktonic foraminiferal assemblage identified in sample Çet-3 from this study indicates a Santonian age. This revised age is consistent with findings from the Haymana and north of Alagöz regions in this study, as well as the observations of Tüysüz *et al.* (2012) in the type locality (Figs. 3, 8, 14).

The Unaz Formation transitions gradually into the Haymana Formation, which is characterized by red-colored, thin-bedded mudstones alternating with green-colored, thick-bedded sandstones (Figs. 13-14, 15.i-j). Although Koçyiğit *et al.* (1988) and Koçyiğit (1991) defined this unit as the "Teşrekyayla Formation" in this locality, we adopt the name "Haymana Formation" *sensu* Schmidt (1960), based on correlations with the Haymana region (Figs. 13-14). Although Koçyiğit *et al.* (1988) and Koçyiğit (1991) reported a middle Campanian to Maastrichtian (Late Cretaceous) age for the 1000-meter-thick formation, correlations with the Haymana region (this study) and north of the Alagöz region (Sariaslan *et al.*, 2020; this study) assign the Haymana Formation to the broader Campanian-Maastrichtian interval (Fig. 14).

4. Biochronology of the radiolarian and planktonic foraminiferal assemblages

4.1. The Seyran Formation within the Soğukçam Limestone Group from the Uyuzhamamı section in the Haymana region

4.1.1. Radiolarian biochronology of the upper part of the Seyran Formation within the Soğukçam Limestone Group

The upper part of the Seyran Formation within the Soğukçam Limestone Group, overlying the limestone breccia (Fig. 3), contains highly-diverse and well-preserved radiolarians, indicating an early Hauterivian to early Aptian (Early Cretaceous) time span (Fig. 16; Pls. 1-8; Table 1). A total of eleven samples (Uy-1 to Uy-11) were collected from this unit along the Uyuzhamamı section (Fig. 3). Only one sample (Uy-8) was devoid of radiolarian content. The age determinations for these samples are as follows.

Eleven meters above the platform carbonates of the Bilecik Limestone Group, the first radiolarian-bearing sample (Uy-1, Fig. 3) was retrieved. This sample contains several significant radiolarian taxa (*e.g.*, *Halesium palmatum* Dumitrica, *Tetrapaurinella staurus* Dumitrica, *Becus gemmatus* Wu, *Archaeodictyomitra longovata* Dumitrica, *Spinosicapsa agolarium* (Foreman), and *Arcanicapsa leiostraca* (Foreman), *etc.*; Table 1). The presence of taxa such as *Halesium palmatum* Dumitrica, *Tetrapaurinella staurus* Dumitrica, *Spinosicapsa agolarium* (Foreman), *Pseudodictyomitra nodocostata* Dumitrica, and *Arcanicapsa leiostraca* (Foreman), which have their last appearance datum (LAD) at the end of the Hauterivian, along with taxa that first appear (FAD) at the beginning of the Hauterivian (*e.g.*, *Archaeodictyomitra longovata* Dumitrica, *Becus gemmatus* Wu, and *Pseudodictyomitra nodocostata* Dumitrica), supports a Hauterivian age for this sample (Jud, 1994; Dumitrica *et al.*, 1997). This age corresponds to Zone F2 (UA 26-28) by Jud (1994) and UAZ 19 by Baumgartner *et al.* (1995). Furthermore, the absence of characteristic taxa from the Berriasian-Valanginian interval [*e.g.*, *Emiluvia chica decussata* Steiger, *E. hopsoni* Pessagno, *E. pessagnoi* Foreman s.l., *Obesacapsula cetia* (Foreman), *O. polyedra* (Steiger), *Parapodocapsa amhitreptera* (Foreman), *Cinguloturris arabica* Jud, *Ristola cretacea* (Baumgartner), *Spinosicapsa coronata* (Steiger), *Tethysetta sphaerica* (Steiger)] corroborates the Hauterivian age (Steiger, 1992; Jud, 1994; Baumgartner *et al.*, 1995; Table 1). Therefore, the age of the pelagic limestones below Uy-1 corresponds to the late Berriasian-Valanginian interval (Fig. 3).

The radiolarian assemblage of sample Uy-2 is less diverse but shares similarities with Uy-1 (Table 1). The first appearance of *Stylospongia* ? *titirez* Jud in Uy-2 indicates the base of Zone F3 (UA 29) by Jud (1994), corresponding to the middle to late Hauterivian (Fig. 16; Table 1).

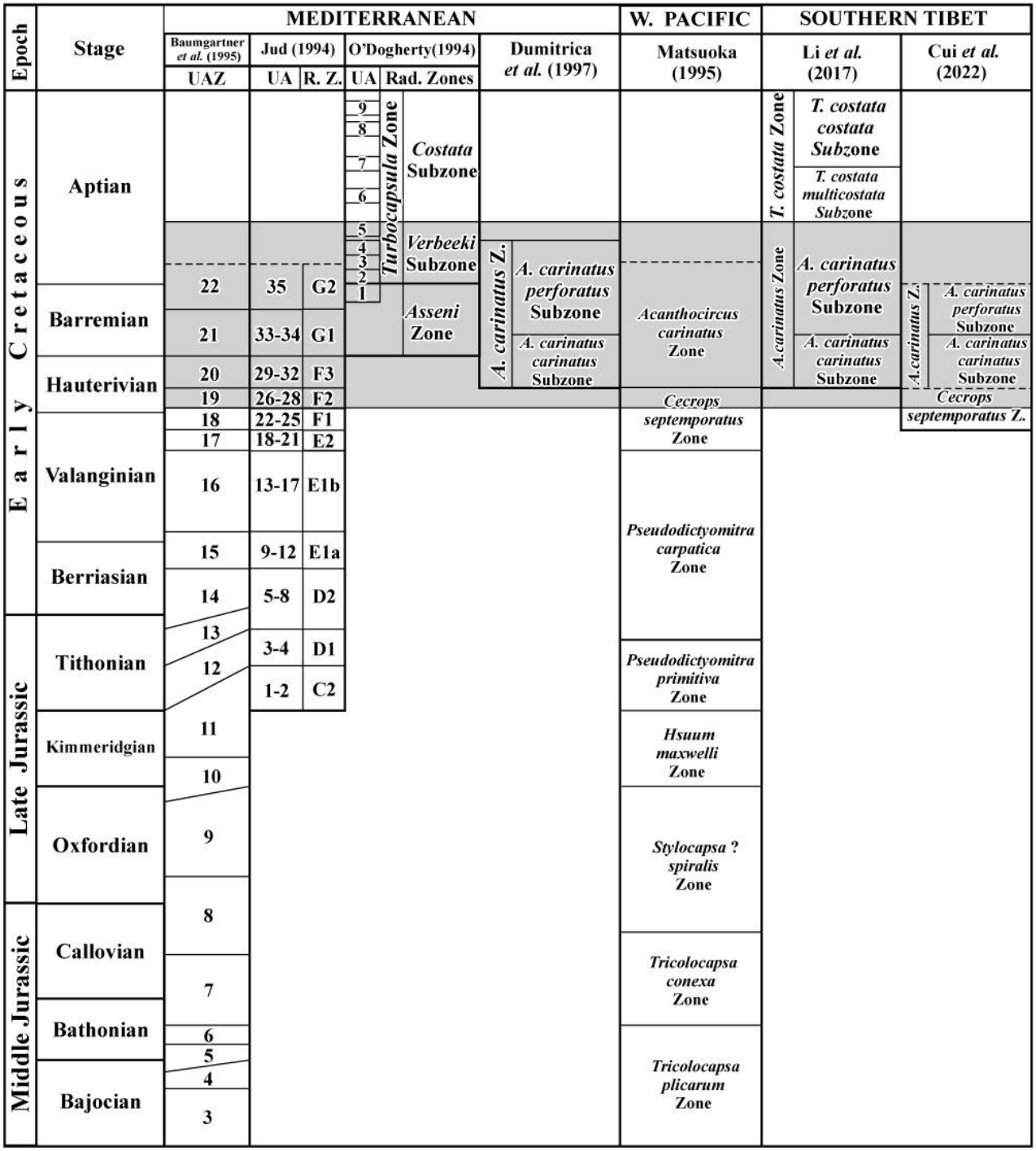

Figure 16: Proposed radiolarian zones and unitary associations for Bajocian (Middle Jurassic) to Aptian (Early Cretaceous) time interval (after JUD, 1994; O'DOGHERTY, 1994; BAUMGARTNER *et al.*, 1995; MATSUOKA, 1995; DUMITRICA *et al.*, 1997; LI *et al.*, 2017; CUI *et al.*, 2021). The shaded area corresponds to the chronostratigraphic position (Hauterivian to early Aptian) of the radiolarian assemblages obtained from the Seyran Formation within the Soğukçam Limestone Group, from the Uyuzhamamı section in the Haymana region.

Higher in the section, a significant radiolarian taxon, *Aurisaturnalis carinaus inconstans* DUMITRICA & DUMITRICA-JUD, is identified for the first and only time in sample Uy-3 (Table 1). According to DUMITRICA and DUMITRICA-JUD (1995), this taxon is a diagnostic marker of the uppermost Hauterivian strata, corresponding to UA 32 (Zone F3) by JUD (1994) and UAZ 20 by BAUMGARTNER *et al.* (1995). Additionally, another key taxon, *Cecrops* ? *sexaspina* JUD, with its last appearance datum (LAD) in the uppermost Hauterivian, is also exclusive to this sample (Zone F3 and UA 31 by JUD, 1994; Fig. 16; Table 1). These findings establish the age of sample Uy-3 as latest Hauterivian, corresponding to the F3 Zone (UA 31-32) by JUD (1994) and UAZ 20 by BAUMGARTNER *et al.* (1995; Fig. 16; Table 1).

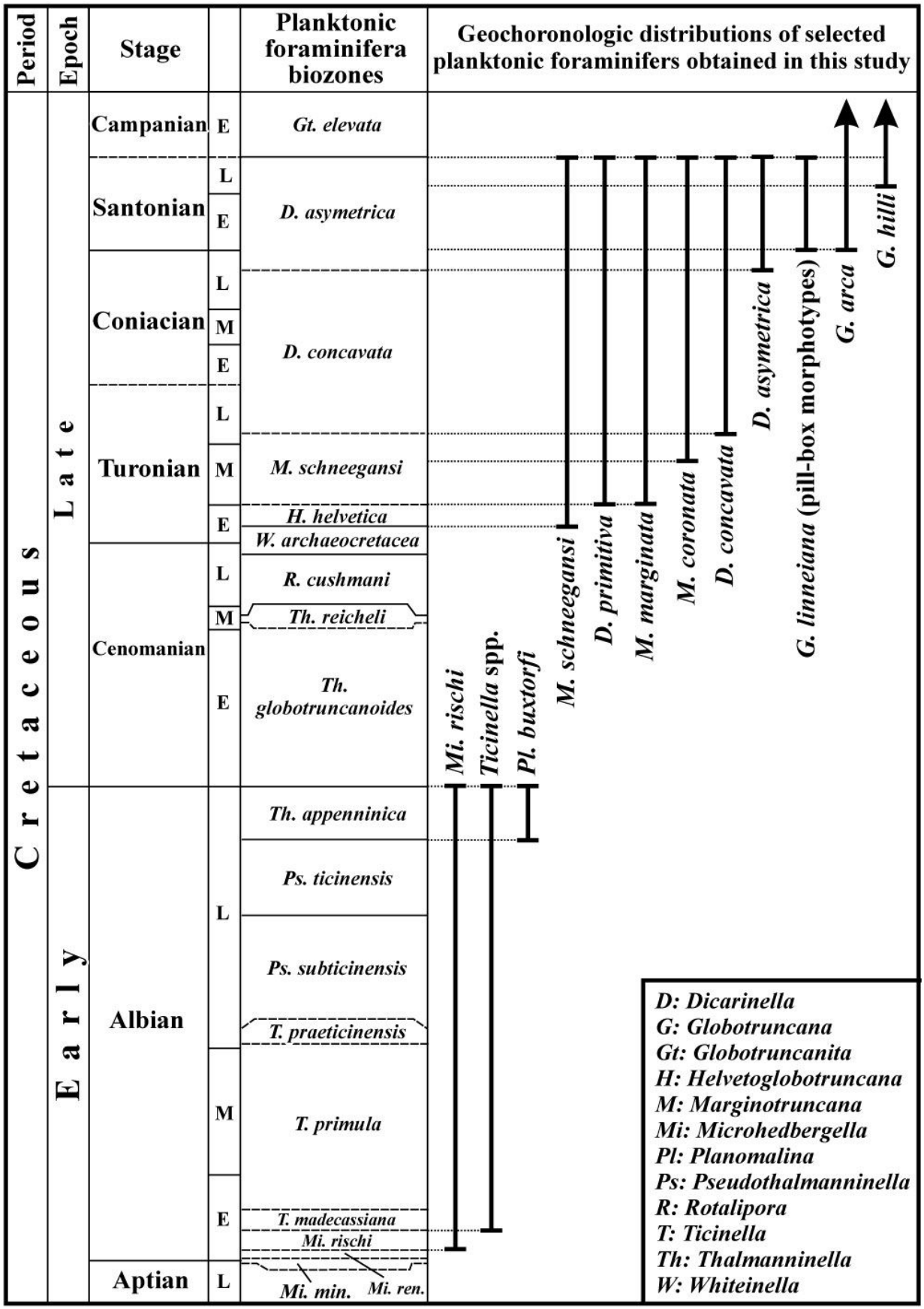

Figure 17: Latest Aptian-Campanian (Cretaceous) planktonic foraminiferal biozones and stratigraphic distributions of some important taxa observed in this study. Biozones are adopted from HUBER and LECKIE (2011) and COCCIONI and PREMOLI SILVA (2015). Stratigraphic distributions of selected taxa are derived from PETRIZZO (2000), PETRIZZO and HUBER (2006a, 2006b), GRADSTEIN *et al.* (2012), LAMOLDA *et al.* (2014), COCCIONI and PREMOLI SILVA (2015), PETRIZZO *et al.* (2022), and the mikrotax database (mikrotax.org).

Towards the upper part of the section, sample Uy-4 contains the very characteristic taxon, *Cecrops septemporatus* (PARONA), which has its last appearance datum (LAD) in Zone G1 (UA 34) by JUD (1994), corresponding to the early Barremian-early late Barremian time interval (Fig. 16; Table 1). Additionally, another important and indicative taxon described by DUMITRICA and DUMITRICA-JUD (1995), *Aurisaturnalis carinatus inconstans* DUMITRICA & DUMITRICA-JUD, which characterizes the same zone, is only present in sample Uy-5 (Table 1). Based on these two important taxa, the ages of samples Uy-4 and Uy-5 are assigned to the early Barremian-early late Barremian (Zone G1, UA 33-34 by JUD 1994, UAZ 21 by BAUMGARTNER *et al.*, 1995; Fig. 16). According to DUMITRICA and DUMITRICA-JUD (1995), the first appearance datum (FAD) of *Aurisaturnalis carinatus perforatus* DUMITRICA & DUMITRICA-JUD occurs in the middle to latest Barremian, corresponding to the base of Zone G2 (UA 35) by JUD (1994) and UAZ 22 by BAUMGARTNER *et al.* (1995; Fig. 16). This taxon first appears in sample Uy-6 (Table 1). Sample Uy-7 exhibits a similar assemblage to sample Uy-6 and contains radiolarians characteristic of the latest Barremian [*e.g.*, *Thanarla pacifica* NAKASEKO & NISHIMURA, *Thanarla pulchra* (SQUINABOL), *Crypthamporella clivosa* (ALIEV)]. This assemblage corresponds to UA1 by O'DOGHERTY (1994, base of the *Hiscocapsa asseni* Zone) and Zone G2 (UA 35) by JUD (1994), as well as UAZ 22 by BAUMGARTNER *et al.* (1995; Fig. 16; Table 1). Although DUMITRICA *et al.* (1997) reported the age of the *Thanarla pacifica* NAKASEKO & NISHIMURA as Hauterivian-Barremian, our results align with O'DOGHERTY (1994), assigning it to the latest Barremian to middle Aptian.

Sample Uy-8, however, lacks radiolarian assemblages, while sample Uy-9 yielded only a rare radiolarian taxon. As a result, determining the exact age of these samples is challenging. By comparing the underlying sample Uy-7 and the overlying samples Uy-10 and Uy-11, the age of these samples is tentatively assigned to the early Aptian (basal part of Zone G2, UA 35 by JUD, 1994; basal part of UAZ 22 by BAUMGARTNER *et al.*, 1995; basal part of the *Verbeeki* Subzone of the *Turbocapsula* Zone, UA 2-3 by O'DOGHERTY, 1994; Fig. 16; Table 1).

The last two samples (Uy-10 and Uy-11) from the Uyuzhamamı section contain similar radiolarian assemblages [*e.g.*, *Dibolachras tytthopora* FOREMAN, *Spinosicapsa typica* (RÜST), *Praexitus alievi* (FOREMAN), *Tethysetta usotanensis* (TUMANDA), *Thanarla pacifica* NAKASEKO & NISHIMURA, *Tethysetta boesii* (PARONA), *Crypthamporella clivosa* (ALIEV), *Crococapsa uterculus* (PARONA)], all of which have their last appearance datum (LAD) in the early Aptian. These samples correspond to UA 3 to 7 by O'DOGHERTY (1994; Fig. 16; Table 1). Additionally, several long-ranging taxa [*e.g.*, *Rhopalosyringium fossile* (SQUINABOL), *Crucella gavalai* O'DOGHERTY, *Paronaella grapevinensis* (PESSAGNO)], first appear in the lower part of the lower Aptian (UA 4 to 5 by O'DOGHERTY (1994). Based on these observations, the age of these samples is assigned to the earliest Aptian, corresponding to the lower part of the *Turbocapsula* Zone (*Verbeeki* Subzone, UA 4-5 by O'DOGHERTY, 1994), the lower part of G2 Zone, UA 35 by JUD (1994), and UAZ 22 by BAUMGARTNER *et al.* (1995; Fig. 16; Table 1).

4.1.2. Planktonic foraminiferal biochronology of the upper part of the Akkaya Formation within the Soğukçam Limestone Group

The upper part of the Akkaya Formation within the Soğukçam Limestone Group, situated over the debris flow deposits composed of pelagic limestones, contains a less-diverse planktonic foraminiferal microfauna, indicating a latest Albian time span (Figs. 17-18; Table 2). A total of fifteen samples (Uy-14 to Uy-24d) were collected from this unit along the Uyuzhamamı section (Fig. 3) for planktonic foraminiferal analysis. However, two samples from the basal part (samples Uy-14 and Uy-15) did not yield planktonic foraminifers but contained some calcified undeterminable radiolarians (Fig. 3). The dating of the remaining twelve samples, based on the planktonic foraminiferal content, is interpreted as follows.

Wackestone-mudstone depositional textures with planktonic foraminifers (mainly Ticinellids) are observed in the upper pelagic limestone unit of the Akkaya Formation, which belongs to the Soğukçam Limestone Group. The planktonic foraminiferal assemblages are dominated by low to mid-high trochospiral coiling, globular-subglobular chambered morphotypes (*i.e.*, *Microhedbergella* spp. and *Ticinella* spp., Figs. 17-18; Table 2). Within the assemblages, relatively small specimens (150-190 microns) with low trochospiral coiling, thin tests, and moderately enlarging chambers could be attributed to *Microhedbergella* sp. cf. *M. rischi* (MOULLADE) (Fig. 18.A). *Ticinella* spp. are identified by their thick, hispid walls and relatively larger tests (180-250 microns) (Fig. 18.B-D). A single specimen with a planispiral coiling and a peripheral keel throughout the test can be attributed to the species *Planomalina buxtorfi* (GANDOLFI) (Fig. 18.E). *Microhedbergella rischi* (MOULLADE) and the genus *Ticinella* REICHEL are characteristic taxa for the Albian strata (PREMOLI SILVA & SLITER, 1995; BELLIER & MOULLADE, 2002; HUBER & LECKIE, 2011). *Planomalina buxtorfi* has a relatively short stratigraphic range within the latest Albian (PETRIZZO & HUBER, 2006a, 2006b; Fig. 17).

Table 1. Distribution of radiolarian taxa obtained from the clayey, pelagic limestone of the Seyran Formation within the Soğukçam Limestone Group along the Uyuzhamamı section, Haymana region.

EPOCH/STAGE	EARLY CRETACEOUS									
	Hauterivian			Barremian				early Aptian		
Unitary Association by JUD (1994)	26-28	29-32		33-34		35				
Unitary Association by BAUMGARTNER *et al.* (1995)	19	20		21		22				
Unitary Association by O'DOGHERTY (1994)						1		2-3	4-5	
TAXA/SAMPLES	Uy-1	Uy-2	Uy-3	Uy-4	Uy-5	Uy-6	Uy-7	Uy-9	Uy-10	Uy-11
Halesium palmatum DUMITRICA	X									
Tetrapaurinella staurus DUMITRICA	X									
Haliodictya ? sp. A	X									
Spinosicapsa agolarium (FOREMAN)	X									
Spinosicapsa limatum (FOREMAN)	X									
Arcanicapsa leiostraca (FOREMAN)	X									
*Cecrops septemporatus (*PARONA)	X	X	X	X						
Crucella angulata YANG	X	X	X	X	X					
Archaeotritrabs gracilis STEIGER	X	?	?	?	?	X				
Archaeodictyomitra mitra DUMITRICA	X	?	X	?	X	X				
Pseudodictyomitra carpatica (LOZYNIAK)	X	?	?	?	?	X				
Alievium regulare (WU& LI)	X	X	X	?	X	X	X			
Haliodictya crucelliforma DUMITRICA	X	X	X	?	X	X	X			
Halesium biscutum JUD	X	?	?	?	?	X	X	X		
Acastea diaphorogona (FOREMAN)	X	X	X	X	X	?	X	?	X	
Triactoma merici TEKIN nov. sp.	X	?	?	X	?	X	?	?	X	
Crucella ? *inflexa* (RÜST)	X	?	?	?	?	?	?	?	X	
Deviatus diamphidius (FOREMAN)	X	?	?	?	X	X	X	?	X	
Paronaella ? *tubulata* STEIGER	X	?	?	?	X	X	?	?	X	
*Godia coronata (*TUMANDA)	X	?	?	X	?	?	X	X	X	
Tetrapaurinella lepida TEKIN nov. sp.	X	?	?	?	X	X	?	?	X	
*Archaeodictyomitra lacrimula (*FOREMAN)	X	?	?	?	?	?	X	?	X	
Archaeodictyomitra longovata DUMITRICA	X	?	?	?	?	?	X	X	X	
Xitus vermiculatus (RENZ)	X	?	X	?	?	?	X	X	X	
Pantanellium squinaboli (TAN SINHOK)	X	X	X	X	?	X	X	X	X	X
Acaeniotyle umbilicata (RÜST)	X	X	?	?	X	X	X	?	X	X
Suna echiodes (FOREMAN)	X	?	X	?	?	X	X	X	X	X
Crucella bossoensis JUD	X	?	X	?	X	X	X	?	X	X
Cyclastrum infundibuliforme RÜST	X	X	X	X	X	X	X	X	X	X
Paronaella ? *annemariae annemariae* JUD	X	?	X	X	X	X	X	X	X	X
Paronaella trifoliacea OZVOLDOVA	X	X	X	X	X	X	X	?	X	X
Halesium crassum (OZVOLDOVA)	X	X	X	?	X	X	X	X	X	X
Halesium ? *lineatum* JUD	X	?	?	?	?	X	?	?	X	X
Halesium medium (STEIGER)	X	X	X	?	X	X	X	?	X	X
Becus gemmatus WU	X	?	X	?	X	?	X	?	X	X
Dicerosaturnalis amissus (SQUINABOL)	X	?	X	X	X	X	X	X	X	X
Archaeodictyomitra leptocostata (WU& LI)	X	?	X	X	?	X	?	X	X	X
Pseudodictyomitra nodocostata DUMITRICA	X	?	?	?	?	X	?	X	X	X
Dibolachras tytthopora FOREMAN	X	?	X	?	X	X	X	?	X	X
Spinosicapsa triacantha tetraradiata (STEIGER)	X	?	X	?	?	?	X	?	X	X
Arcanicapsa trachyostraca (FOREMAN)	X	?	X	?	?	?	X	X	X	X
Dicerosaturnalis major (SQUINABOL)		X								
Godia ? *orbicula* TEKIN nov. sp.		X	?	X						
Svinitzium pseudopuga DUMITRICA		X	X	?	?	X				
Hexapyramis precedis JUD		X	?	X	X	?	X			
Crucella collina JUD		X	?	X	?	X	X			
Loopus nudus (SCHAAF)		X	X	?	X	X	?	X		
Dicerosaturnalis trizonalis dicranacanthos (SQUINABOL)		X	X	?	X	?	?	X	X	
Pantanellium aff. *cantuchapai* PESSAGNO & MACLEOD *sensu* JUD		X	X	?	?	X	X	?	X	X

EPOCH/STAGE	EARLY CRETACEOUS									
	Hauterivian			Barremian		early Aptian				
Unitary Association by JUD (1994)	26-28	29-32		33-34		35				
Unitary Association by BAUMGARTNER *et al.* (1995)	19	20		21		22				
Unitary Association by O'DOGHERTY (1994)						1		2-3	4-5	
TAXA/SAMPLES	**Uy-1**	**Uy-2**	**Uy-3**	**Uy-4**	**Uy-5**	**Uy-6**	**Uy-7**	**Uy-9**	**Uy-10**	**Uy-11**
Angulobracchia portmanni s.l. BAUMGARTNER		X	X	?	X	X	X	X	X	X
Godia ? *satoi* (TUMANDA)		X	X	X	X	X	X	?	X	X
Stylospongia ? *titirez* JUD		X	X	?	X	X	X	X	?	X
Cecrops ? *sexaspina* JUD			X							
Dicroa periosa FOREMAN			X							
Homoeparonaella irregularis (SQUINABOL)			X							
Tritrabs ewingi s.l. (PESSAGNO)			X							
Aurisaturnalis carinatus inconstans DUMITRICA & DUMITRICA-JUD			X							
Eospongosaturninus breggiensis DUMITRICA & HUNGERBÜHLER			X							
Pyramispongia spinosa TEKIN nov. sp.			X							
Archaeodictyomitra mostleri TEKIN nov. sp.			X							
Pseudodictyomitra matsuokai DUMITRICA			X							
Pseudoeucyrtis sp. A			X							
Acanthocircus italicus (SQUINABOL)			X	?	X					
Acanthocircus multidentatus (SQUINABOL)			X	?	X					
Paronaella ? *annemariae oezgenerdemae* TEKIN nov. subsp.			X	?	?	X				
Acanthocircus horridus SQUINABOL			X	?	X	X				
Acanthocircus hueyi (PESSAGNO)			X	?	X	X				
Acanthocircus levis (DONOFRIO & MOSTLER)			X	?	?	?	X			
Pyramispongia sphaerica TEKIN nov. sp.			X	X	?	X	X			
Spongocapsula obesa JUD			X	?	?	?	X	X		
Homoeparonaella peteri JUD			X	?	X	?	X	?	X	
Godia florealis (JUD)			X	?	?	?	?	?	X	
Pseudoeucyrtis tenuis (RÜST)			X	?	X	?	X	?	X	
Stylosphaera macroxiphus (RÜST)			X	?	X	?	X	?	?	X
Godia lenticulata JUD			X	X	?	?	?	?	X	X
Acanthocircus venetus (SQUINABOL)			X	?	X	?	?	?	?	X
Praexitus alievi (FOREMAN)			X	?	X	?	X	?	X	X
Xitus normalis (WU & LI)			X	?	X	X	X	X	X	X
Triactoma sp. A				X						
Homoeparonaella elegans bulbosa TEKIN nov. subsp.				X	X					
Spongocapsula coronata (SQUINABOL)				X	X	X	X	X	X	X
Triactoma tithonianum RÜST					X					
Aurisaturnalis carinatus carinatus DUMITRICA & DUMITRICA-JUD					X					
Solenotryma ichikawai MATSUOKA & YAO					X					
Becus multispinosus TEKIN nov. sp.					X	X	X			
Archaeospongoprunum obesum TEKIN nov. sp.					X	X	X			
Acanthocircus simplex (SQUINABOL)					X	?	X			
Pseudoxitus laguncula DUMITRICA					X	X	?	X		
Acaeniotyle helicta FOREMAN					X	?	X	?	X	
Clavaxitus clava (PARONA)					X	X	?	?	X	
Crolanium bipodium (PARONA)					X	?	X	?	X	
Cyclastrum ? *planum* JUD					X	?	?	?	?	X
Archaeospongoprunum tortilum TEKIN nov. sp.					X	?	?	?	X	X
Savaryella cruciforma TEKIN nov. sp.					X	X	X	X	X	X
Savaryella pseudoguexi breva TEKIN nov. subsp.					X	X	X	?	X	X
Pseudoeucyrtis zhamoidai (FOREMAN)					X	X	X	?	X	X
Crucella remanei JUD						X				
Pseudocrucella ? *elisabethae* (RÜST)						X				

EPOCH/STAGE	EARLY CRETACEOUS									
	Hauterivian			Barremian				early Aptian		
Unitary Association by JUD (1994)	26-28	29-32		33-34		35				
Unitary Association by BAUMGARTNER *et al.* (1995)	19	20		21		22				
Unitary Association by O'DOGHERTY (1994)						1		2-3	4-5	
TAXA/SAMPLES	**Uy-1**	**Uy-2**	**Uy-3**	**Uy-4**	**Uy-5**	**Uy-6**	**Uy-7**	**Uy-9**	**Uy-10**	**Uy-11**
Alievium ? *fatuum* DUMITRICA						X				
Pyramispongia sp. B						X				
Aurisaturnalis carinatus perforatus DUMITRICA & DUMITRICA-JUD						X				
Pseudodictyomitra thurowi DUMITRICA						X				
Hemicryptocapsa capita TAN SIN HOK						X				
Archaeospongoprunum ankaraense TEKIN nov. sp.						X	?	?	X	X
Archaeospongoprunum carrierensis globosum TEKIN nov. subsp.						X	X	?	X	X
Obeliscoites dorysphaeroides (NEVIANI)						X	?	?	X	X
Pseudocrolanium puga (SCHAAF)						X	X	X	X	X
Noviitus robustus WU						X	?	?	X	X
Crococapsa asseni (TAN SIN HOK)						X	X	X	X	X
Pantanellium masirahense DUMITRICA							X			
Homoeparonaella sp. A							X			
Pyramispongia barmsteinensis (STEIGER)							X			
Archaeodictyomitra excellens (TAN SIN HOK)							X			
Napora praespinifera (PESSAGNO)							X			
Triactoma haymanaense TEKIN nov. sp.							X	?	X	
Cyclastrum ? *trigonum* (RÜST)							X	?	X	
Mirifusus chenodes (RENZ)							X	?	X	
Tethysetta usotanensis (TUMANDA)							X	?	X	
Thanarla pulchra (SQUINABOL)							X	?	X	
Becus helenae (SCHAAF)							X	?	X	X
Godia concava (LI & WU)							X	?	?	X
Haliodictya ? *quadrata* TEKIN nov. sp.							X	?	X	X
Haliodictya ? sp. B							X	?	?	X
Thanarla pacifica NAKASEKO & NISHIMURA							X	?	?	X
Tethysetta boesii (PARONA)							X	?	?	X
Pseudoxitus seriola DUMITRICA							X	?	?	X
Crypthamporella clivosa (ALIEV)							X	X	?	X
Neorelumbra tippitae KIESSLING								X		
Spinosicapsa spinosa (SQUINABOL)								X	X	
Xitus sandovali JUD									X	
Rhopalosyringium fossile (SQUINABOL)									X	
Trimulus parmatus O'DOGHERTY									X	
Archaeodictyomitra sp. A									X	
Suna hybum (FOREMAN)									X	X
Crucella gavalai O'DOGHERTY									X	X
Paronaella grapevinensis (PESSAGNO)									X	X
Spongostichomitra elatica (ALIEV)									X	X
Spinosicapsa producta TEKIN nov. sp.									X	X
Pantanellium sp. A										X
Archaeospongoprunum sp. A										X
Archaeospongoprunum carrierensis carrierensis PESSAGNO										X
Bernoullius spelae JUD										X
Vitorfus campbelli PESSAGNO										X
Amphipyndax mediocris (TAN SIN HOK)										X
Pseudoeucyrtis corpulentus DUMITRICA										X
Crococapsa uterculus (PARONA)										X

Table 2. Distribution of planktonic foraminiferal taxa obtained from the pelagic clayey limestone of the Akkaya Formation within the Soğukçam Limestone Group in the Uyuzhamamı section, Haymana region.

EPOCH/STAGE	EARLY CRETACEOUS														
	earliest Albian														
BIOZONE			*Thalmanninella appenninica*												
TAXA / SAMPLES	Uy -14	Uy -15	Uy -16	Uy -17	Uy -18	Uy -19	Uy -20	Uy -21	Uy -22	Uy -23	Uy -24	Uy -24a	Uy -24b	Uy -24c	Uy -24d
Planomalina buxtorfi (GANDOLFI)			X												
Microhedbergella sp.			X	X	X	X	X	X	X	X	X	X	X	X	X
Ticinella sp.			X	X	X	X	X	X	X	X	X	X	X	X	X
Microhedbergella rischi (MOULLADE)				cf.											

4.2. Biochronology of the pelagic assemblages from blocks within the Elmadağ Olistostrome at the Yakacık, north of Alagöz, and Haymana regions

In three different regions (Yakacık, north of Alagöz, and Haymana), pelagic blocks were dated based on the radiolarian and planktonic foraminiferal assemblages. These are listed in chronological order below:

4.2.1. Radiolarian biochronology of the blocks within the Elmadağ Olistostrome at the Yakacık region

Although several spot samples (Damla-1 to Damla-9) were collected from the southeastern bank of Damlaağaçderesi creek, only two of these samples (Damla-1 and Damla-6) yielded determinable radiolarians in the Yakacık region (Fig. 10). In addition to these samples, one of the mega-block (Acısu) was studied in detail based on five samples (Acı-1 to Acı-5; Figs. 11-12). From this block, well-preserved radiolarians were obtained from two samples (Acı-3 and Acı-4). The radiolarian assemblages from these samples are discussed chronologically as follows.

4.2.1.1. Sample Damla-6

The pelagic limestone block, with gray chert nodules, contains a radiolarian microfauna [*i.e.*, *Emiluvia salensis* PESSAGNO (Pl. 9, fig. A), *Paronaella kotura* BAUMGARTNER (Pl. 9, fig. B), *Homoeparonaella argolidensis* BAUMGARTNER (Pl. 9, fig. C), *Tritrabs exotica* (PESSAGNO) (Pl. 9, fig. D), *Haliodictya* ? *antiqua antiqua* (RÜST) (Pl. 9, fig. E), *H.* ? *hojnosi* RIEDEL & SANFILIPPO (Pl. 9, fig. F), *Perispyridium ordinarium* (PESSAGNO) (Pl. 9, fig. G), *Cinguloturris carpatica* DUMITRICA (Pl. 9, fig. H), and *Spinosicapsa triacantha tetraradiata* (STEIGER) (Pl. 9, fig. I)] characteristic of a Middle to Late Jurassic age (BAUMGARTNER *et al.*, 1995). The first appearance datum (FAD) of *Cinguloturris carpatica* DUMITRICA occurs at the base of upper Bathonian-lower Callovian strata, corresponding to the base of UA7 by BAUMGARTNER *et al.* (1995), while the last appearance datums (LAD) of two key taxa (*Haliodictya* ? *hojnosi* RIEDEL & SANFILIPPO and *Paronaella kotura* BAUMGARTNER) is at the top of the lower Kimmeridgian (UA10 by BAUMGARTNER *et al.*, 1995). Based on these FAD and LAD, the age of the sample can be assigned as late Bathonian to early Kimmeridgian. However, according to several studies (DUMITRICA & MELLO, 1982; GORICAN, 1994; SASHIDA & UEMATSU, 1996; HORI, 1999), *Cinguloturris carpatica* DUMITRICA first appears at the base of the Callovian. Additionally, a diverse radiolarian assemblage from UAZ 7 was described from a sample above lower Callovian ammonites, supporting the interpretation that UAZ 7 is mainly Callovian in age (BECCARO, 2006). Based on these interpretations, the age of this sample is therefore assigned to the Callovian (late Middle Jurassic; middle part of UA7 by BAUMGARTNER *et al.*, 1995) to early Kimmeridgian (Late Jurassic; UA10 by BAUMGARTNER *et al.*, 1995; Fig. 16).

4.2.1.2. Samples from the Acısu section

Sample Acı-3 from the Acısu section contains rich radiolarian microfauna [*e.g.*, *Emiluvia pessagnoi* FOREMAN s.l. (Pl. 9, fig. J), *E. orea* s.l. BAUMGARTNER (Pl. 9, fig. K), *Tetratrabs zealis* (OZVOLDOVA) (Pl. 9, fig. L), *Angulobracchia digitata* BAUMGARTNER (Pl. 9, fig. M), *Paronaella kotura* BAUMGARTNER (Pl. 9, fig. N), *P. mulleri* PESSAGNO (Pl. 9, fig. O), *Perispyridium ordinarium* (PESSAGNO) (Pl. 9, fig. P), *Cinguloturris carpatica* DUMITRICA (Pl. 9, fig. Q), *Praewilliriedellium convexum* (YAO) (Pl. 9, fig. R)]. The First Appearance Datum (FAD) of *Cinguloturris carpatica* is at the base of the Callovian, while the Last Appearance Datums (LAD) of *Paronaella kotura* BAUMGARTNER, *P. mulleri* PESSAGNO, and *Angulobracchia digitata* BAUMGARTNER occur at the top of the lower Kimmeridgian. Based on this range, the age of sample Acı-3 is assigned to the early Callovian (late Middle Jurassic) to early Kimmeridgian (Late Jurassic), corresponding to the middle part of UA7-10 by BAUMGARTNER *et al.*, 1995; Fig. 16).

Stratigraphically younger sample Acı-4 in the Acısu section contains a different radiolarian assemblage compared to the underlying sample Acı-3. This assemblage includes *Homoeparonaella argolidensis* BAUMGARTNER (Pl. 9, fig. S), *Transhsuum* sp. aff. *T. maxwelli* (PESSAGNO) (Pl. 9, fig. T), *Cinguloturris primorika* KEMKIN & TAKETANI (Pl. 9, fig. U), *Mirifusus* sp. (Pl. 9, fig. V), *Svinitzium mizutanii* DUMITRICA (Pl. 9, fig. W), *Palinandromeda* sp. aff. *P. podbielensis* (OZVOLDOVA) (Pl. 9, fig. X), and *Spongocapsula palmerae* PESSAGNO (Pl. 9, fig. Y), as well as ammonoid remains (Pl. 9, fig. Z). The taxon range zone of *Cinguloturris primorika* KEMKIN & TAKETANI as reported by KEMKIN and TAKETANI (2004) and SUZUKI and GAWLICK (2009) supports an age assignment for this sample to the early Callovian (late Middle Jurassic) to middle-late Ti-

thonian (Late Jurassic). This age roughly corresponds to the middle part of UA7-12 by BAUMGARTNER *et al.* (1995; Fig. 16).

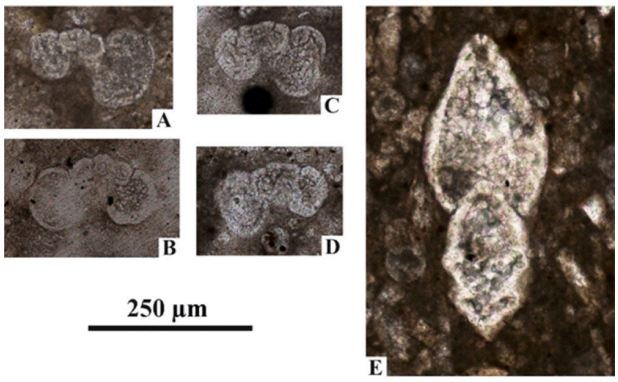

Figure 18: Thin-section photomicrographs of the planktonic foraminifers from the upper part of the Akkaya Formation within the Soğukçam Limestone Group studied in the Uyuzhamamı section, Haymana region: **A.** *Microhedbergella* sp. cf. *M. rischi* (MOULLADE): Uy-17; **B-D.** *Ticinella* spp.: B. Uy-16, C-D. Uy-24b; **E.** *Planomalina buxtorfi* (GANDOLFI): Uy-16. The scale bar is indicated at the bottom of the figure.

4.2.1.3. Sample Damla-1

Sample Damla-1 contains a diverse radiolarian microfauna, including *Cecrops septemporatus* (PARONA) (Pl. 9, fig. AK), *Triactoma tithonianum* RÜST (Pl. 9, fig. AL), *Crucella angulata* YANG (Pl. 9, fig. AM), *C. collina* JUD (Pl. 9, fig. AN), *Paronaella* ? *annemariae* JUD (Pl. 9, fig. AO), *P.* ? *tubulata* STEIGER (Pl. 9, fig. AP), *Godia florealis* (JUD) (Pl. 9, fig. AQ), *Halesium crassum* (OZVOLDOVA) (Pl. 9, fig. AR), *Haliodictya* ? *crucelliforma* DUMITRICA (Pl. 9, fig. AS), *Archaeodictyomitra mitra* DUMITRICA (Pl. 9, fig. AT), *Mirifusus* sp. (Pl. 9, fig. AU), *Xitus elegans* (SQUINABOL) (Pl. 9, fig. AV), *X. normalis* (WU & LI) (Pl. 9, fig. AW), *Obesacapsula verbana* (PARONA) (Pl. 9, fig. AX), and *Arcanicapsa leiostraca* (FOREMAN) (Pl. 9, fig. AY). According to DUMITRICA *et al.* (1997), *Xitus normalis* (WU & LI) in the assemblage first appears at the base of the Hauterivian, while *Cecrops* ? *sexaspina* JUD last appears near the top of the Hauterivian (JUD, 1994; DUMITRICA *et al.*, 1997). The assemblage is assigned to the early Hauterivian (base of the Zone F2, UA26 by JUD, 1994) to late Hauterivian (near the top of Zone F2, UA31 by JUD, 1994; Fig. 16).

4.2.2. Radiolarian biochronology of the block in the Elmadağ Olistostrome at the base of the Güdük section, north of Alagöz region

Sample Güd-2, retrieved from a block of the Elmadağ Olistostrome in the lower part of the Güdük section (Fig. 8), reveals a radiolarian assemblage including *Cecrops septemporatus* (PARONA) (Pl. 9, fig. AA), *C.* ? *sexaspina* JUD (Pl. 9, fig. AB), *Crucella angulata* YANG (Pl. 9, fig. AC), *Cyclastrum infundibuliforme* RÜST (Pl. 9, fig. AD), *Paronaella trifoliacea* OZVOLDOVA (Pl. 9, fig. AE), *D. trizonalis dicranacanthos* (SQUINABOL) (Pl. 9, fig. AF), *Spongocapsula coronata* (SQUINABOL) (Pl. 9, fig. AG), *Spinosicapsa agolarium* (FOREMAN) (Pl. 9, fig. AH), *S.* sp. aff. *S. coronata* (STEIGER) *sensu* JUD (Pl. 9, fig. AI), and *Arcanicapsa leiostraca* (FOREMAN) (Pl. 9, fig. AJ), characteristic mainly of the late Valanginian to late Hauterivian time interval (JUD, 1994; BAUMGARTNER *et al.*, 1995; DUMITRICA *et al.*, 1997). The co-occurrence of *Spongocapsula coronata* (SQUINABOL) and *Spinosicapsa* sp. aff. *S. coronata* (STEIGER) *sensu* JUD places the assemblage within the late Valanginian (base of F1 Zone, UA22 by JUD, 1994) to the early middle Hauterivian (base of F3 Zone, UA29 by JUD, 1994; Fig. 16).

4.2.3. Planktonic foraminiferal biochronology of the Çitrik block within the Elmadağ Olistostrome in the Haymana region

Clayey limestones interlayered within the marl of the Çitrik block are characterized by carbonate mudstone with few planktonic foraminiferal assemblages (Fig. 5). The planktonic foraminiferal assemblage, comprising *Marginotruncana* sp. cf. *M. pseudolinneiana* and *Marginotruncana* sp. (Fig. 19), suggests a Turonian-Santonian age interval for the Çitrik block within the Elmadağ Olistostrome (Fig. 17). Taking into consideration its position beneath the Santonian Unaz Formation, a Turonian-Coniacian age can be assigned to the Çitrik block.

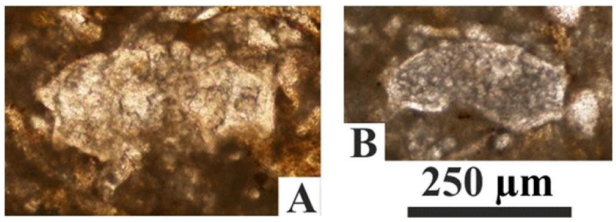

Figure 19: Thin-section photomicrographs of the Turonian-Coniacian planktonic foraminifers observed from the Çitrik block within the Elmadağ Olistostrome in the Çitrik section, Haymana region: **A.** *Marginotruncana* sp. cf. *M. marginata* (REUSS), Çit-2; **B.** *Marginotruncana* sp., Çit-2. Scale bar is indicated at the bottom of the figure.

4.3. Biochronology of the planktonic foraminiferal assemblages from the Unaz Formation in the Haymana, north of Alagöz, and west of Memlik regions

In this study, planktonic foraminiferal assemblages of the Unaz Formation were studied in detail in three different sections: the Uyuzhamamı section in the Haymana region, the Güdük section in the north of Alagöz region, and the Çetinyatak section in the west of Memlik region. The biochronology of the planktonic foraminiferal assemblages from these sections is as follows.

4.3.1. The Unaz Formation in the Uyuzhamamı section, Haymana region

The pelagic limestones of the Unaz Formation in the Uyuzhamamı section are represented by wackestone-carbonate mudstone with planktonic foraminifers, predominantly marginotruncanids. The planktonic foraminiferal assemblage comprises *Dicarinella asymetrica* (SIGAL) (Fig. 20.A), *Globotruncana hilli* PESSAGNO (Fig. 20.C-D), *Margi-*

notruncana sp. cf. *M. marginata* (REUSS), *M. pseudolinneiana* PESSAGNO (Fig. 20.E-G), and *M.* sp. aff. *M. sigali* (REICHEL) (Fig. 20.H) (Table 3). Within the assemblage, *Dicarinella asymetrica* is the eponymous taxon of the *D. asymetrica* Zone, which is characteristic of the latest Coniacian to Santonian age (Fig. 17). *Globotruncana hilli* is a taxon commonly reported in several Tethys Campanian-Maastrichtian strata. It has also been rarely recorded in the middle to upper parts of the *Dicarinella asymetrica* Zone in the Exmouth Plateau (NW Australia) (PETRIZZO, 2000), the Gubbio section (Italy) (COCCIONI & PREMOLI SILVA, 2015), and the SE Indian Ocean (PETRIZZO *et al.*, 2022). The first occurrence (FO) of *Globotruncana hilli* was recently reported from the uppermost Santonian strata of the Bottaccione section (MINIATI *et al.*, 2020; GALE *et al.*, 2023). According to the mikrotax database, its first appearance is accepted as being the latest Santonian. Considering the co-occurrence of the two important taxa (*Dicarinella asymetrica* and *Globotruncana hilli*) in sample Uy-28a, which is located just 1.5 meters above the base of the Unaz Formation (Fig. 3), the age of this formation is interpreted to be primarily the late Santonian (Table 3).

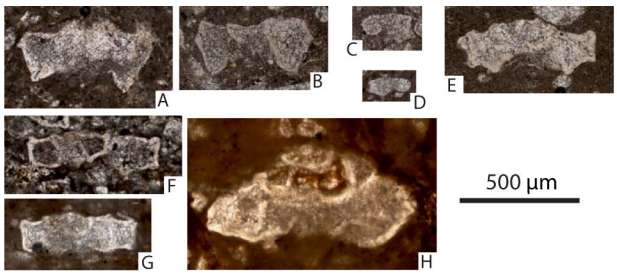

Figure 20: Thin-section photomicrographs of the Santonian planktonic foraminifers observed in the Unaz Formation from the Uyuzhamamı section, Haymana region. **A.** *Dicarinella asymetrica* (SIGAL): Uy-28a; **B.** *Dicarinella* sp. cf. *D. asymetrica* (SIGAL): Uy-31; **C-D.** *Globotruncana hilli* PESSAGNO: C. Uy-28a, D. Uy-29; **E-G.** *Marginotruncana pseudolinneiana* PESSAGNO: E. Uy-27. F. Uy-28, G. Uy-29; **H.** *Marginotruncana* sp. aff. *M. sigali* (REICHEL): Uy-29. The scale bar is indicated at the bottom of the figure.

4.3.2. The Unaz Formation in the Güdük section, north of Alagöz region

Wackestone depositional texture with planktonic foraminifers and recrystallized allochems are observed in the limestones from the Unaz Formation at the Güdük section (Fig. 8). Planktonic foraminifers are abundant and diverse in the lower part of the succession, while they become rare in the upper part (Fig. 21, Table 4). The amount of recrystallized allochems increases in some levels at the upper part of the section, whereas planktonic foraminifers and other clasts show inclination in some intervals.

The planktonic foraminifers observed in the Güdük section are dominated by double-keeled marginotruncanids, which are associated with rare dicarinellids (Fig. 21). The planktonic foraminiferal assemblages include *Dicarinella asymetrica* (SIGAL) (Fig. 21.A-C), *D. concavata* (BROTZEN) (Fig. 21.F-H), *D. primitiva* (DALBIEZ) (Fig. 21.K), *Globotruncana arca* (CUSHMAN) (Fig. 21.L), *G. linneiana* (ORBIGNY) (Fig. 21.N), *Marginotruncana coronata* (BOLLI) (Fig. 21.O), *M.* sp. cf. *M. marginata* (REUSS) (Fig. 21.P-R), *M. paraconcavata* PORTHAULT, *M. pseudolinneiana* PESSAGNO (Fig. 21.S-T), *M.* sp. cf. *M. schneegansi* (SIGAL) (Fig. 21.U), *M.* sp., and *Muricohedbergella* sp. cf. *M. flandrini* (PORTHAULT) (Fig. 21.W-X). Within the assemblage, the lowest occurrence of *Dicarinella asymetrica*, the eponymous taxon of the *D. asymetrica* Zone, is observed in sample Güd-3a at the base of the succession. This taxon is found in several stratigraphic levels throughout the section (Table 4). These data suggest that the age of the approximately 10.25 m thick pelagic succession is not older than the latest Coniacian and not younger than the Santonian (ION & SZASZ, 1994; ION *et al.*, 1999; ROBASZYNKI *et al.*, 2000; GALE *et al.*, 2007; LAMOLDA & PAUL, 2007; GRADSTEIN *et al.*, 2012; LAMOLDA *et al.*, 2014; COCCIONI & PREMOLI SILVA, 2015). Some morphotypes of *D. asymetrica* and *D. concavata* recorded in the Güdük section have slightly wider carinal bands (Fig. 21) compared to the typical *D. asymetrica* and *D. concavata*. The first occurrence of *Globotruncana arca* is observed at the base of the Güdük section (sample Güd-3, Table 4). The taxon is widely

Table 3. Distribution of planktonic foraminiferal taxa obtained from the Unaz Formation in the Uyuzhamamı section, Haymana region.

EPOCH/STAGE	LATE CRETACEOUS									
			Santonian							
BIOZONE			*Dicarinella asymetrica*							
TAXA/SAMPLES	Uy-27	Uy-28	Uy-28a	Uy-29	Uy-30	Uy-31	Uy-32	Uy-33	Uy-34	Uy-35
Marginotruncana marginata (REUSS)	cf.					cf.				
Marginotruncana sp.	X	X	?	X	?	X				
Marginotruncana pseudolinneiana PESSAGNO		X	X	X	?	X	X	X		
Marginotruncana tarfayaensis (LEHMANN)			cf.							
Globotruncana hilli PESSAGNO			X	X						
Dicarinella asymetrica (SIGAL)			X	?	?	cf.				
Dicarinella sp.				X						
Marginotruncana sigali (REICHEL)				aff.						

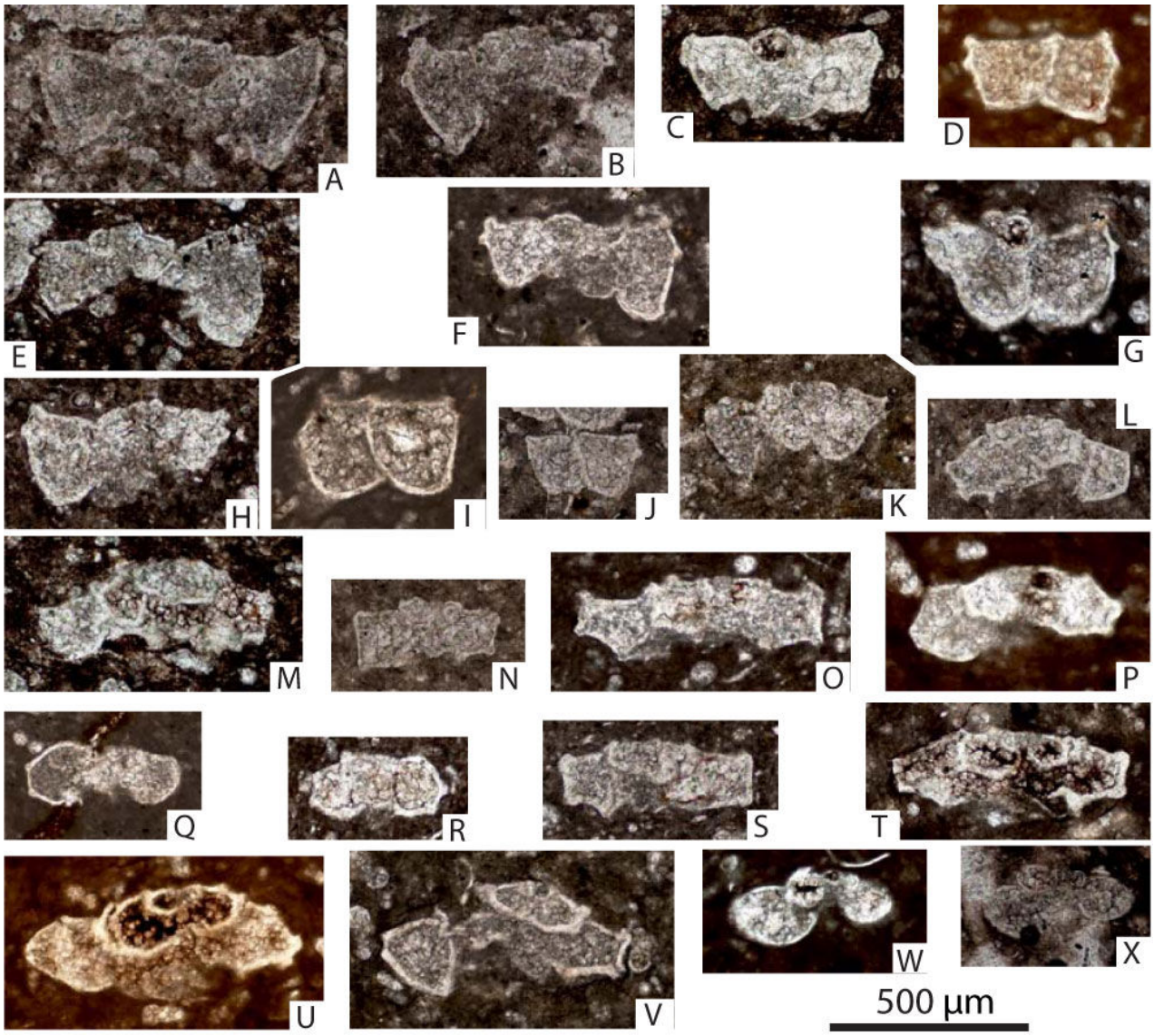

Figure 21: Thin-section photomicrographs of the Santonian planktonic foraminifers observed in the Unaz Formation from the Güdük section, north of Alagöz region. **A-C.** *Dicarinella asymetrica* (SIGAL): A. Güd-8; B. Güd-3a; C. Güd-15; **D-E.** *Dicarinella* sp. cf. *D. asymetrica* (SIGAL): D. Güd-3a, E. Güd-13; **F-H.** *Dicarinella concavata* (BROTZEN): F-G. Güd-4; H. Güd-7; **I-J.** *Dicarinella* sp. cf. *D. concavata* (BROTZEN): I. Güd-3, J. Güd-4; **K.** *Dicarinella primitiva* (DALBIEZ): Güd-15a; **L.** *Globotruncana arca* (CUSHMAN): Güd-3; **M.** *Globotruncana* sp. cf. *G. arca* (CUSHMAN): Güd-13; **N.** *Globotruncana linneiana* (D'ORBIGNY): Güd-3; **O.** *Marginotruncana coronata* (BOLLI): Güd-3a; **P-R.** *Marginotruncana* sp. cf. *M. marginata* (REUSS): **P-Q.** Güd-3, R. Güd-10; **S-T.** *Marginotruncana pseudolinneiana* PESSAGNO: S. Güd-10, T. Güd-5; **U.** *Marginotruncana* sp. cf. *M. schneegansi* (SIGAL): Güd-5; **V.** *Marginotruncana* sp. cf. *M. tarfayaensis* (LEHMANN): Güd-15a; **W-X.** *Muricohedbergella* sp. cf. *M. flandrini* (PORTHAULT), W. Güd-13, X. Güd-11. The scale bar is indicated at the bottom of the figure.

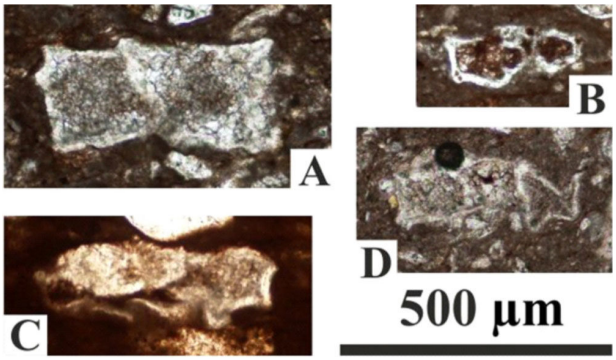

◀ **Figure 22:** Thin-section photomicrographs of the Santonian planktonic foraminifers observed in the Unaz Formation from the Çetinyatak section, west of Memlik region. **A.** *Dicarinella* sp. cf. *D. asymetrica* (SIGAL): Çet-3; **B.** *Marginotruncana* sp. cf. *M. pseudolinneiana* PESSAGNO: Çet-3; **C-D.** *Marginotruncana* sp.: both are from Çet-3. The scale bar is indicated at the bottom of the figure.

Table 4. Distribution of planktonic foraminiferal taxa obtained from the Unaz Formation in the Güdük section, north of Alagöz region.

EPOCH/STAGE	LATE CRETACEOUS																
	Santonian																
BIOZONE	*Dicarinella asymetrica*																
TAXA / SAMPLES	Güd -3	Güd -3a	Güd -4	Güd -5	Güd -6	Güd -7	Güd -8	Güd -9	Güd -10	Güd -11	Güd -12	Güd -13	Güd -14	Güd -15	Güd -15a	Güd -16	Güd -17
Globotruncana linneiana (ORBIGNY) 'pill-boxmorphotype'	X	?	X														
Dicarinella sp.	X	?	?	?	X												
Marginotruncana marginata (REUSS)	cf.		cf.						cf.								
Dicarinella concavata (BROTZEN)	cf.	?	X	?	?	X											
Globotruncana arca (CUSHMAN)	X											cf.			cf.		
Marginotruncana pseudolinneiana PESSAGNO	X	X	X	X	X	X	X	X	X	X	X	X	X	X	X		
Marginotruncana coronata (BOLLI)	X	X	X	?	?	?	?	?	?	X			cf.				
Dicarinella asymetrica (SIGAL)		X	?	?	?	?	X	?	?	?	?	cf.	?	X			
Marginotruncana paraconcavata PORTHAULT			X												cf.		
Marginotruncana tarfayaensis (LEHMANN)			X												cf.		
Marginotruncana schneegansi (SIGAL)				cf.													
Muricohedbergella flandrini (PORTHAULT)										cf.	?	cf.					
Dicarinella primitiva (DALBIEZ)															X		

known from several Campanian-Maastrichtian successions; however, its first appearance is within the Santonian at the base of the *Dicarinella asymetrica* Zone (Fig. 17).

4.3.3. The Unaz Formation in the Çetinyatak section, west of Memlik region

Wackestone with rare planktonic foraminifers, recrystallized allochems, and abundant siliciclastics are observed in the Çetinyatak section, with inclination being common in many taxa (Fig. 22). A few planktonic foraminifers are obtained from sample Çet-3, including *Dicarinella* sp. cf. *D. asymetrica* (SIGAL) (Fig. 22.A), *Marginotruncana pseudolinneiana* PESSAGNO (Fig. 22.B-C), and *M.* sp. (Fig. 22.D). The presence of *Dicarinella* sp. cf. *D. asymetrica* suggests the *D. asymetrica* Zone, indicating the latest Coniacian-Santonian time interval (Fig. 17). Based on a comparison with planktonic foraminifers from the Uyuzhamamı and Güdük sections, the age of the Unaz Formation in this section is assigned to the Santonian.

5. Results and discussion

5.1. The Bilecik Limestone Group

The Bilecik Limestone Group constitutes the basal part of the sequence studied in the Uyuzhamamı section in the Haymana region. It is composed of gray- to beige-colored, medium- to thick-bedded platform carbonates of Tithonian to early Berriasian age based on the study of OKAY and ALTINER (2016).

5.2. The Soğukçam Limestone Group

Lithological units of the Bilecik Limestone Group are unconformably overlain by a rather continuous middle Berriasian to uppermost Albian pelagic rock sequence, with a minor gap during the middle to late Aptian time interval (Figs. 2-3). These rock units are included in the Soğukçam Limestone Group and are represented by two formations (the Seyran and Akkaya formations). The rank of the "Soğukçam Limestone" has been raised to the "Soğukçam Limestone Group" in this study.

5.2.1. The Seyran Formation

The Seyran Formation, originally described by YÜKSEL (1970), was revised in this study to include the lower two units, while the upper unit was reassigned to the Akkaya Formation, as described by OKAY and ALTINER (2016; Fig. 3).

In its basal part, the Seyran Formation is characterized by an 11-meter-thick limestone breccia, which was assigned to the middle Berriasian by OKAY and ALTINER (2016). The boundary between the overlying Seyran Formation and the underlying Bilecik Limestone Group may correspond to the early/middle Berriasian boundary (*i.e.*, a version of the Kbe2 sequence boundary), which has been overprinted by local tectonism and represents a drowning unconformity (GODET, 2013). According to GODET (2013), drowning unconformities indicate that "changes in nutrient input, clastic delivery, temperature, or a combination of them may be responsible for a decrease in light penetration in the water column and the progressive suffocation and poisoning of photosynthetic carbonate producers". This drowning event suggests that the middle Berriasian marks the time of platform collapse, transitioning into a deep, pelagic environment as evidenced by radiolarian-rich, thin-bedded clayey limestones (FLÜGEL, 2004) during the late Berriasian to early Aptian time interval (Fig. 3).

The basal limestone breccia of the Seyran Formation is overlain by micritic, clayey and cherty pelagic limestone with abundant radiolarians (Fig. 3). The lower part of this sequence lacks fossil microfauna but can be ascribed to the late Berriasian-Valanginian based on well-dated strata above and below. In contrast, the upper part of these limestones yielded a diverse and abundant radiolarian assemblage (Fig. 3), which indicates an early Hauterivian to early Aptian age based on a total of 146 taxa. These data suggest that the

early Hauterivian to early Aptian (Early Cretaceous) interval was the time of a well-stratified basin, with minimal tectonic activities (FLÜGEL, 2004). Due to these facts, the age of the Seyran Formation can be assigned to the middle Berriasian to early Aptian, primarily based on radiolarian dating (Fig. 3). Therefore, the age assignment of this formation as Cenomanian-Turonian by YÜKSEL (1970, 1973) and as Berriasian by OKAY and ALTINER (2016) (Soğukçam Limestone in their study) should be revised.

5.2.2. The Akkaya Formation

The type locality of the Akkaya Formation is located at the outcrops of the Elmadağ Olistostrome (Fig. 2). However, this formation was first defined from the Uyuzhamamı region by OKAY and ALTINER (2016). Because of this, the Akkaya Formation was included in this study, but the age assignment by OKAY and ALTINER (2016) has been revised.

The Akkaya Formation overlies the Seyran Formation with a typical disconformity surface, indicating a relatively minor gap in deposition (Fig. 3). It can be subdivided into two parts: 1) debris flow deposits and 2) clayey pelagic limestones. The debris flow deposits at the basal part consist of closely-packed calciturbidites containing clasts and blocks from the Bilecik and Soğukçam limestone groups. An Albian age was assigned by OKAY and ALTINER (2016) to this unit, based on the foraminiferal assemblages found in the matrix of these debris flow deposits. These debris flow deposits may indicate tectonic destabilization in their depositional environment, possibly linked to the initiation of the South Atlantic Ocean opening during the late Barremian (126 Ma) (TORSVIK *et al.*, 2009). Post-rift and drift processes began in the South Atlantic Ocean at the onset of the early Albian (110 Ma), triggering the subsequent southwest-to-northeast clockwise rotational movement of the African Plate (TORSVIK *et al.*, 2009). As a result of these movements, the closure of the Neotethys Ocean (*e.g.*, Intra-Pontide and IAE of Northern Neo-Tethys *sensu* ŞENGÖR and YILMAZ, 1981) began during the late early (Albian) to Late Cretaceous time interval (TORSVIK *et al.*, 2009). The upper part of the Akkaya Formation comprises clayey, pelagic limestones with abundant glauconite and planktonic foraminifers. According to VELDE (2014), glauconite primarily forms from fecal pellets in an environment with low depositional rates, independent of the water depth. The presence of glauconite, the absence of chert interlayers in the clayey limestone, and the rare silica content (with planktonic foraminifers replacing radiolarians) suggest that these limestones were deposited in a shallower pelagic condition with low sedimentation rates (FLÜGEL, 2004).

The planktonic foraminiferal assemblage of this unit suggests a latest Albian age, though a late Albian age cannot be ruled out. Therefore, an Albian age has been roughly assigned to this formation (Fig. 3). Based on this evidence, it can be concluded that the middle to late Aptian time interval corresponds to the sedimentation gap between the deposition of the underlying Seyran Formation and the overlying Akkaya Formation within the Soğukçam Limestone Group. This group is unconformably overlain by the Elmadağ Olistostrome (Fig. 3).

5.3. THE ELMADAĞ OLISTOSTROME

This unit is widely distributed around the Ankara region and was examined in all areas in this study (Fig. 1.B). Due to the unconformable relationship of the Elmadağ Olistostrome with the underlying middle Berriasian to latest Albian Soğukçam Limestone Group and the overlying Santonian Unaz Formation in the Uyuzhamamı section from Haymana region, the depositional age of this olistostrome can be constrained to the Cenomanian to Coniacian interval (Fig. 3). However, due its overlying position on the accretionary prism of the IAE Ocean, with the final deposition age being Turonian (Late Cretaceous, BRAGIN & TEKIN, 1996) in the west of the Memlik region, the depositional age of this olistostrome can also be assigned to the Coniacian (Fig. 3).

The thickness of the Elmadağ Olistostrome varies in different regions (*e.g.*, 165 m in the Uyuzhamamı section, Haymana region, and 12 meters in the Çetinyatak section, west of the Memlik region, Fig. 23). In general, there are two distinct types of blocks and pebbles (pelagic limestones and brecciated platform carbonates) within the mélange. Gray- to beige-colored, micritic pelagic limestone blocks and pebbles are common in the mélange, with sizes ranging from mega-blocks (over 100 meters in size) to small pebbles (OKAY & ALTINER, 2016). The radiolarian ages from pelagic blocks mainly range from the early Callovian (late Middle Jurassic) to late Hauterivian (Early Cretaceous) (BRAGIN & TEKIN, 1999; this study), while the planktonic foraminiferal assemblages reveal the presence of younger blocks, dated to the late Aptian to Coniacian age (OKAY & ALTINER, 2017; SARIASLAN *et al.*, 2020; this study; Fig. 24). This configuration may indicate that pelagic blocks of Callovian to Albian age primarily originated from the Soğukçam Limestone Group. While the first pelagic sediments within the Soğukçam Limestone Group appeared in the middle Berriasian-Hauterivian (Early Cretaceous) in the Haymana region, the first pelagic sedimentation over the Bilecik Limestone Group occurred in the Callovian (late Middle Jurassic) to Oxfordian (early Late Jurassic) interval in the Pontides (ALTINER *et al.*, 1991). The younger blocks, dated as Cenomanian-Coniacian in the olistostrome (*e.g.*, the Turonian-Coniacian Çitrik block), may have synsedimentary origins within the foreland flysch,

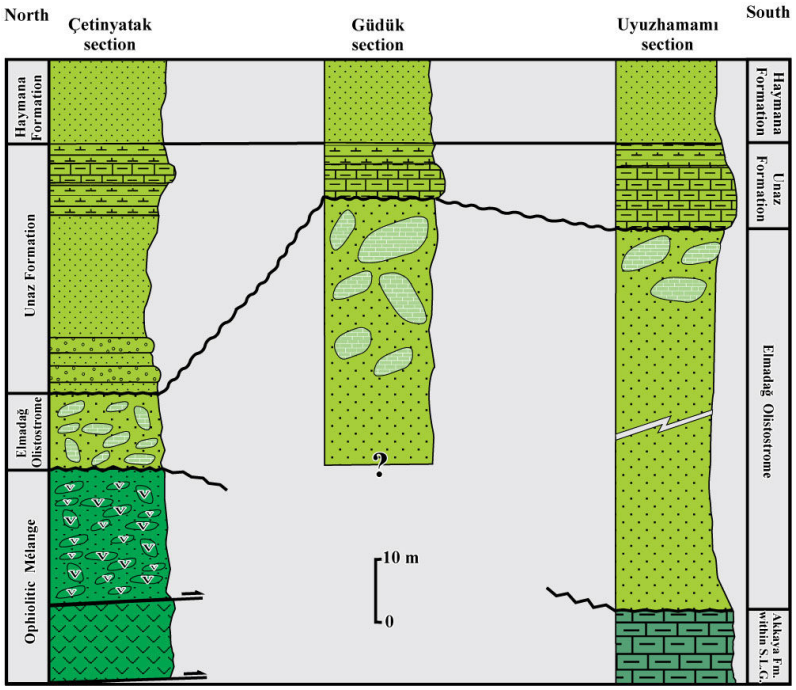

◀ **Figure 23:** Correlation of the Elmadağ Olistostrome, Unaz, and Haymana formations in different stratigraphic sections (the Çetinyatak section in the west of Memlik region, the Güdük section in the north of Alagöz region and the Uyuzhamamı section in the Haymana region) in this study to the west of Ankara region. Abbreviation: Akkaya Fm. within the S.L.G.: The Akkaya Formation within the Soğukçam Limestone Group.

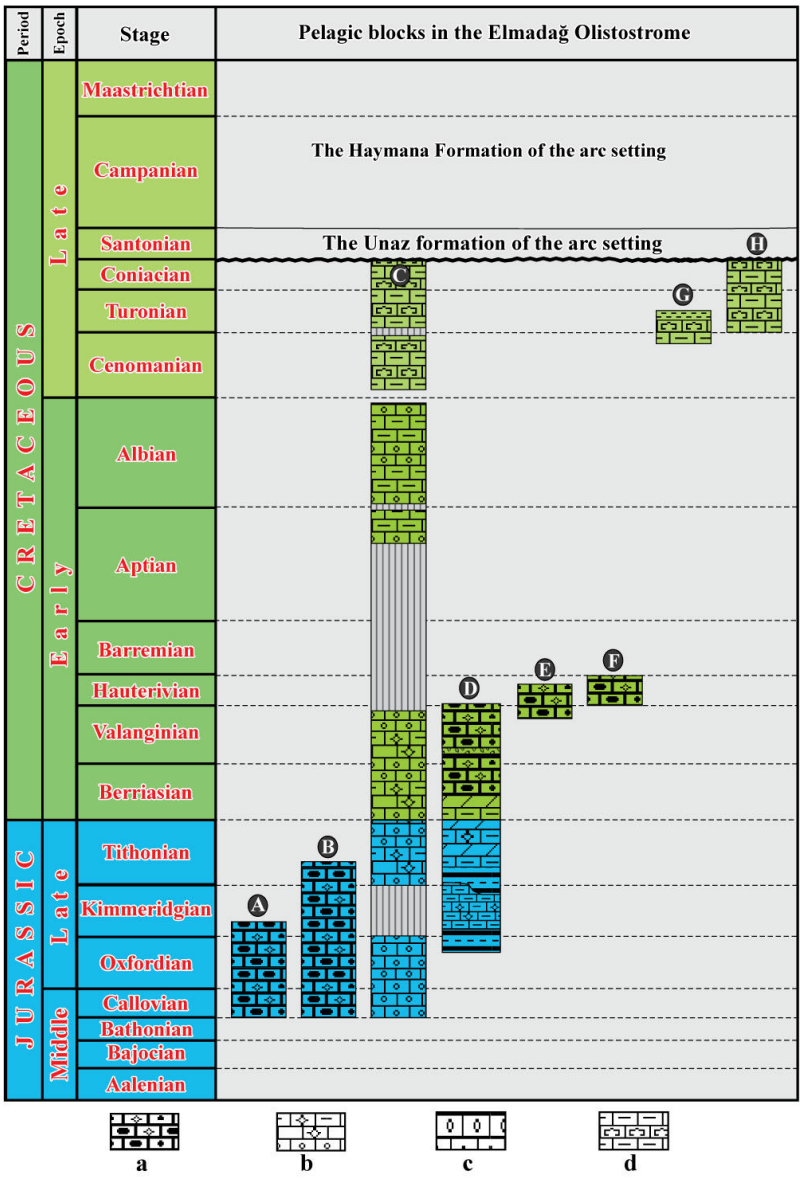

◀ **Figure 24:** Chronostratigraphic distribution of the pelagic blocks in the Elmadağ Olistostrome based on this study and previous studies (Bragin & Tekin, 1999; Okay & Altiner, 2017; Sariaslan *et al.*, 2020); **A.** Radiolarian dating (early Callovian-early Kimmeridgian) on the small block (sample Damla-6) from the Yakacık region in this study; **B.** Radiolarian dating (early Callovian-middle Tithonian) on the Acısu block (samples Acı-3 and Acı-4) from the Yakacık region in this study; **C.** Composite planktonic foraminiferal datings (partial ages from Callovian to Coniacian) from the different blocks around the Ankara region by Okay and Altiner (2017), **D.** Radiolarian ages from the middle Oxfordian to late Valanginian mega-block from the Elmadağ Olistostrome (Alacaatlı, Ankara city center) by Bragin and Tekin (1999); **E.** Radiolarian dating (late Late Valanginian- early Late Hauterivian) on sample Güd-2 from the base of the Güdük section, north of Alagöz region in this study; **F.** Radiolarian dating (Hauterivian) on the small block (sample Damla-1) in the Yakacık region in this study; **G.** Planktonic foraminiferal dating (latest Cenomanian-middle Turonian) in the north of Alagöz region by Sariaslan *et al.* (2020); **H.** Planktonic foraminiferal dating (Turonian to Coniacian) from the Çitrik section (sample Çit-2) in the Haymana region in this study. Key: **a.** Radiolarian bearing cherty limestone, **b.** Alternating calciturbidite and radiolarian bearing clayey limestone, **c.** Calciturbidite, **d.** Planktonic foraminifer bearing clayey limestone.

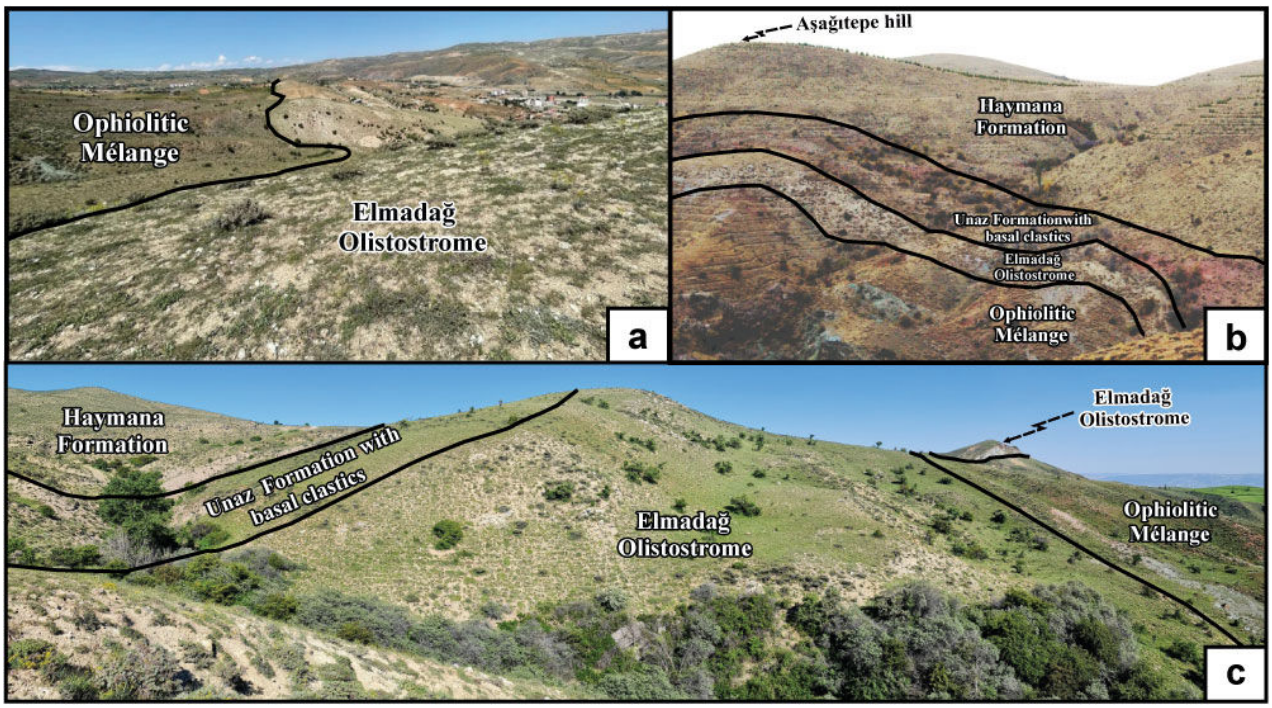

Figure 25: Field photographs showing the contact relations of the Elmadağ Olistostrome with the underlying and overlying units: a. View from the Çaltepe (in the west of Yakacık region) towards NE, showing the relation between the ophiolitic mélange and the overlying Elmadağ Olistostrome (see Fig. 10), b. View from the south of Yapılıyol hill in the east of west of Memlik region to NW direction showing the contact relations between the ophiolitic mélange, Elmadağ Olistostrome, Unaz, and Haymana formations (see Fig. 13), c. View from northwest of the west of the Memlik region to the east, showing the contact relations between the ophiolitic mélange, Elmadağ Olistostrome, Unaz, and Haymana formations (see Fig. 13).

formed in front of the advancing nappes moving from north to south. Considering the three different regions, the Elmadağ Olistostrome unconformably overlies the Soğukçam Limestone Group in the Haymana region, while in both the Yakacık and west of Memlik regions, it has an unconformable relation with the underlying ophiolitic mélange of the accretionary prism of the Neotethys IAE Ocean (Fig. 23). These observations significantly contrast with the previous interpretations (*e.g.*, BATMAN *et al.*, 1978; OKAY & ALTINER, 2016). BATMAN *et al.* (1978) suggested that the Akkayatepe Mélange, a local equivalent of the Elmadağ Olistostrome, formed as a result of tectonic activity in the Başağaçtepe Limestones (locally equivalent of the Soğukçam Limestone Group). They linked the formation of this blocky material to gravitational movements within a tectonically active environment (BATMAN *et al.*, 1978). In contrast, according to KOÇYIĞIT (1991), the general tectono-stratigraphic column for the Ankara region indicated that the sedimentary mélange (the Damlaağaçderesi Formation *sensu* KOÇYIĞIT, 1991), equivalent of Elmadağ Olistostrome, unconformably overlies older carbonate sequences (Bilecik and Soğukçam limestone groups) and is tectonically overlain by the ophiolitic mélange (*i.e.*, Anatolian Complex *sensu* KOÇYIĞIT, 1991). The unconformable lower contact of the sedimentary mélange (Elmadağ Olistostrome) with the older units was also observed in this study in the Haymana region, but the nature of the upper contact between the Elmadağ Olistostrome and the ophiolitic mélange remains uncertain. KOÇYIĞIT's (1991) observations on the upper contact were based on a slightly overturned contact in the Alcı region (southwest of Ankara, Fig. 1.B). He proposed that the sedimentary mélange formed in an extensional regime, where the limestone blocks slid into the matrix. Meanwhile, OKAY and ALTINER (2017) attributed the formation of the olistostrome to uplift in a fore-arc basin situated above the accretionary complex, positioned over the subducting aseismic ridge. All these three interpretations suggest that the Elmadağ olistostromal unit formed via gravitational movements within a basin. However, considering its position over older units (*i.e.*, over the Soğukçam Limestone Group of the Sakarya Continent Cover sediments and the Ankara Ophiolitic Mélange of the Neotethys IAE Ocean; Fig. 25) as well as its morphological characteristics, we propose an external origin for the olistostrome. Specifically, it is likely to have formed in a trench-like basin in front of the southward-advancing nappes derived from the Neotethys Intra-Pontide Ocean (Fig. 1.A). According to ŞENGÖR and YILMAZ (1981) and ŞENGÖR *et al.* (1984), this branch of Neo-Tethys opened in the Early Jurassic to the north of the Sakarya Continent. However, recent research on the Intra-Pontide Suture Zone in northern Türkiye suggests that deposition within this basin may date back to the Permian. Evidence includes findings from the Ezine Zone in the Biga peninsula (BECCALETTO, 2004; BECCALETTO & JENNY, 2004), the Çetmi Mélange in the Biga peninsula (BECCALETTO, 2004;

BECCALETTO *et al.*, 2005), the Arkotdağ Mélange in the NE Bolu City (GÖNCÜOĞLU *et al.*, 2008), the Arkotdağ Mélange in the Bayramören-Araç-Akpınar area, west of Kastamonu (TEKIN *et al.*, 2012b; GÖNCÜOĞLU *et al.*, 2014), the sedimentary cover of the Aylıdağ ophiolitic sequence in the Araç area, west of Kastamonu city (GÖNCÜOĞLU *et al.*, 2012; Fig. 26).

Pelagic limestones interspersed with debris flow deposits from the upper Olenekian to middle Carnian within the Çamköy Formation in the Ezine Zone, and red nodular limestones of the upper Olenekian to Ladinian within the Çetmi Mélange in the Biga peninsula, were documented by BECCALETTO (2004), BECCALETTO and JENNY (2004), and BECCALETTO *et al.* (2005; Fig. 26). Additionally, the deposition of alternating radiolarian chert and mudstone occurred from the late Bajocian (Middle Jurassic) to Aptian (Early Cretaceous), as reported by BECCALETTO (2004) and BECCALETTO *et al.* (2005; Fig. 26). Comparable interbedded radiolarian chert and mudstone sequences, ranging from the late Anisian (Middle Triassic) to the early Turonian (Late Cretaceous), were documented within the Arkotdağ Mélange in the Intra-Pontide Suture Zone of northern Türkiye by TEKIN *et al.* (2012b) and GÖNCÜOĞLU *et al.* (2008, 2014; Fig. 26). Evidence pointing to a possible northernly origin of the olistostrome includes our preliminary studies around the Ankara region. These studies demonstrate that the Sakarya Continent sediments are tectonically overlain by Middle Jurassic cherts, which are attributed to Intra-Pontide origins.

5.4. THE UNAZ FORMATION

The Kocatepe Formation, initially introduced by YÜKSEL (1970) has been referenced in numerous subsequent studies (*e.g.*, OKAY & ALTINER, 2016; SARIASLAN *et al.*, 2020, *etc.*). However, our recent field observations indicate that the formation requires revision. These observations reveal that the Kocatepe Formation was incorrectly mapped as the Haymana Formation in several areas, such as the Kocatepe hill southeast of Haymana town and regions around the Haymana anticline (Figs. 2, 6.e-f). When compared to the Pontides region, the Upper Cretaceous pelagic limestones observed in the Ankara region show a strong correlation with the "Unaz Formation" as described by TÜYSÜZ *et al.* (1997, 2012).

The Unaz Formation was examined in this study across three key sections: the Uyuzhamamı section in the Haymana region, the Güdük section, north of the Alagöz region, and the Çetinyatak section, west of the Memlik region (Fig. 23). In the Uyuzhamamı and Güdük sections, the Unaz Formation unconformably overlies the Elmadağ Olistostrome, with a sharp and distinct contact between the two formations. It is predominantly composed of gray- to beige-colored, thin-bedded, clayey limestone transitioning into red- to purple-colored, thin-bedded, clayey limestones rich in planktonic foraminifers. Additionally, in the Güdük section, the upper portion of the formation includes pale violet- to purple-colored, very fine-grained, thin-bedded marl (Figs. 8, 23). The lithological composition of the Unaz Formation in the Çetinyatak section (west of Memlik region) shows some differences compared to the other two sections. Here, it predominantly consists of red- to purple-colored, thin-bedded clayey limestones, which are underlain by clastic deposits including conglomerates, sandstones, and siltstones (Fig. 23). The type locality of the Unaz Formation is located in the western Black Sea region, north of the study area (TÜYSÜZ *et al.*, 2012). In this area, pink- to red-colored, thin-bedded clayey limestones of the Unaz Formation overlie the Dereköy Formation in a suddenly subsided basin (TÜYSÜZ *et al.*, 2012). This is followed by the deposition of more voluminous volcanic materials, including andesite, basalt, agglomerate, tuff, and volcaniclastics, of the Campanian Cambu Formation, representing the second volcanic phase (TÜYSÜZ *et al.*, 2012). In the Ankara region, due to subsidence in the arc basin during the Santonian stage, the Elmadağ Olistostrome was covered by the pelagic limestones of the Unaz Formation, forming a very sharp contact. Basal clastics are only present in the northern part of the region, specifically in the area west of Memlik, at the base of the Unaz Formation. The overlying volcaniclastics, which belong to the Campanian-Maastrichtian Haymana Formation in the Ankara region, correlate with the second volcanic phase represented by the Cambu Formation in the northwestern Black Sea region.

The thickness of the upper carbonate portion of the Unaz Formation varies across different localities: it measures 14.5 meters along the Uyuzhamamı section in the Haymana region, 10.25 meters in the Güdük section, north of the Alagöz region, and 12.5 meters along the Çetinyatak section, west of Memlik (Fig. 23). With basal clastics, the total thickness of the Unaz Formation at the Çetinyatak section (west of Memlik region) is approximately 40.5 meters (Fig. 14). The age of the Unaz Formation is primarily Santonian, correlating to the *Dicarinella asymetrica* Zone. However, the co-occurrence of *Globotruncana hilli* and *Dicarinella asymetrica* near the base of this formation in the Uyuzhamamı section (the Haymana region) suggests a late Santonian age, though the possibility of an early Santonian age cannot be ruled out, based on other sections. Overall, the age of the Unaz Formation does not correspond to the Coniacian as reported by YÜKSEL (1970), nor does it align with the Turonian to early Campanian range by OKAY and ALTINER (2016). Therefore, these previous age assignments require revision. The age determined in this study, however, is consistent with the findings of TÜYSÜZ *et al.* (2012), whose results from the western Black Sea region, to the north of the study area.

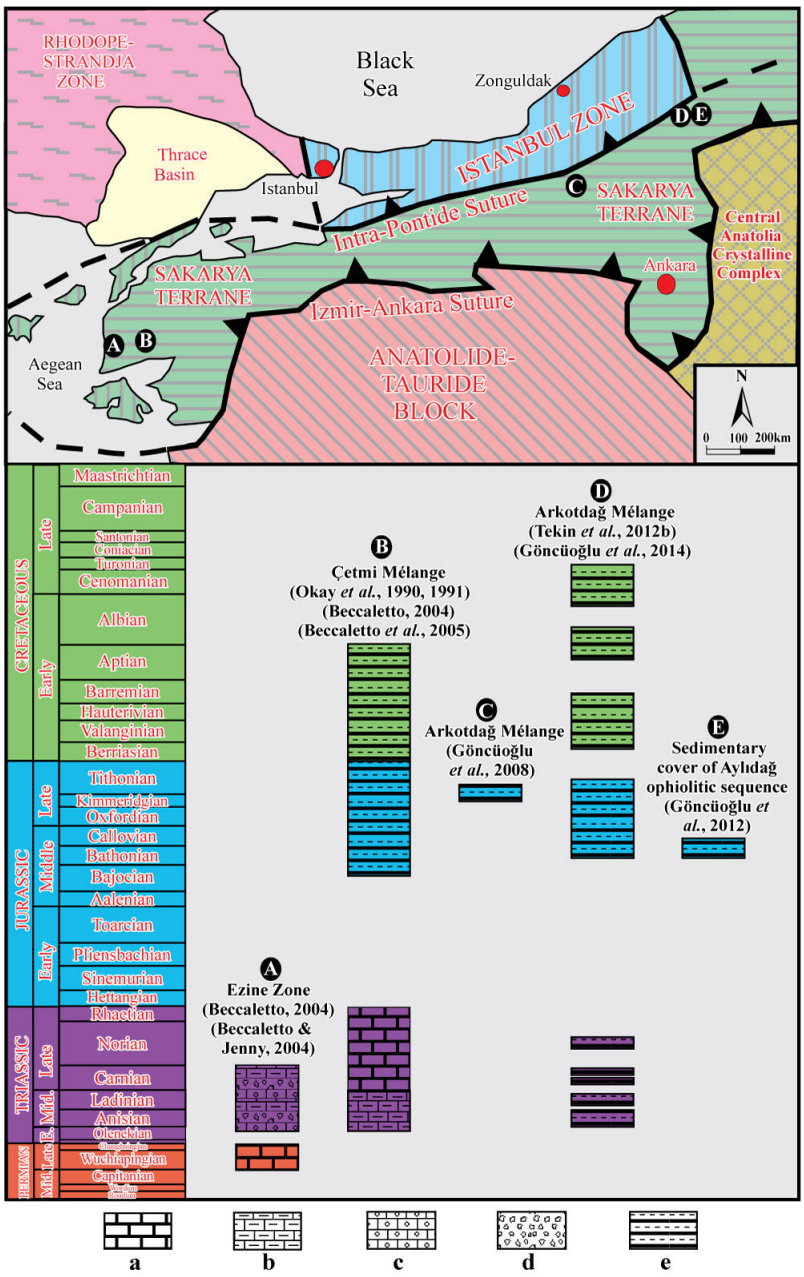

◀ **Figure 26:** Distribution of blocks/tectonic slices in the Intra-Pontide Suture Zone presented in the previous studies (location map from OKAY & TÜYSÜZ, 1999); A. The Ezine Zone in the Biga peninsula from BECCALETTO (2004) and BECCALETTO and JENNY (2004), B. The Çetmi Mélange in the Biga peninsula from OKAY *et al.* (1990, 1991), BECCALETTO (2004) and BECCALETTO *et al.* (2005) C. The Arkotdağ Mélange in the NE Bolu city from GÖNCÜOĞLU *et al.* (2008), D. The Arkotdağ Mélange in the Bayramören-Araç-Akpınar area, west of Kastamonu city from TEKIN *et al.* (2012b) and GÖNCÜOĞLU *et al.* (2014), E. Sedimentary cover of the Aylıdağ ophiolitic sequence in the Araç area, west of Kastamonu city from GÖNCÜOĞLU *et al.* (2012). Key: a. Platform limestone, b. Pelagic limestone, c. Calciturbidite, d. Debris flow deposit, e. Alternating radiolarian chert and mudstone.

5.5. GEODYNAMIC REMARKS

In the northern Tethys realm during the Late Cretaceous subduction-related activity and basin development were widespread, as seen in the Ulus Basin, Sinop Basin, and Haymana Basin (*e.g.*, KOÇYIĞIT, 1991; TÜYSÜZ, 2018). During this period, the Sakarya Terrane was positioned above the northwardly subducting IAE oceanic lithosphere, acting as an active margin. KOÇYIĞIT (1991) proposed that this subduction system, which hosted the Haymana fore-arc basin, continued until the middle Eocene. However, based on new and existing evidence, we propose a revised geodynamic scenario for the Cretaceous evolution of the Sakarya Terrane, suggesting that the subduction system may not have persisted as long as previously suggested (Fig. 27).

During the Albian time, the Sakarya Terrane was still covered by the last deposits of the Soğukçam Limestone Group, while the northern branches of the Neotethys Ocean (IAE and Intra-Pontide oceans) were undergoing contraction, driven by the opening of the South Atlantic Ocean (Fig. 27). For the IAE Ocean, contraction is evidenced by the formation of intra-oceanic subduction zones and associated accretionary prisms. A key piece of evidence for this is the presence of oceanic arc relics, such as the Albian-Cenomanian Kösdağ Unit, which has zircon U-Pb ages ranging from 112 to 95 Ma (AYGÜL *et al.*, 2015; BERBER *et al.*, 2021). In the Albian, the Intra-Pontide Ocean was also undergoing a contraction, with the accretion of oceanic materials to the northern margin of the Sakarya Terrane (*e.g.*, MARRONI *et al.*, 2020).

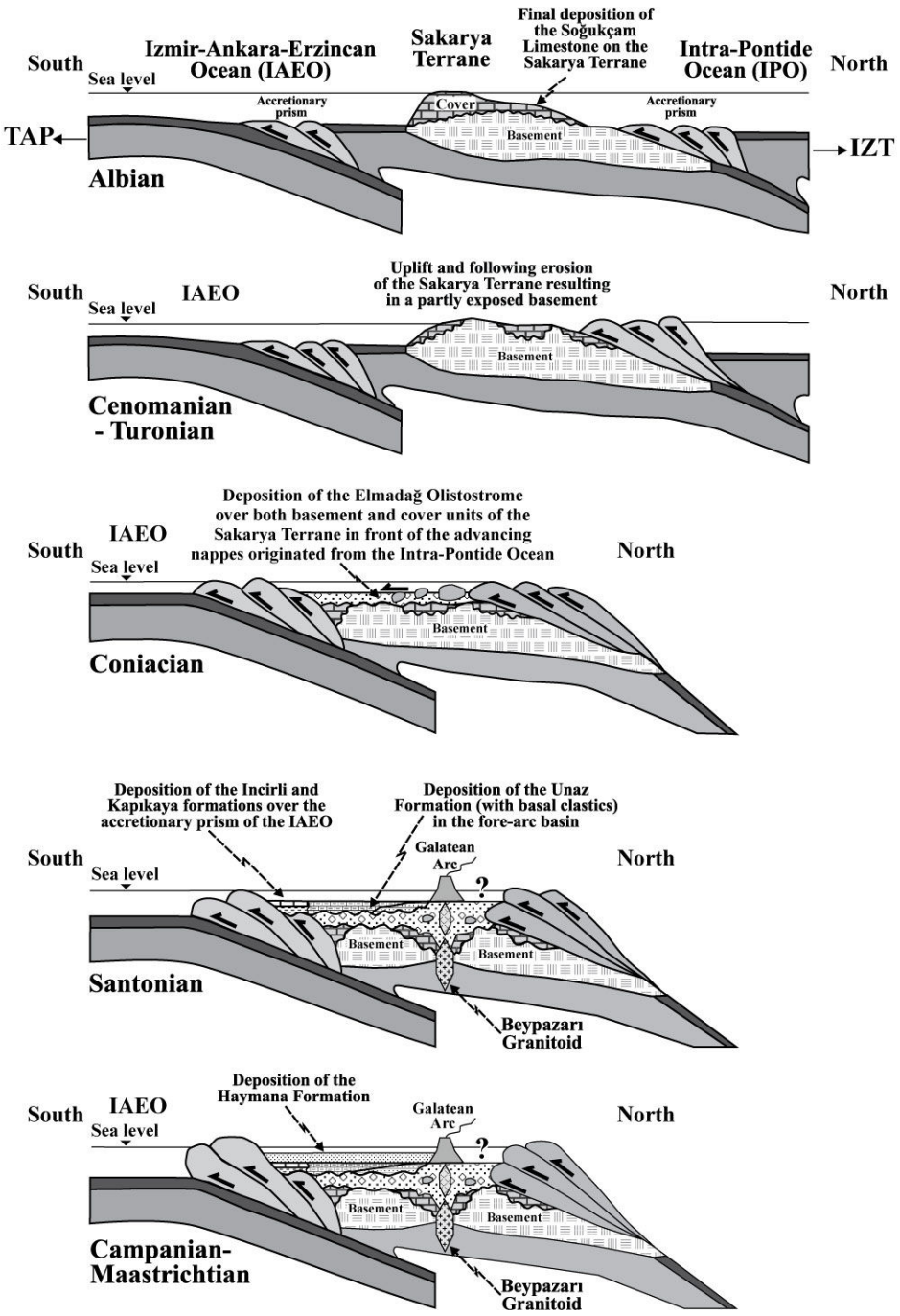

◀ **Figure 27:** Geodynamic evolution of the Ankara region and surroundings during the Albian- Maastrichtian (Cretaceous) time interval. Abbreviations; TAP: Tauride-Anatolide Platform, IZT: Istanbul-Zonguldak Terrane.

The intra-oceanic subduction continued in the IAE Ocean during the Cenomanian to Turonian, evidenced by the Kösdağ and Kartal arcs, with the Kartal Arc yielding Cenomanian plagioclase Ar-Ar ages (99 Ma, BEYAZPIRINÇ *et al.*, 2019). The continued contraction led to the intra-oceanic decoupling and subduction, which is reflected in the formation of subophiolitic metamorphic soles, with Cenomanian-Conician Ar-Ar ages (101-93 Ma, HARRIS *et al.*, 1994; ÖNEN, 2003). In contrast, the lifetime of the Intra-Pontide Ocean nearly came to an end towards the end of the Turonian (*e.g.*, TÜYSÜZ, 2018; MARRONI *et al.*, 2020; Fig. 27). For the Sakarya Terrane, the Cenomanian-Turonian interval was marked by non-deposition, uplift, and significant erosion, which exposed parts of the basement (Fig. 27). In the Coniacian, the Soğukçam Limestone Group and the ophiolitic mélange were unconformably overlain by the Elmadağ Olistostrome, which was deposited in front of the advancing nappes originating from the north of the Sakarya Terrane, *i.e.*, from the Intra-Pontide realm (Fig. 27). The deposition of the olistostrome can be envisioned as occurring through the mobilization of continental margin units, followed by the infill of sediments in trench-like basins, as explained by GAWLICK *et al.* (1999) and MISSONI and GAWLICK (2011). The Elmadağ Olistostrome likely began to develop after the closure of the Intra-Pontide Ocean.

The Santonian stage was characterized by the deposition of the Unaz Formation over the Elma-

dağ Olistostrome (Fig. 27). In the central and western Pontides, these units are interpreted to have formed in an extensional environment related to continental back-arc rifting, which ultimately led to the opening of the Black Sea Basin (TÜYSÜZ *et al.*, 2012; TÜYSÜZ, 2018; KESKIN & TÜYSÜZ, 2018). For the Ankara region, we propose a similar extensional system for the deposition of the Unaz and Haymana formations. However, this event appears to be unrelated to rifting; it occurred within a continental arc setting known as the Galatean Arc (KOÇYIĞIT, 1991; OKAY *et al.*, 2019). While the IAE slab triggered arc magmatism in the Santonian, Black Sea rifting, initiated by the Intra-Pontide slab, had already progressed in the north. During the deposition of the Unaz Formation in the Santonian, the Incirli Formation (composed of graded-bedded fluvial conglomerate at the base and pinkish to yellowish-colored sandstone and marl on top) and the overlying Kapıkaya Formation (made up of reefal limestone) deposited in relatively shallow sea conditions at the southern distal end of this continental arc setting (KOÇYIĞIT & LÜNEL, 1987; KOÇYIĞIT *et al.*, 1988; ROJAY & SÜZEN, 1997; Fig. 27). This arc magmatism in the Sakarya Terrane appears to have been short-lived, possibly taking place in the Campanian, as indicated by the paleontological and radiometric ages obtained from the Saraçköy Volcanics, Beypazarı Granitoid, and the sandstones from the Alcı (local equivalent of the Haymana Formation) and Haymana formations (KOÇYIĞIT *et al.*, 2003; SPECIALE *et al.*, 2012; OKAY *et al.*, 2019, 2020; Fig. 27). In the Central Pontides, the late Santonian-middle Campanian Tafano Unit could be an extension of this continental arc magmatism (ELLERO *et al.*, 2015; SAYIT *et al.*, 2022). After the Santonian, accretion and mélange formation in the IAE Ocean may have continued until the Maastrichtian (*e.g.*, TÜYSÜZ *et al.*, 1995; ROJAY, 2013). However, there seems to be no evidence of subduction or in-situ oceanic crust beyond the Late Cretaceous for this oceanic domain. The youngest age obtained thus far from the chert blocks within the Ankara Ophiolitic Mélange (the IAE Suture Belt) is Turonian (BRAGIN & TEKIN, 1996). The age of blueschist metamorphism, which characterizes the age of subduction, does not exceed the Campanian (78.2 Ma Ar-Ar phengite age; OKAY *et al.*, 2020). The Sarıkaraman Ophiolite, a Central Anatolian Ophiolite obducted onto the TAP platform, is cut by the post-collisional Terlemez Granitoid (a Central Anatolian Granitoid) of late Campanian-early Maastrichtian age (81.5-67.1 Ma hornblende K-Ar amphibole age; YALINIZ *et al.*, 1999). The Central Anatolian ophiolites and granites are unconformably overlain by the latest Maastrichtian-early Paleocene sediments. Therefore, it appears that the IAE Ocean was consumed during the latest Cretaceous, which negates the possibility of active subduction beneath the Sakarya Terrane until the middle Eocene, as suggested by KOÇYIĞIT (1991; Fig. 27).

Acknowledgements

Dr. Yavuz BEDI (General Directorate of Mineral Research and Exploration, Ankara, Türkiye) and Umutcan ERYILMAZ (Hacettepe University, Ankara, Türkiye) are gratefully acknowledged for their help during field investigations. We also express our gratitude to Dr. Melikan AKBAŞ (Konya Technical University, Konya, Türkiye) for his technical support. Our sincere thanks go to the reviewers, Špela GORIČAN (Research Center of the Slovenian Academy of Sciences and Arts, Ljubljana, Slovenia), Francesca FALZONI (Consiglio Nazionale delle Ricerche, Milano, Italy), and two anonymous reviewers for their valuable remarks and comments during the editing of this study.

Bibliographic references

AKYOL Z., ARPAT E., ERDOĞAN B., GÖĞER E., GÜNER Y., ŞAROĞLU F., ŞENTÜRK I., TÜTÜNCÜ K. & UYSAL S. (1974).- 1/50.000 scale geologic map of Türkiye, quadrangle series, Zonguldak E29a, E29b, E29c, E29d, Kastamonu E30a, E30d.- Mineral Research and Exploration Institute of Turkey (MTA), Ankara [in Turkish].

ALKAYA F. & MEISTER C. (1995).- Liassic Ammonites from the central and eastern Pontides (Ankara and Kelkit areas), Turkey.- *Revue de Paléobiologie*, Genève, vol. 13, no. 1, p. 123-195.

ALTINER D., KOÇYIĞIT A., FARINACCI A., NICOSIA U. & CONTI M.A. (1991).- Jurassic-Lower Cretaceous stratigraphy and paleogeographic evolution of the southern part of north-western Anatolia (Turkey). *In*: FARINACCI A., AGER D.V. & NICOSIA U. (eds.), Geology and Paleontology of Western Pontides.- *Geologica Romana*, vol. XXVII, p. 13-80.

ALTINLI I.E. (1965).- Yenişehir havzasının jeolojik ve hidrojeolojik incelenmesi.- *İstanbul Üniversitesi Fen Fakültesi Mecmuasi*, B, vol. 30, no. 1-2, s. 31-51 [in Turkish].

ALTINLI I.E. (1975a).- Orta Sakarya Jeolojisi. *In*: Proceedings of the 50th Anniversary of the Turkish Republic Earth Science Congress.- Mineral Research and Exploration Institute of Turkey (MTA), Ankara, p. 159-191 [in Turkish].

ALTINLI I.E. (1975b).- Bilecik Jurasiği. *In*: Proceedings of the 50th Anniversary of the Turkish Republic Earth Science Congress.- Mineral Research and Exploration Institute of Turkey (MTA), Ankara, p. 103-111 [in Turkish].

ALTINLI I.E., GÜRPINAR O. & ERSEN S. (1970).- Erenköy-Deresakarı (Bilecik Ili) alanının jeolojisi.- *İstanbul Üniversitesi Fen Fakültesi Mecmuası* (Serie B), vol. 35, no. 1-2, p. 77-83 [in Turkish].

AYGÜL M., OKAY A.I., OBERHANSLI R., SCHMIDT A. & SUDO M. (2015).- Late Cretaceous infant intra-oceanic arc volcanism, the central Pontides, Turkey: Petrogenetic and tectonic implications.- *Journal of Asian Earth Sciences*, vol. 111, p. 312-327.

BAILEY E.B. & MCCALLIEN W.J. (1950).- The Ankara Mélange and the Anatolian Thrust.- *Bulletin of the Mineral Research and Exploration*, Ankara, vol. 40, p. 17-22.

BATMAN B. (1978).- Geological evolution of the northern part of Haymana Region and study of mélange in the area I. Stratigraphic units.- *Yerbilimleri*, Ankara, vol. 4, no. 1-2, p. 95-124 [in Turkish with English abstract].

BATMAN B., KULAKSIZ S. & GÖRMÜŞ S. (1978).- A study related to deformation properties of lithostratigraphic sequence of Jurassic-Cretaceous age in the Alacaatli region (SW Ankara).- *Yerbilimleri*, Ankara, vol. 4, no. 1-2, p. 135-153 [in Turkish with English abstract].

BAUMGARTNER P.O. (1980).- Late Jurassic Hagiastridae and Patulibracchiidae (Radiolaria) from the Argolis Peninsula (Peloponnesus, Greece).- *Micropaleontology*, Flushing - NY, vol. 26, no. 3, p. 274-322.

BAUMGARTNER P.O., O'DOGHERTY L., GORIČAN S., DUMITRICA-JUD R., DUMITRICA P., PILLEVUIT A., URQUHART E., MATSUOKA A., DANELIAN T., BARTOLINI A., CARTER E.S., DE WEVER P., KITO N., MARCUCCI M. & STEIGER T. (1995).- Radiolarian catalogue and systematics of Middle Jurassic to Early Cretaceous Tethyan genera and species. *In*: BAUMGARTNER P.O., GORICAN S., URQUHART E., PILLEVUIT A. & DE WEVER P. (eds.), Middle Jurassic to Lower Cretaceous Radiolaria of Tethys: Occurrences, systematics, biochronology.- *Mémoires de Géologie*, Lausanne, vol. 23, p. 37-685.

BELLIER J.-P. & MOULLADE M. (2002).- Lower Cretaceous planktic foraminiferal biostratigraphy of the western North Atlantic (ODP Leg 171B), and taxonomic clarification of some key index species.- *Revue de Micropaléontologie*, Paris, vol. 45, p. 9-26.

BECCALETTO L. (2004).- Geology, correlations, and geodynamic evolution of the Biga Peninsula (NW Turkey).- *Mémoires de Géologie*, Lausanne, vol. 43, 146 p.

BECCALETTO L. & JENNY M. (2004).- Geology and correlation of the Ezine Zone: A Rhodope Fragment in NW Turkey?- *Turkish Journal of Earth Sciences*, Ankara, vol. 13, p. 145-176.

BECCALETTO L., BARTOLINI A.C., MARTINI R., HOCHULI P.A. & KOZUR H. (2005).- Biostratigraphic data from the Cetmi Mélange, northwest Turkey: Palaeogeographic and tectonic implications.- *Palæogeography*, *Palæoclimatology*, *Palæoecology*, vol. 221, p. 215-244.

BECCARO P. (2006).- Radiolarian biostratigraphy of Middle-Upper Jurassic pelagic successions of western Sicily and the southern Alps (Italy).- *Mémoires de Géologie*, Lausanne, Special Publication 45, p. 1-114

BERBER F., SAYIT K. & GÖNCÜOĞLU M.C. (2021).- Geochemistry and U-Pb ages from the Kösdağ Metavolcanics in the southern central Pontides (Turkey): Complementary data for early Late Cretaceous island arc development in the Northern Neotethys.- *Turkish Journal of Earth Sciences*, Ankara, vol. 30, p. 59-80.

BEYAZPIRINÇ M., AKÇAY A.E., YILMAZ A. & SÖNMEZ M.K. (2019).- A Late Cretaceous ensimatic arc developed during closure of the northern branch of Neo-Tethys (central-northern Turkey).- *Geoscience Frontiers*, vol. 10, p. 1015-1028.

BILGIN A.Z. (2014).- 1:100 000 scale Turkish Geological Maps, Ankara-I28 Quadrangle.- Mineral Research and Exploration Institute of Turkey (MTA), Ankara, vol. 208, 40 p. [in Turkish].

BINGÖL E., AKYÜREK B. & KORKMAZER B. (1975).- Biga Yarımadasi'nın jeolojisi ve Karakaya Formasyonu'nun bazı özellikleri. *In*: Proceedings of the 50th Anniversary of the Turkish Republic Earth Science Congress.- Mineral Research and Exploration Institute of Turkey (MTA), Ankara, p. 70-77 [in Turkish].

BOCCALETTI M., BORTOLOTTI V. & SAGRI M. (1966).- Ricerche sulle ofioliti delle Catene Alpine. I Osservazioni sull'Ankara Mélange nella zona di Ankara.- *Bollettino della Società Geologica Italiana*, Roma, vol. 85, p. 485-508.

BORTOLOTTI V., CHIARI M., GÖNCÜOĞLU M.C., MARCUCCI M., PRINCIPI G., TEKIN U.K. SACCANI E. & TASSINARI R. (2013).- Age and geochemistry of basalt-chert associations in the ophiolites of the Izmir-Ankara Mélange east of Ankara, Turkey: Preliminary data.- *Ofioliti*, Pisa, vol. 38, no. 2, p. 157-173.

BORTOLOTTI V., CHIARI M., GÖNCÜOĞLU M.C., PRINCIPI G., SACCANI E., TEKIN U.K. & TASSINARI R. (2018).- The Jurassic-Early Cretaceous basalt-chert association in the ophiolites of the Ankara Mélange east of Ankara, Turkey: Age and geochemistry.- *Geological Magazine*, Cambridge (UK), vol. 155, no. 2, p. 451-478.

BOZKURT E., HOLDSWORTH B.K. & KOÇYIĞIT A. (1997).- Implications of Jurassic chert identified in the Tokat Complex, northern Turkey.- *Geological Magazine*, Cambridge (UK), vol. 134, p. 91-97.

BRAGIN N.Yu. & TEKIN U.K. (1996).- Age of radiolarian-chert blocks from the Senonian Ophiolitic Mélange (Ankara, Turkey).- *Island Arc*, vol. 5, p. 114-122.

BRAGIN N.Yu. & TEKIN U.K. (1999).- Stratigraphy and the Upper Jurassic-Lower Cretaceous radiolarians from the carbonate-siliceous deposits, Ankara Region (Turkey).- *Stratigraphy and Geological Correlation*, vol. 7, no. 2, p. 130-140.

CHAPUT E. (1931).- Notice explicative de la carte géologique à 1/135.000 de la région d'Angora (Ankara).- *Istanbul Darülfünunu Geologie Enstitüsü Neşriyatı*, vol. 7.

CHAPUT E. (1936).- Voyages d'études géologiques et géomorphogéniques en Turquie.- *Mémoires de l'Institut Français d'Archéologie de Stamboul*, Paris, II, 312 p.

COCCIONI R. & PREMOLI SILVA I. (2015).- Revised Upper Albian-Maastrichtian planktonic foraminiferal biostratigraphy and magnetostratigraphy of the classical Tethyan Gubbio section

(Italy).- *Newsletters on Stratigraphy*, vol. 48, no. 1, p. 47-90.

CUI X., LUO H., AITCHISON J.C., LI X. & FANG P. (2021).- Early Cretaceous radiolarians and chert geochemistry from western Yarlung Tsangpo Suture Zone in Jiangyema section, Purang county, SW Tibet.- *Cretaceous Research*, vol. 125, p. 1-16.

ÇAPAN U.Z. (1981).- Ankara Melanjı hakkında görüşler ve melanjın Gökdere-Aktepe yöresindeki özelliklerine ait gözlemler. *In*: OYGÜR V., SOYSAL Y. & TERLEMEZ I. (eds.), Proceedings of the Symposium on Geology of the Central Anatolia.- Geological Society of Turkey 35th Annual Meeting, Ankara, p. 27-31 [in Turkish with English abstract].

ÇAPAN U.Z. & BUKET E. (1975).- Geology of the Aktepe-Gökdere region and the ophiolitic mélange.- *Bulletin of the Geological Society of Turkey*, Ankara, vol. 18, p. 11-16 [in Turkish with English abstract]. URL: https://www.jmo.org.tr/resimler/ekler/981f2b708044d6f_ek.pdf

ÇAPAN U.Z., LAUER J.P. & WHITECHURCH H. (1983).- The Ankara Mélange (central Anatolia): An important element for the reconstruction of Tethyan closure.- *Yerbilimleri*, Ankara, vol. 10, p. 35-43 [in Turkish with English abstract].

DANGERFIELD A., HARRIS R., SARIFAKIOĞLU E. & DILEK Y. (2011).- Tectonic evolution of the Ankara Mélange and associated Eldivan Ophiolite near Hancılı, central Turkey. *In*: WAKABAYASHI J. & DILEK Y. (eds.), Mélanges: Processes of formation and societal significance.- *Geological Society of America Special Paper*, Boulder - CO, vol. 480, p. 143-169.

DELI A. & ORHAN H. (2007).- Stratigraphy of Jurassic-Cretaceous aged deposits outcropping around Alacaatlı-Beytepe village (southwest Ankara).- *Selcuk University Journal of Engineering Science and Technology*, vol. 22, p. 60-78 [in Turkish with English abstract].

DELIKAN A. & ORHAN H. (2020).- Sedimentology of Jurassic pelagic carbonate platforms in the Ankara region (central Anatolia-Turkey).- *Facies*, Erlangen, vol. 66, no. 3, p. 1-21.

DE WEVER P., DUMITRICA P., CAULET J.P., NIGRINI C. & CARIDROIT M. (2001).- Radiolarians in the sedimentary record.- Gordon and Breach Science Publications, London, 524 p.

DUMITRICA P. (1970).- Cryptocephalic and Cryptothoracic Nasseleria in some Mesozoic deposits of Romania.- *Revue Roumaine de Géologie, Géophysique et Géographie* (Série Géologie), Bucarest, vol. 14, no. 1 p. 45-124.

DUMITRICA P. (1989).- Internal skeletal structures of the Superfamily Pyloniacea (Radiolaria), a basis of a new systematic.- *Revista Española de Micropaleontologia*, Madrid, vol. 21, no. 2, p. 207-264.

DUMITRICA P. & MELLO J. (1982).- On the age of the Meliata Group and Silica Nappe radiolarites (Localities Drzhovce and Buhonova, Slovak Karst, CSSR).- *Geologicke Prace*, vol. 77, p. 17-28.

DUMITRICA P. & DUMITRICA-JUD R. (1995).- *Aurisaturnalis carinatus* (FOREMAN), an example of phyletic gradualism among saturnalid-type radiolarians.- *Revue de Micropaléontologie*, Paris, vol. 38, no. 3, p. 195-216.

DUMITRICA P., IMMENHAUSER A. & DUMITRICA-JUD R. (1997).- Mesozoic radiolarian biostratigraphy from Masirah ophiolite, Sultanate of Oman, Part 1. Middle Triassic, Uppermost Jurassic and Lower Cretaceous spumellarians and multisegmented nassellarians.- *Bulletin of the National Museum of Natural Sciences*, Taipei, vol. 9, 106 p.

DUMITRICA P., TEKIN U.K. & BEDI Y. (2013).- Taxonomic study of spongy spumellarian Radiolaria with three and four coplanar spines or arms from the middle Carnian (Late Triassic) of the Köseyahya nappe (Elbistan, SE Turkey) and other Triassic localities.- *Paläontologische Zeitschrift*, vol. 87, no. 3, p. 345-395.

DURU M. & AKSAY A. (2002).- 1:100000 scale Turkish Geological Maps, Bolu-H29 Quadrangle.- Mineral Research and Exploration Institute of Turkey (MTA), Ankara, 42, 25 p. [in Turkish].

EHRENBERG C.G. (1838).- Über die Bildung der Kreidefelsen und des Kreidemergels durch unsichtbare Organismen.- *Abhandlungen der Königlichen Akademie der Wissenschaften zu Berlin* (Physikalische Klasse), Jahre 1838, p. 59-147.

EHRENBERG C.G. (1847).- Über die mikroskopischen kieselschaligen Polycystinen als mächtige Gebirgsmasse von Barbados und über das Verhältniss der aus mehr als 300 neuen Arten bestehenden ganz eigentümlichen Formengruppe jener Felsmasse zu den jetz lebenden Thieren und zur Kreidebildung. Eine neue Anregung zur Erforschung des Erdlebens.- *Bericht der Konigliche Preussischen Akademie der Wissenschaften zu Berlin*, p. 40-60. URL: https://www.biodiversitylibrary.org/page/11226274

EHRENBERG C.G. (1875).- Fortsetzung der mikrogeologischen Studien als Gesammt-Übersicht der mikroskopischen Paläontologie gleichartig analysirter Gebirgsarten der Erde, mit specieller Rücksicht auf den Polycystinen-Mergel von Barbados.- *Königliche Preussichen Akademie der Wissenschaften zu Berlin, Abhandlungen*, Jahre 1875, p. 1-226.

ELLERO A., OTRRIA G., SAYIT K., CATANZARITI R., FRASSI C., GÖNCÜOĞLU M.C., MARRONI M. & PANDOLFI L. (2015).- Geological and geochemical evidence for a Late Cretaceous continental arc in the central Pontides, northern Turkey.- *Ofioliti*, Pisa, vol. 40, no. 2, p.73-90.

ELLIS G. (1993).- Late Aptian-Early Albian Radiolaria of the Windalia Radiolarite (type section), Carnavor basin, Western Australia.- *Eclogae Geologicae Helvetiae*, Basel, vol. 86, no. 3, p. 943-995.

ERK S. (1981).- Stratigraphy of the sedimentary rocks of the Ankara Mélange. *In*: OYGÜR V., SOYSAL Y. & TERLEMEZ I. (eds.), Proceedings of the Symposium on Geology of the central Ana-

tolia.- Geological Society of Turkey 35th Annual Meeting, p. 35-40 [in Turkish].

EROL O. (1956).- A study of the geology and geomorphology of the region SE of Ankara in Elma Dağı and its surroundings.- *Institute of Mineral Research and Exploration, Special Publication* (Serie D), Ankara, vol. 9, 99 p. [in Turkish with English summary].

EROSKAY S.O. (1965).- Paşalar Boğazı-Gölpazarı sahasının jeolojisi.- *Istanbul Üniversitesi Fen Fakültesi Mecmuası B*, vol. 30, p. 135-159 [in Turkish].

ESMERAY-ŞENLET S., ÖZKAN-ALTINER S., ALTINER D. & MILLER K.G. (2015).- Planktonic foraminiferal biostratigraphy, microfacies analysis and sequence stratigraphy across the Cretaceous/ Paleogene boundary in the Haymana Basin, central Anatolia, Turkey.- *Journal of Sedimentary Research*, Tulsa - OK, vol. 85, p. 489-508.

FLÜGEL E. (2004).- Microfacies of carbonate rocks: Analysis, interpretation and application.- Springer-Verlag, New York - NY, 976 p.

FOREMAN H.P. (1973).- Radiolaria from DSDP leg 20. *In*: HEEZEN B.C. & MACGREGOR I.D. (eds.), Leg 20 of the cruises of the Drilling Vessel Glomar Challenger, Yokohama, Japan to Suva, Fiji, September - November 1971.- *Initial Reports of the Deep Sea Drilling Project*, Washington - DC, vol. 20, p. 249-305. DOI: 10.2973/ dsdp.proc.20.113.1973

GALE A.S., KENNEDY J.W., LEES J.A., PETRIZZO M.R. & WALASZCZYK I. (2007).- An integrated study (inoceramid bivalves, ammonites, calcareous nannofossils, planktonic foraminifera, stable carbon isotopes) of the Ten Mile Creek section, Lancaster, Dallas County, north Texas, a candidate Global Boundary Stratotype Section and point for the base of the Santonian Stage.- *Acta Geologica Polonica*, Warszawa, vol. 57, p. 113-160.

GALE A.S., MUTTERLOSE J. & BATENBURG S. (2020).- The Cretaceous Period. *In*: GRADSTEIN F.M., OGG J.G., SCHMITZ M.D. & OGG G.M. (eds.), Geologic Time Scale 2020.- Elsevier, Amsterdam, 1357 p.

GALE A. S., BATENBURG S., COCCIONI R., DUBICKA Z., ERBA E., FALZONI F., HAGGART J., HASEGAWA T., IFRIM C., JARVIS I., JENKYNS H., JURAWSKA A., KENNEDY J., MARON M., MUTTONI G., PEARCE M., PETRIZZO M. R., PREMOLI SILVA I., THIBAULT N., VOIGT S., WAGREICH M. & WALASZCY I. (2023).- The Global Boundary Stratotype Section and Point (GSSP) of the Campanian Stage at Bottaccione (Gubbio, Italy) and its Auxiliary Sections: Seaford Head (UK), Bocieniec (Poland), Postalm (Austria), Smoky Hill, Kansas (U.S.A), Tepayac (Mexico).- *Episodes*, Seoul, vol. 46, no. 3, p. 451-490.

GANNSER A. (1959).- Ausseralpine Ophiolitproblеme.- *Eclogae Geologicae Helvetiae*, Basel, vol. 52, p. 659-680.

GAWLICK H.-J., FRISCH W., VECSEI A., STEIGER T. & BÖHM F. (1999).- The change from rifting to thrusting in the Northern Calcareous Alps as recorded in Jurassic sediments.- *Geologische Rundschau*, vol. 87, p. 644-657.

GODET A. (2013).- Drowning unconformities: Palaeoenvironmental significance and involvement of global processes.- *Sedimentary Geology*, vol. 293, p. 45-66.

GORICAN S. (1994).- Jurassic and Cretaceous radiolarian biostratigraphy and sedimentary evolution of the Budva Zone (Dinarides, Montenegro).- *Mémoires de Géologie*, Lausanne, vol. 18, p. 1-120.

GÖKÇEN S.L. & KELLING G. (1983).- The Paleogene Yamak sand-rich submarine-fan complex, Haymana Basin, Turkey.- *Sedimentary Geology*, vol. 34, p. 219-243.

GÖKTEN E., KAZANCI N. & ACAR S. (1988).- Stratigraphy and tectonics of the Late Cretaceous – Pliocene series in the northwest of Ankara (Bağlum-Kazan).- *Bulletin of the Mineral Research and Exploration*, Ankara, vol. 108, p. 69-81 [in Turkish].

GÖNCÜOĞLU M.C., DIRIK K. & KOZLU H. (1997).- Pre-Alpine and Alpine Terranes in Turkey: explanatory notes to the terrane map of Turkey.- *Annales Géologiques des Pays Helléniques*, Athènes, vol. 37, p. 515-536.

GÖNCÜOĞLU M.C., YALINIZ M.K. & TEKIN U.K. (2006a).- Geochemical features and radiolarian ages of volcanic rocks from the Izmir-Ankara Suture Belt, western Turkey. *In*: Mesozoic Ophiolite belts of the northern part of the Balkan Peninsula. Proceedings of the International Symposium (Belgrade, Banja Luca).- Faculty of Mining and Geology, Beograd, p. 41-44.

GÖNCÜOĞLU M.C., YALINIZ M.K. & TEKIN U.K. (2006b).- Geochemistry, tectono-magmatic discrimination and radiolarian ages of basic extrusives within the Izmir-Ankara Suture Belt (NW Turkey): Time constraints for the Neotethyan evolution.- *Ofioliti*, Pisa, vol. 31, no. 1, p. 25-38.

GÖNCÜOĞLU M.C., SAYIT K. & TEKIN U.K. (2010).- Oceanization of the Northern Neotethys: Geochemical evidence from ophiolitic mélange basalts within the Izmir-Ankara suture belt, NW Turkey.- *Lithos*, vol. 116, p. 175-187.

GÖNCÜOĞLU M.C., GÜRSU S., TEKIN U.K. & KÖKSAL S. (2008).- New data on the evolution of the Neotethyan oceanic branches in Turkey: Late Jurassic ridge spreading in the Intra-Pontide Branch.- *Ofioliti*, Pisa, vol. 33, no. 2, p. 153-164.

GÖNCÜOĞLU M.C., TURHAN N., ŞENTÜRK K., ÖZCAN A. & UYSAL S. (2000).- A geotraverse across NW Turkey: Tectonic units of the central Sakarya region and their tectonic evolution. *In*: BOZKURT E., WINCHESTER J. & PIPER J.A. (eds.), Tectonics and magmatism in Turkey and the Surrounding Area.- *Geological Society of London, Special Publications*, vol. 173, p. 139-161.

GÖNCÜOĞLU M.C., MARRONI M., SAYIT K., TEKIN U.K., OTTRIA G., PANDOLFI L. & ELLERO A. (2012).- The Aylı Dağ Ophiolite Sequence (central-northern Turkey): A fragment of Middle Jurassic oceanic lithosphere within the Intra-Pontide Suture Zone.- *Ofioliti*, Pisa, vol. 37, no. 2, p. 77-92.

GÖNCÜOĞLU M.C., MARRONI M., PANDOLFI L., ELLERO A., OTTRIA G., CATANZARITI R., TEKIN U.K. & SAYIT K. (2014).- The Arkot Dağ Mélange in Araç area, central Turkey: Evidence of its origin within the geodynamic evolution of the Intra-Pontide Suture Zone.- *Journal of Asian Earth Sciences*, vol. 85, p. 117-139.

GRADSTEIN F.M., OGG J.G., SCHMITZ M.D. & OGG G.M. (eds., 2012).- The Geologic Time Scale 2012.- Elsevier, Amsterdam, 1144 p.

GRANIT Y. & TINTANT H. (1960).- Observations préliminaires sur le Jurassique de la région de Bilecik (Turquie).- *Comptes Rendus Hebdomadaires des Séances de l'Académie des Sciences*, Paris, vol. 251, p. 1801-1803.

GÜLYÜZ E., ÖZKAPTAN M., KAYMAKÇI N., PERSANO C. & STUART F.M. (2019).- Kinematic and thermal evolution of the Haymana Basin, a fore-arc to foreland basin in central Anatolia (Turkey).- *Tectonophysics*, vol. 766, p. 326-339.

HAECKEL E. (1862).- Die radiolarien (Rhizopoda radiolaria): Eine Monographie.- Riemer, Berlin, 572 p. DOI: 10.5962/bhl.title.10155

HAECKEL E. (1881).- Entwurf eines Radiolarien-Systems auf Grund von Studien der Challenger-Radiolarien.- *Janische Zeitschrift für Naturwissenschaft*, vol. 15, p. 418-472.

HARRIS N.B.W., KELLEY S. & OKAY A.I. (1994).- Post-collision magmatism and tectonics in northwest Anatolia.- *Contributions to Mineralogy and Petrology*, vol. 117, p. 241-252.

HOJNOS R. (1916).- Beitrage zur kenntis der Ungarischen fossilen radiolarien.- *Földtani Közlöny*, Budapest, vol. 46, p. 340-365.

HORI N. (1999).- Latest Jurassic radiolarians from the northeastern part of the Torinoko Block, Yamizo Mountains, central Japan.- *Scientific Reports of the Institute of Geoscience, University of Tsukuba* (Section B), vol. 20, p. 47-114.

HUBER B.T. & LECKIE R.M. (2011).- Planktonic foraminiferal species turnover across deep-sea Aptian/Albian boundary sections.- *Journal of Foraminiferal Research*, Lawrence - KS, vol. 41, no. 1, p. 53-95.

ION J. & SZASZ L. (1994).- Biostratigraphy of the Upper Cretaceous of Romania.- *Cretaceous Research*, vol. 15, p. 59-87.

ION J., ANTONESCU E., MELINTE M. & SZASZ L. (1999).- Integrated biostratigraphy of the Lower and Middle Coniacian in Romania.- *Acta Palaeontologica Romaniae*, Cluj Napoca, vol. 2, p. 213-221.

JUD R. (1994).- Biochronology and systematics of Early Cretaceous Radiolaria of the western Tethys.- *Mémoires de Géologie*, Lausanne, vol. 19, p. 1-147.

KARABEYOĞLU U., ÖZKAN-ALTINER S. & ALTINER D. (2019).- Quantitative analysis of planktonic foraminifera across the Cretaceous-Paleogene transition and observations on the extinction horizon, Haymana Basin, Turkey.- *Cretaceous Research*, vol. 104, p. 1-25.

KAZANCI N. & GÖKTEN E. (1986).- Sedimentary characteristics of terrestrial Paleocene deposits in northern Ankara region, Turkey.- *Communications Faculty of Sciences University of Ankara* (Series C, Biology), vol. 4, p. 153-163.

KEMKIN I.V. & TAKETANI Y. (2004).- New radiolarian species from Late Jurassic chert-terrigenous deposits of the Taukha Terrane, southern Sikhote-Alin.- *Paleontological Research*, Tokyo, vol. 8, no. 4, p. 325-336.

KESKIN M. & TÜYSÜZ O. (2018).- Stratigraphy, petrogenesis and geodynamic setting of Late Cretaceous volcanism on the SW margin of the Black Sea, Turkey. *In*: SIMMONS M.D., TARI G.C. & OKAY A.I. (eds.), Petroleum Geology of the Black Sea.- *Geological Society of London, Special Publications*, vol. 464, p. 95-130.

KOÇYIĞIT A. (1991).- An example of an accretionary forearc basin from northern central Anatolia and its implications for the history of subduction of Neo-Tethys in Turkey.- *Geological Society of America, Bulletin*, Boulder - CO, vol. 102, p. 22-36.

KOÇYIĞIT A. & LÜNEL A.T. (1987).- Geology and tectonic setting of Alcı region.- *METU Journal of Pure and Applied Sciences*, Ankara, vol. 20, no. 1, p. 35-57.

KOÇYIĞIT A., ÖZKAN S. & ROJAY B. (1988).- Examples from the fore arc basin remnant at the active margin of Northern Neo-Tethys: Emplacement age of the Anatolian Nappe.- *METU Journal of Pure and Applied Sciences*, Ankara, vol. 21, no. 1-3, p. 183-210.

KOÇYIĞIT A., WINCHESTER J.A., BOZKURT E. & HOLLAND G. (2003).- Saraçköy Volcanic Suite: Implications for the subductional phase of arc evolution in the Galatean Arc Complex, Ankara, Turkey.- *Geological Journal*, vol. 38, p. 1-14.

KOZUR H. & MOSTLER H. (1972).- Beiträge zur Erforschung der mesozoischen Radiolarien. Teil I, Revision der Oberfamilie Coccodiscacea HAECKEL, 1862 emend. und Beschreibung ihrer triassischen Vertreter.- *Geologisch-Paläontologische Mitteilungen Innsbruck*, Band 2, Heft 8/9, p. 1-60. URL: https://www2.uibk.ac.at/downloads/c715/gpm_02/02_08_09_001-060.pdf

KOZUR H. & MOSTLER H. (1978).- Beiträge zur Erforschung der mesozoischen Radiolarien. Teil II. Oberfamilie Trematodiscacea HAECKEL 1862 emend. und Beischreibung ihrer triassischen Vertreter.- *Geologisch-Paläontologische Mitteilungen Innsbruck*, Band 8, p. 123-182. URL: https://www2.uibk.ac.at/downloads/c715/gpm_08/8_123-182.pdf

KOZUR H. & MOSTLER H. (1994).- Anisian to middle Carnian radiolarian zonation and description of some stratigraphically important radiolarians.- *Geologisch-Paläontologische Mitteilungen Innsbruck*, Sonderband 3, p. 39-255. URL: https://www.zobodat.at/pdf/GeolPalaeMitt_SB003_0039-0255.pdf

LAMOLDA M.A. & PAUL C.R.C. (2007).- Carbon and oxygen stable isotopes across the Coniacian/Santonian boundary at Olazagutia, northern Spain.- *Cretaceous Research*, vol. 28, no. 1, p. 37-45.

LAMOLDA M.A., PAUL C.R.C., PERYT D. & PONS J.M. (2014).- The Global Boundary Stratotype and Section point (GSSP) for the base of the Santonian stage, 'Cantera de Margas', Olazagutia, northern Spain.- *Episodes*, Seoul, vol. 37, no. 1, p. 2-13.

LEUCHS K. (1939).- Ladinische und karnische Transgression in Anatolien.- *Zentralblatt für Mineralogie, Geologie und Paläontologie* (Abteilung A), Jarhgang 1939, no. 11, p. 305-313.

LI X., MATSUOKA A., LI Y.L. & WANG C.S. (2017).- Phyletic evolution of the mid-Cretaceous radiolarian genus Turbocapsula from southern Tibet and its applications in zonation.- *Marine Micropaleontology*, vol. 130, p. 29-42.

LOKMAN K. & LAHN E. (1946).- Géologie de la région de Haymana (Ankara Vil.).- *Bulletin of the Mineral Research and Exploration*, Ankara, vol. 36, p. 292-299.

MARRONI M., GÖNCÜOĞLU M.C., FRASSI C., SAYIT K., PANDOLFI L., ELLERO A. & OTTRIA G. (2020).- The Intra-Pontide ophiolites in northern Turkey revisited: From birth to death of a Neotethyan oceanic domain.- *Geoscience Frontiers*, vol. 11, p. 129-149.

MATSUOKA A. (1995).- Middle Jurassic to Early Cretaceous radiolarian occurrence in Japan and western Pacific (ODP Sites 800-801). *In*: BAUMGARTNER P.O., O'DOGHERTY L., GORICAN S., URQUHART E., PILLEVUIT A. & DE WEVER P. (eds.), Middle Jurassic to Lower Cretaceous Radiolaria of Tethys: Occurrences, Systematics, Biochronology.- *Mémoires de Géologie*, Lausanne, vol. 23, p. 937-966.

MEKIK F.A. (2000).- Early Cretaceous Pantanelliidae (Radiolaria) from northwest Turkey.- *Micropaleontology*, Flushing - NY, vol. 46, no. 1, p. 1-30.

MEKIK F.A., LING H. Y., ÖZKAN-ALTINER S. & ALTINER D.D. (1999).- Preliminary radiolarian biostratigraphy across the Jurassic-Cretaceous boundary from northwestern Turkey.- *Geodiversitas*, Paris, vol. 21, no. 4, p. 715-738.

MINIATI F., PETRIZZO M.R., FALZONI F. & ERBA E. (2020).- Calcareous plankton biostratigraphy boundary interval in the Bottaccione section (Umbria-Marche Basin, central Italy).- *Rivista Italiana di Paleontologia e Stratigrafia*, Milano, vol. 126, p. 771-789.

MISSONI S. & GAWLICK H.J. (2011).- Jurassic mountain building and Mesozoic-Cenozoic geodynamic evolution of the Northern Calcareous Alps as proven in the Berchtesgaden Alps (Germany*).- Facies*, Erlangen, vol. 57, p. 137-186.

MOIX P. & GORICAN S. (2013).- Jurassic and Cretaceous radiolarian assemblages from the Bornova Mélange in northern Karaburun Peninsula (western Turkey) and its connection to the Izmir-Ankara Mélanges.- *Geodinamica Acta*, vol. 26, no. 1-2, p. 56-67.

MUZAVOR S.N.X. (1977).- Die oberjurassiche Radiolarien-Fauna von Oberaudorf am Inn.- Inaugural-Dissertation zur Erlangung des Doktorgrades des Fachbereiches Geowissenschaften der Ludwig-Maximilians-Universität, München, 163 p.

MÜLLER J. (1858).- Uber die Thalassicollen, Polycystinen und Acanthometren des Mittelmeeres.- *Abhandlungen der Preussischen Akademie der Wissenschafteler zu Berlin*, Jahrang 1858, p. 1-62.

NORMAN T. (1975).- Ankara melanjı'nın yapısı hakkında. *In*: Proceedings of the 50th Anniversary of the Turkish Republic Earth Science Congress.- Mineral Research and Exploration Institute of Turkey (MTA), Ankara, p. 70-77 [in Turkish].

NOWACK E. (1928).- Eine Reise von Angora zum Schwarzen Meer.- *Zeitschrift der Gesellschaft für Erdkunde zu Berlin*, no. 9/10, p. 414-426.

O'DOGHERTY L. (1994).- Biochronology and paleontology of mid-Cretaceous radiolarians from northern Apennines (Italy) and Betic Cordillera (Spain).- *Mémoires de Géologie*, Lausanne, vol. 21, 415 p.

O'DOGHERTY L., CARTER E.S., DUMITRICA P., GORICAN S., DE WEVER P., BANDINI A.N., BAUMGARTNER P.O. & MATSUOKA A. (2009).- Catalogue of Mesozoic radiolarian genera. Part 2: Jurassic-Cretaceous.- *Geodiversitas*, Paris, vol. 31, no. 2, p. 271-356.

OKAY A.I. (1989).- Tectonic units in the Pontides, northern Turkey. *In*: ŞENGÖR A.M.C. (ed.), Tectonic Evolution of the Tethyan Region.- Kluwer Academic Publishers, Dordrecht, p. 109-116.

OKAY A.I. & GÖNCÜOĞLU M.C. (2004).- The Karakaya Complex: A review of data and concepts.- *Turkish Journal of Earth Sciences*, Ankara, vol. 13, no. 2, p. 77-95.

OKAY A.I. & ALTINER D. (2016).- Carbonate sedimentation in an extensional active margin: Cretaceous history of the Haymana region, Pontides.- *International Journal of Earth Sciences*, vol. 105, no. 7, p. 2013-2030.

OKAY A.I. & ALTINER D. (2017).- Alacaatlı Olistostromları: Ankara'da Alcı ve Bağlum bölgelerinin jeolojisi.- Field Trip Book, 70th Geological Congress of Turkey, 41 p. [in Turkish with English abstract].

OKAY A.I. & TÜYSÜZ O. (1999).- Tethyan sutures of northern Turkey. *In*: DURAND B., JOLIVET L., HORVÁTH F. & SÉRANNE M. (eds.), The Mediterranean basins: Tertiary extension within the Alpine orogen.- *Geological Society of London*, *Special Publications*, vol. 156, p. 475-515.

OKAY A.I., ALTINER D. & KYLANDER-CLARK R.C. (2019).- Major Late Cretaceous mass flows in central Turkey: Recording the disruption of the Mesozoic continental margin.- *Tectonics*, vol. 38, p. 960-989.

OKAY A.I., SIYAKO M. & BÜRKAN B.A. (1990).- Geology and tectonic evolution of the Biga peninsula.- *Turkish Association Petroleum Geologists, Bulletin*, Ankara, vol. 2, no. 1, p. 83-121 [in Turkish with English abstract].

OKAY A.I., SIYAKO M. & BÜRKAN B.A. (1991).- Geology and tectonic evolution of the Biga peninsula, northwest Turkey.- *Bulletin of Technical University of Istanbul*, vol. 44, p. 191-256.

OKAY A.I., SUNAL G., SHERLOCK S., KYLANDER-CLARK A.R. & ÖZCAN E. (2020).- Izmir-Ankara Suture as a Triassic to Cretaceous plate boundary – Data from central Anatolia.- *Tectonics*, vol. 38, p. 1-21.

OKAY A.I., ALTINER D., DANELIAN T., TOPUZ G., ÖZCAN E. & KYLANDER-CLARK R.C. (2022).- Subduction-accretion complex with boninitic ophiolite slices and Triassic limestone seamounts: Ankara Mélange, central Anatolia.- *Geological Magazine*, Cambridge (UK), vol. 159, p. 1699-1726.

OKUYUCU C., TEKIN U.K., GÜZGÜN C. & SAYIT K. (2024).- Latest Carboniferous-Early Permian rifting of the Northern Gondwanan margin and the opening of the Northern Neotethys: New evidence from the Carboniferous and Permian foraminiferal assemblages from the Beyşehir-Hoyran Nappes, central Taurides (southern Turkey).- *Journal of Earth Science*, vol. 35, no. 2, p. 394-415.

OZVOLDOVA L. (1975).- Upper Jurassic radiolarians from the Kysuca series in the Klippen Belt.- *Zapadne Karpaty* (Seria Paleontologia), vol. 1, p. 73-86.

ÖNEN A.P. (2003).- Neotethyan ophiolitic rocks of the Anatolides of NW Turkey and comparison with Tauride ophiolites.- *Journal of the Geological Society of London*, vol. 160, p. 947-962.

ÖZCAN E. & ÖZKAN-ALTINER S. (1997).- Late Campanian-Maastrichtian evolution of orbitoid foraminifera in Haymana basin succession (Ankara, Central Turkey).- *Revue de Paléobiologie*, Genève, vol. 16, no. 1, p. 271-290.

PESSAGNO E.A. Jr (1971).- Jurassic and Cretaceous Hagiastridae from the Blake Bahama Basin (Site 5A, JOIDES Leg 1) and the Great Valley Sequence, California Coast Ranges.- *Bulletins of American Paleontology*, Ithaca - NY, vol. 60, no. 264, p. 1-83.

PESSAGNO E.A. Jr (1973).- Upper Cretaceous Spumellariina from the Great Valley Sequence, California Coast Ranges.- *Bulletins of American Paleontology*, Ithaca - NY, vol. 63, no. 276, p. 49-103.

PESSAGNO E.A. Jr (1976).- Radiolarian zonation and stratigraphy of the Upper Cretaceous portion of the Great Valley Sequence, California Coast Ranges.- *Special Publication in Micropaleontology*, Flushing - NY, vol. 2, p. 1-95.

PESSAGNO E.A. Jr (1977a).- Upper Jurassic Radiolaria and radiolarian biostratigraphy of the California Coast Ranges.- *Micropaleontology*, Flushing - NY, vol. 23, no. 1, p. 56-113.

PESSAGNO E.A. Jr (1977b).- Lower Cretaceous radiolarian biostratigraphy of the Great Valley Sequence and Franciscan Complex, California Coast Ranges.- *Cushman Foundation for Foraminiferal Research, Special Publication*, Lawrence - KS, vol. 15, p. 1-87.

PESSAGNO E.A. Jr & NEWPORT R.L. (1972).- A new technique for extracting Radiolaria from radiolarian cherts.- *Micropaleontology*, Flushing - NY, vol. 18, no. 2, p. 231-234.

PESSAGNO E.A. Jr & BLOME C.D. (1980).- Upper Triassic and Jurassic Pantanelliinae from California, Oregon and British Columbia.- *Micropaleontology*, Flushing - NY, vol. 26, no. 3, p. 225-273.

PESSAGNO E.A. Jr, LONGARIA J.F., MACLEOD N. & SIX W.M. (1987).- Studies of North American Jurassic Radiolaria Part. I. Upper Jurassic (Kimmeridgian-Upper Tithonian) Pantanellidae from the Taman Formation, east central Mexico, tectonostratigraphic, chronostratigraphic and phylogenic implications.- *Cushman Foundation for Foraminiferal Research, Special Publication*, Lawrence - KS, vol. 23, no. 1, p. 1-51.

PETRIZZO M.R. (2000).- Upper Turonian-lower Campanian planktonic foraminifera from southern mid-high latitudes (Exmouth Plateau, NW Australia): Biostratigraphy and taxonomic notes.- *Cretaceous Research*, vol. 21, p. 479-505.

PETRIZZO M.R. & HUBER B.T. (2006a).- Biostratigraphy and taxonomy of Late Albian planktonic foraminifera from ODP Leg 171B (western North Atlantic Ocean).- *Journal of Foraminiferal Research*, Lawrence - KS, vol. 36, no. 2, p. 166-190.

PETRIZZO M.R. & HUBER B.T. (2006b).- On the phylogeny of the Late Albian genus *Planomalina*.- *Journal of Foraminiferal Research*, Lawrence - KS, vol. 36, no. 3, p. 233-240.

PETRIZZO M.R., AMAGLIO G., WATKINS D.K., MACLEOD K.G., HUBER B.T., HASEGAWA T. & WOLFGRING E. (2022).- Biotic and paleoceanographic changes across the Late Cretaceous Oceanic Anoxic Event 2 in the southern high latitudes (IODP sites U1513 and U1516, SE Indian Ocean).- *Paleoceanography and Paleoclimatology*, vol. 37, no. 9, p. 1-30.

PHILIPPSON A. (1919).- Kleinasien.- *Handbuch der regionalen Geologie*, Heidelberg, Band V, Abt. 2, 183 p.

PREMOLI SILVA I. & SLITER W.V. (1995).- Cretaceous planktonic foraminiferal biostratigraphy and evolutionary trends from the Bottacione section, Gubbio, Italy.- *Palaeontographica Italica*, Pisa, vol. 82, p. 1-89.

RIEDEL W.R. (1967).- Subclass Radiolaria. *In*: HARLAND W.B. (ed.), The fossil record. A symposium with documentation.- Geological Society of London, p. 291-298.

ROBERTSON A.H.F., PARLAK O. & USTAÖMER T. (2023).- Neotethyan Ankara Mélange, central Turkey in its Triassic-Eocene regional tectonic setting including accretionary mélanges, magmatic arcs and continental units.- *International Geology Review*, vol. 65, no. 20, p. 3192-3247.

ROBASZYNSKI F., GONZALES DONOSO J.M., LINARES D., AMÉDRO F., CARON M., DUPUIS C., DHONDT A.V. & GARTNER, S. (2000).- Le Crétacé supérieur de la région de Kalaat Senan, Tunisie centrale. Litho-biostratigraphie intégrée : Zones d'ammonites, de foraminifères planctoniques et de nannofossiles du Turonien supérieur au Maas-

trichtien.- *Bulletin des Centres de Recherches Exploration-Production elf-Aquitaine*, Pau, vol. 22, p. 359-490.

ROJAY B. (2013).- Tectonic evolution of the Cretaceous Ankara Ophiolitic Mélange during the Late Cretaceous to pre-Miocene interval in central Anatolia, Turkey.- *Journal of Geodynamics*, vol. 65, p. 66-81.

ROJAY B. & SÜZEN L. (1997).- Tectonostratigraphic evolution of an arc-trench basin on accretionary ophiolitic mélange prism, central Anatolia, Turkey.- *Turkish Association of Petroleum Geologists, Bulletin*, Ankara, vol. 9, p. 1-12.

ROJAY B., ALTINER D., ÖZKAN-ALTINER S., ÖNEN A.P., JAMES S. & THIRLWALL M.F. (2004).- Geodynamic significance of the Cretaceous pillow basalts from North Anatolian Ophiolitic Mélange Belt (central Anatolia, Turkey): Geochemical and paleontological constraints.- *Geodinamica Acta*, vol. 17, no. 5, p. 349-361.

RÜST D. (1885).- Beiträge zur Kenntniss der Fossilen Radiolarien aus Gesteinen des Jura.- *Palaeontographica*, Pisa, vol. 31, p. 269-321.

SALAMON-CALVI W. (1940).- Geologische Wanderungen bei Ankara.- *Maden Tetkik ve Arama*, Ankara, t. 5, p. 389-400, 610-619.

SARIFAKIOĞLU E., DILEK Y. & SEVIN M. (2014).- Jurassic-Paleogene intraoceanic magmatic evolution of the Ankara Mélange, north-central Anatolia, Turkey.- *Solid Earth*, vol. 5, p. 77-108.

SASHIDA K. & UEMATSU H. (1996).- Late Jurassic radiolarians from the Torinosu type limestone embedded in the Early Cretaceous Hinodani Formation of the northern Shimanto Terrane, Shikoku, Japan.- *Science Reports of the Institute of Geoscience*, *University of Tsukuba* (Section B, Geological Sciences), vol. 17, p. 33-69.

SAYIT K. & GÖNCÜOĞLU M.C. (2013).- Geodynamic evolution of the Karakaya Mélange Complex, Turkey: A review of geological and petrological constraints.- *Journal of Geodynamics*, vol. 65, p. 56-65.

SAYIT K., BEDI Y., TEKIN U.K., GÖNCÜOĞLU M.C. & OKUYUCU C. (2017).- Middle Triassic Back-Arc Basalts from the blocks in the Mersin Mélange, southern Turkey: Implications for the geodynamic evolution of the Northern Neotethys.- *Lithos*, vol. 268-271, p. 102-113.

SAYIT K., BEDI Y., TEKIN U.K. & OKUYUCU C. (2020).- Carnian (Upper Triassic) lavas and tuffites from the Mersin Mélange: Evidence for intraoceanic arc rifting in the Northern Neotethys.- *The Journal of Geology*, Chicago - IL, vol. 128, no. 5, p. 445-464.

SAYIT K., GÖNCÜOĞLU M.C., ELLERO A., OTTRIA G., FRASSI C., MARRONI M. & PANDOLFI L. (2022).- Late Cretaceous arc magmatism in the southern central Pontides: constraints for the closure of the northern Neotethyan branches.- *Ofioliti*, Pisa, vol. 47, no. 1, p. 19-35.

SCHAAF A. (1981).- Late Early Cretaceous Radiolaria from leg 62 of the DSDP. *In*: THIEDE J., VALUER T.L., ADELSECK C.G., BOERSMA A., CEPEK P., DEAN W.E., FUJII N., KOPORULIN V.I., REA D.K., SANCETTA C., SAYRE W.O., SEIFERT K., SCHAAF A., SCHMIDT R.R., WINDOM K. & VINCENT E. (eds.), Leg 62 of the cruises of the Drilling Vessel Glomar Challenger. Marjuro Atoll, Marshall Islands to Honolulu, Hawaii. July-September 1978.- *Initial Report of the Deep Sea Drilling Project*, Washington - DC, vol. 62, p. 419-470. DOI: 10.2973/dsdp.proc.62.112.1981

SARIASLAN N., ÖZKAN-ALTINER S. & ALTINER D. (2020).- Timing of depositional regime changes during the Late Cretaceous evolution of the southern Pontides (Ankara, central Anatolia, Turkey).- *Cretaceous Research*, vol. 112, p. 1-15.

SCHMIDT G.C. (1960, unpublished).- Geological evolution of the licences 360-363 and 365-367, district 11.- Archive of the Turkish Petroleum Affairs, Ankara.

SERVAIS M. (1982, unpublished).- Collision et suture téthysienne en Anatolie Centrale : Étude structurale et métamorphique (HP-BT) de la zone nord Kütahya.- PhD thesis, Université de Paris-Sud 11, Orsay, 349 p.

SESTINI G. (1971).- The relation between flysch and serpentinites in north central Turkey. *In*: CAMPBELL A.S. (ed.), Geology and history of Turkey.- The Petroleum Exploration Society of Turkey, Tripoli, p. 369-383.

SIREL E., DAĞER Z. & SÖZERI B. (1986).- Some biostratigraphic and paleogeographic observations on the Cretaceous-Tertiary boundary in the Haymana-Polatli region (central Turkey). *In*: WALLISER O. (ed.), Global bioevents.- *Lecture Notes on Earth Sciences*, vol. 8, p. 385-396.

SPECIALE P.A., CATLOS E.J., YILDIZ G.O., SHIN T.A. & BLACK K.N. (2012).- Zircon ages from the Beypazarı granitoid pluton (north central Turkey): Tectonic implications.- *Geodinamica Acta*, vol. 25, no. 3-4, p. 162-182.

SQUINABOL S. (1904).- Radiolarie Cretacee degli Euganei.- *Atti e Memorie della R. Accademia di Scienze Lettere ed Arti in Padova* (Nuova Serie), vol. XX, p. 171-204.

STEIGER T. (1992).- Systematik, Stratigraphie und Palökologie der Radiolarien des Oberjura-Unterkreide-Grenzbereiches im Osterhorn-Trolikum (Nördliche Kalkalpen, Salzburg und Bayern).- *Zitteliana*, vol. 19, p. 1-188.

SUZUKI H. & GAWLICK H. (2009).- Jurassic radiolarians from cherty limestones below the Hallstatt salt mine (Northern Calcareous Alps, Austria).- *Neues Jahrbuch für Geologie und Paläontologie - Abhandlungen*, Band 251, Heft 2, p. 155-197.

ŞENALP M. & GÖKÇEN S.L. (1978).- Sedimentological studies of the oil-saturated sandstones of the Haymana Region (SW Ankara).- *Bulletin of the Geological Society of Turkey*, Ankara, vol. 21, p. 87-94 [in Turkish with English abstract].

ŞENGÖR A.M.C. & YILMAZ Y. (1981).- Tethyan evolution of Turkey: A plate tectonic approach.- *Tectonophysics*, vol. 75, p. 181-241.

ŞENGÖR A.M.C., YILMAZ Y. & SUNGURLU O. (1984).- Tectonics of the Mediterranean Cimmerides: Nature and evolution of the western termina-

tion of Palaeotethys. *In*: ROBERTSON A.H.F. & DIXON J.E. (eds.), The geological evolution of the eastern Mediterranean.- *Geological Society of London*, *Special Publications*, vol. 13, p. 77-112.

TAKEMURA A. (1986).- Classification of Jurassic Nassellarians (Radiolaria).- *Paleontographica*, Pisa, vol. 195, no. 1-3, p. 29-74.

TEKIN U.K. & GÖNCÜOĞLU M.C. (2007).- Discovery of oldest (late Ladinian to middle Carnian) radiolarian assemblages from the Bornova Flysch Zone in western Turkey: Implications for the evolution of the Neotethyan Izmir-Ankara Ocean.- *Ofioliti*, Pisa, vol. 32, no. 2, p. 131-150.

TEKIN U.K. & GÖNCÜOĞLU M.C. (2009).- Late Middle Jurassic (late Bathonian-early Callovian) radiolarian cherts from the Neotethyan Bornova Flysch Zone, Spil mountains, western Turkey.- *Stratigraphy and Geological Correlation*, vol. 17, no. 3, p. 298-308.

TEKIN U.K. & TUNCER A. (2024, unpublished).- Dating of sedimentary units of the Karakaya Complex (SE and NE of Ankara city center) using Radiolarian and Foraminiferal faunas, geochemistry/petrography of its volcanic/volcanosedimentary units and evaluation of its geodynamic evolution.- Report of Scientific Research Department, Hacettepe University, Project Number: FHD-2022-20129, 126 p. [in Turkish with English abstract]

TEKIN U.K., GÖNCÜOĞLU M.C. & TURHAN N. (2002).- First evidence of late Carnian radiolarians from the Izmir-Ankara Suture Complex, central Sakarya, Turkey: Implications for the opening age of the Izmir-Ankara branch of Neo-Tethys.- *Géobios*, Villeurbanne, vol. 35, no. 1, p. 127-135.

TEKIN U.K., GÖNCÜOĞLU M.C. & UZUNÇIMEN S. (2012a).- Radiolarian assemblages from an olistolith with Middle - Late Jurassic to early Late Cretaceous pelagic deposition within the Bornova Flysch Zone in western Turkey.- *Bulletin de la Société Géologique de France*, Paris, vol. 183, no. 4, p. 307-318.

TEKIN U.K., GÖNCÜOĞLU M.C., PANDOLFI L. & MARRONI M. (2012b).- Middle-Late Triassic radiolarian cherts from the Arkotdağ Mélange in northern Turkey: Implications for the life span of the northern Neotethyan branch.- *Geodinamica Acta*, vol. 25, no. 3-4, p. 305-319.

TEKIN U.K., GÖNCÜOĞLU M.C., ÖZKAN-ALTINER S. & YALINIZ M.Y. (2006, unpublished).- Dating of Neotethyan volcanics using Planktonic Foraminifera, Bornova Flysch Zone, NW Anatolia.- Report for Turkish Scientific Council, Report Number: YDABCAG 103Y027, 236p. [in Turkish with English abstract].

TEKIN U.K., BEDI Y., OKUYUCU C., GÖNCÜOĞLU M.C. & SAYIT K. (2016).- Radiolarian biochronology of upper Anisian to upper Ladinian (Middle Triassic) blocks and tectonic slices of volcano-sedimentary successions in the Mersin Mélange, southern Turkey: New insights for the evolution of Neotethys.- *Journal of African Earth Sciences*, vol. 124, p. 409-426.

TEKIN U.K., OKUYUCU C., SAYIT K., BEDI Y., NOBLE P.J., KRYSTYN L. & GÖNCÜOĞLU M.C. (2019).- Integrated Radiolaria, benthic foraminifera and conodont biochronology of the pelagic Permian blocks/tectonic slices and geochemistry of associated volcanic rocks from the Mersin Mélange, southern Turkey: Implications for the Permian evolution of the northern Neotethys.- *Island Arc*, vol. 28, no. 2, p. 1-36.

THUROW J. (1988).- Cretaceous radiolarians of the North Atlantic Ocean; ODP Leg 103 (Sites 638, 640 and 641) and DSDP legs 93 (site 603) and 47 B (site 398). *In*: BOILLOT G., WINTERER E.L., MEYER A.W., APPLEGATE J., BALTUCK M., BERGEN J.A., COMAS M.C., DAVIES T.A., DUNHAM K.W., EVANS C.A., GIRARDEAU J., GOLDBERG D., HAGGERTY J.A., JANSA L.F., JOHNSON J.A., KASAHARA J., LOREAU J.-P., LUNA E., MOULLADE M., OGG J.G., SARTI M., THUROW J., WILLIAMSON M.A. & MAZZULLO E.K. (eds.), Leg 103 of the cruises of the Drilling Vessel JOIDES Resolution, Ponta Delgada, Azores, to Bremerhaven, Germany, 25 April 1985-19 June 1985.- *Proceedings of the Ocean Drilling Program, Scientific Results*, Washington - DC, vol. 103, p. 379-418. DOI: 10.2973/odp.proc.sr.103.148.198

TOKER V. (1979).- Upper Cretaceous planktonic foraminifera and the biostratigraphic investigation of the Haymana area (SW Ankara).- *Bulletin of the Geological Society of Turkey*, Ankara, vol. 22, p. 121-132 [in Turkish with English abstract].

TOKER V. (1980).- Nannoplankton biostratigraphy of the Haymana region (SW Ankara).- *Bulletin of the Geological Society of Turkey*, Ankara, vol. 23, p. 165-178 [in Turkish with English abstract].

TORSVIK T.H., ROUSSE S., LABAILS C. & SMETHURST M.A. (2009).- A new scheme for the opening of the South Atlantic Ocean and the dissection of an Aptian salt basin.- *Geophysical Journal International*, vol. 177, p. 1315-1333.

TÜYSÜZ O. (1999).- Geology of the Cretaceous sedimentary basins of the western Pontides.- *Geological Journal*, vol. 34, p. 75-93.

TÜYSÜZ O. (2018).- Cretaceous geological evolution of the Pontides. *In*: SIMMONS M.D., TARI G.C. & OKAY A.I., (eds.), Petroleum geology of the Black Sea.- *Geological Society of London, Special Publications*, vol. 464, p. 69-94.

TÜYSÜZ O. & TEKIN U.K. (2007).- Timing of imbrication of an active continental margin facing the northern branch of Neotethys, Kargı Massif, northern Turkey.- *Cretaceous Research*, vol. 28, no. 3, p. 754-764.

TÜYSÜZ O., DELLALOĞLU A.A. & TERZIOĞLU N. (1995).- A magmatic belt within the Neo-Tethyan suture zone and its role in the tectonic evolution of northern Turkey.- *Tectonophysics*, vol. 243, p. 173-191.

TÜYSÜZ O., KIRICI S. & SUNAL G. (1997, unpublished).- Geology of Cide-Kurucaşile region.- Turkish Petroleum Corporation Internal Report, Ankara, no. 3736 [in Turkish].

TÜYSÜZ O., YILMAZ I.Ö., SVABENICKA L. & KIRICI S. (2012).- The Unaz Formation: A key unit in the western Black Sea Region, N Turkey.- *Turkish Journal of Earth Sciences*, Ankara, vol. 21, p. 1009-1028.

ÜNALAN G. (1981).- Stratigraphy of the Ankara Mélange southwest of Ankara. *In*: Proceedings of the Symposium on Geology of the Central Anatolia.- Geological Society of Turkey 35th Annual Meeting, Ankara, p. 46-52 [in Turkish with English abstract].

ÜNALAN G. & YÜKSEL V. (1978).- Example of an ancient graben; the Haymana-Polatlı Basin.- *Bulletin of the Geological Society of Turkey*, Ankara, vol. 21, p. 165-169 [in Turkish with English abstract].

ÜNALAN G., YÜKSEL V., TEKELI T., GÖNENÇ O., SEYIT Z. & HÜSEYIN S. (1976).- Upper Cretaceous-Lower Tertiary stratigraphy and paleogeographic evolution of the Haymana-Polatlı region (SW of Ankara).- *Bulletin of the Geological Society of Turkey*, Ankara, vol. 19, p. 159-176 [in Turkish with English abstract].

VELDE B. (2014).- Green clay minerals. *In*: HOLLAND H.D. & TUREKIAN K.K. (eds.), Sediments, diagenesis and sedimentary rocks, green clay minerals.- Treatise on Geochemistry, Second Edition, Elsevier, Cambridge - MA, p. 351-364.

VÖRÖS A. (2014).- A taxonomic and nomenclatural revision of the historical brachiopod collection from the Lower Jurassic of Yakacık (Ankara, Turkey).- *Földtani Közlöny*, Budapest, vol. 144, no. 3, p. 231-254.

WU H.R. (1986).- Some new genera and species of Cenomanian Radiolaria from southern Xizang (Tibet).- *Acta Micropaleontologica Sinica*, Nanjing, vol. 3, no. 4, p. 347-360.

WU H.R. & LI H.S. (1982).- Radiolaria from the olistostrome of the Zonghou Formation, Gyangze, southern Xizan (Tibet).- *Acta Paleontologica Sinica*, Nanjing, vol. 21, no. 1, p. 64-71.

YALINIZ K.M., AYDIN N.S., GÖNCÜOĞLU M.C. & PARLAK O. (1999).- Terlemez quartz monzonite of central Anatolia (Aksaray-Sarikaraman): Age, petrogenesis and geotectonic implications for ophiolite emplacement.- *Geological Journal*, vol. 34, p. 233-242.

YALINIZ K.M., FLOYD P.A. & GÖNCÜOĞLU M.C. (2000).- Geochemistry of volcanic rocks from the Çicekdağ Ophiolite, central Anatolia, Turkey, and their inferred tectonic setting within the northern branch of the Neotethyan Ocean. *In*: BOZKURT E., WINCHESTER J.A. & PIPER J.D.A. (eds.), Tectonics and magmatism in Turkey and the surrounding area.- *Geological Society of London, Special Publications*, vol. 173, p. 203-218.

YÜKSEL S. (1970, unpublished).- Étude géologique de la région d'Haymana (Turquie Centrale).- Thèse, Faculté des Sciences de l'Université de Nancy, 179 p.

YÜKSEL S. (1973).- Évolution verticale de la série sédimentaire et répartition latérale des faciès de la région de Haymana.- *Bulletin of the Mineral Research and Exploration*, Ankara, vol. 80, p. 49-53.

Appendix

Taxonomic notes on the new radiolarian assemblages from the pelagic carbonates of the Seyran Formation within the Soğukçam Limestone Group

Radiolarian-bearing limestone samples in this study were processed using diluted acetic acid (5-10% CH_3COOH), while the chert samples containing radiolarians were etched with diluted hydrofluoric acid (5-10 % HF), following the methods of DUMITRICA (1970) and PESSAGNO and NEWPORT (1972). The illustrated radiolarian specimens and types from this study are housed in the collections of Hacettepe University, Department of Geological Engineering, Türkiye.

Previously, radiolarians from the Soğukçam Limestone have been partly studied by MEKIK *et al.* (1999) and MEKIK (2000) in northern Türkiye. In this study, detailed analyses of the clayey micritic limestones of the Seyran Formation within the Soğukçam Limestone Group revealed a highly diverse and well-preserved assemblage of radiolarians, including 146 taxa, with fourteen new species and four new subspecies from early Hauterivian to the early Aptian time interval (Pls. 1-8).

In this appendix, remarks on some taxa and the nomenclature of the new species are provided.

Subclass Radiolaria MÜLLER, 1858
Order Polycystina EHRENBERG, 1838
Suborder Spumellariina EHRENBERG, 1875
Superfamily Actinommaceae HAECKEL, 1862
Family Pantanelliidae PESSAGNO, 1977a
Subfamily Pantanelliinae PESSAGNO, 1977a
Genus *Pantanellium* PESSAGNO, 1977a

Type species: *Pantanellium riedeli* PESSAGNO, 1977a.

Pantanellium sp. aff. *P. cantuchapai* PESSAGNO & MACLEOD *in* PESSAGNO *et al.*, 1987, *sensu* JUD, 1994

(Pl. 1, figs. H-J)

aff. 1987 *Pantanellium cantuchapai* PESSAGNO & MACLEOD *in* PESSAGNO *et al.*, p. 20, Pl. 1, figs. 8-9, 13-15, 22; Pl. 7, fig. 2.

1994 *Pantanellium* sp. aff. *P. cantuchapai* PESSAGNO & MACLEOD *in* PESSAGNO *et al.*, JUD, p. 89, Pl. 15, figs. 7-9.

Locality and age: Samples Uy-2, Uy-3, Uy-6, Uy-7, Uy-10, Uy-11, the Seyran Formation, Soğukçam Limestone Group, Haymana Basin, south of Ankara, central Türkiye; Early Cretaceous, Hauterivian-early Aptian (Table 1).

Remarks: This species is distinguished from the holotype of *Pantanellium cantuchapai* PESSAGNO & MACLEOD *in* PESSAGNO *et al.* (1987, Pl. 1, figs. 8-9, 13-15, 22; Pl. 7, fig. 2) by its longer and wider polar spines and narrower cortical shell, in accordance with the definition by JUD (1994).

Pantanellium sp. A

(Pl. 1, fig. O)

Locality and age: Sample Uy-11, Seyran Formation, Soğukçam Limestone Group, Haymana Basin, south of Ankara, central Türkiye; Early Cretaceous, early Aptian (Table 1).

Description: The subspherical cortical shell is composed of large, polygonal (mainly hexagonal and pentagonal) pore frames with slightly elevated rims. Four pores are visible on the cortical shell along the axis perpendicular to the polar spines. One polar spine is short and slightly twisted dextrally, while the other is long and straight. Polar spines are tricarinate, featuring three shallow grooves and relatively wider ridges. They decrease in size towards the distal end and terminate in sharp tips.

Remarks: This taxon can be distinguished from other species of the genus *Pantanellium* PESSAGNO by its unequal polar spines, with one spine slightly twisted dextrally.

Family Xiphostylidae HAECKEL, 1881
Genus *Triactoma* RÜST, 1885

Type species: *Triactoma tithonianum* RÜST, 1885.

Triactoma haymanaense TEKIN nov. sp.

(Pl. 1, figs. AH-AJ)

Etymology: This species is named after the town of Haymana, referring to its type locality.

Types: Holotype: Sample Uy-10 (Pl. 1, fig. AH; registration number (DN): HU.JMB.0164). Paratypes: Both from sample Uy-7 (Pl. 1, fig. AI; DN: HU.JMB.0165 and 17AJ; DN: HU.JMB.0166).

Locality and age: Samples Uy-7 and Uy-10, Seyran Formation, Soğukçam Limestone Group, Haymana Basin, south of Ankara, central Türkiye; Early Cretaceous, early Barremian-early Aptian (Table 1).

Material: Five specimens, three of which are photographed and measured.

Diagnosis: Cortical shell lenticular with a sharp side, including numerous small pores within polygonal pore frames on the surface. Three primary spines approximately equal in length, tricarinate, thin, and tapering distally.

Description: The cortical shell is circular in outline and lenticular with a sharp distal side. It features many small, subspherical pores within polygonal (mainly trigonal and hexagonal) pore frames, which have slightly elevated rims. Three primary spines are approximately the same length, thin, and taper gradually towards their sharp ends. Tricarinate primary spines are straight to very slightly twisted dextrally, characterized by thin ridges and shallow grooves.

Measurements (µm): Based on the three specimens.

	HT	Min.	Max.	Mean
Diameter of cortical shell	200	200	260	226
Length of primary spines	110	110	140	130

Remarks: This species can be distinguished from *Triactoma tithonianum* RÜST (1885, p. 289, Pl. 28 (3), fig. 5) by its a lenticular cortical shell with smaller and more numerous pores rather than a spherical to subtriangular shell. It also differs from *T. tithonianum* in having shorter, equally sized primary spines positioned at varied angles unlike the spines in *T. tithonianum*, which are arranged at 120° angles and are of different lengths.

***Triactoma merici* TEKIN nov. sp.**

(Pl. 1, figs. AK-AN)

Etymology: Name in honor of the late Prof. Dr. Engin MERIÇ (Istanbul University, Türkiye) for his significant contributions to Cretaceous to Recent foraminiferal taxonomy.

Types: Holotype: Sample Uy-1 (Pl. 1, fig. AK; DN: HU.JMB.0167), Paratypes: Samples Uy-1 (Pl. 1, fig. AL; DN: HU.JMB.0168), Uy-6 (Fig. 7AM; DN: HU.JMB.0169), Uy-10 (Pl. 1, fig. AN; DN: HU.JMB.0170).

Locality and age: Samples Uy-1, Uy-4, Uy-6 and Uy-10, Seyran Formation, Soğukçam Limestone Group, Haymana Basin, south of Ankara, central Türkiye; Early Cretaceous, early Hauterivian-early Aptian (Table 1).

Material: More than ten specimens, of which four are photographed and measured.

Diagnosis: Cortical shell lenticular, slightly inflated at the center, containing many small, irregular pores within polygonal pore frames. Three primary spines positioned at right angles, approximately equal in length. Spines tricarinate with wide ridges and shallow grooves, gradually tapering distally and terminating in blunt ends.

Description: The cortical shell has a lenticular shape with convex sides, slightly inflated in the center and tapering toward the edges. The surface of the shell is covered with numerous small, irregular, circular to subcircular pores within slightly elevated polygonal pore frames. The primary spines are arranged at 120° angles in a single plane. They are tricarinate with wide, elevated ridges and shallow grooves, tapering gradually and ending blunty.

Measurements (µm): Based on the four specimens.

	HT	Min.	Max.	Mean
Diameter of cortical shell	183	160	200	176
Length of primary spines	166	120	166	143

Remarks: This species can be distinguished from *Triactoma foremanae* MUZAVOR (1977, p. 55, Pl. 1, fig. 11) of Middle to Late Jurassic age, by its lenticular cortical shell with numerous irregular pores rather than large pores in regular polygonal frames and by blunt-ended, less pronounced tricarinate primary spines, unlike the sharp-ended primary spines of *T. foremanae*. It also differs from *T. haymanaense* TEKIN nov. sp. described in this study by having a smaller cortical shell and broader, more robust primary spines with blunt ends, as opposed to the sharp-ended primary spines of *T. haymanaense*.

***Triactoma* sp. A**

(Pl. 1, fig. AP)

Locality and age: Sample Uy-4, Seyran Formation, Soğukçam Limestone Group, Haymana Basin, south of Ankara, central Türkiye; Early Cretaceous, early to early late Barremian (Table 1).

Description: The cortical shell is large, ranging from hemispherical to lenticular in shape, with numerous small, spherical to hemispherical pores set within pore frames. Three primary spines are nearly equal in length and arranged at 120° angles. They are very wide at the base, gradually tapering distally to a sharp tip. These spines feature wide ridges and deep grooves and exhibit strong dextral twisting.

Remarks: This species can be differentiated from other species within the genus *Triactoma* RÜST by its large test and the wider, strongly dextrally twisted primary spines near the base.

Superfamily Pyloniacea (HAECKEL, 1881) DUMITRICA, 1989
Subsuperfamily Dactyliospaerilae SQUINABOL, 1904
Family Hagiastridae RIEDEL, 1967
Genus *Savaryella* JUD, 1994

Type species: *Savaryella guexi* JUD, 1994.

***Savaryella cruciforma* TEKIN nov. sp.**

(Pl. 2, figs. O-U)

Etymology: Derived from the Latin *cruciforma*, meaning "cross-shaped", in reference to the cross-like arrangement of rays.

Types: Holotype: Sample Uy-10 (Pl. 2, fig. O; DN: HU.JMB.0171). Paratypes: Samples Uy-6 (Pl. 2, fig. P; DN: HU.JMB.0172), Uy-7 (Pl. 2, fig. Q; DN: HU.JMB.0173), Uy-7 (Pl. 2, fig. R; DN: HU.JMB.0174), Uy-10 (Pl. 2, fig. S; DN: HU.JMB.0175), Uy-11 (Pl. 2, fig. T; DN: HU.JMB.0176), Uy-11 (Pl. 2, fig. U; DN: HU.JMB.0177).

Locality and age: Samples Uy-5, Uy-6, Uy-7, Uy-8, Uy-9, Uy-10, and Uy-11, Seyran Formation, Soğukçam Limestone Group, Haymana Basin, south of Ankara, central Türkiye; Early Cretaceous, early to early late Barremian- early Aptian (Table 1).

Material: More than thirty specimens, nineteen of which are photographed and measured.

Diagnosis: Test with four equal-length rays arranged mostly at right angles, though occasionally slightly inclined. Central part and initial sections of rays flattened to slightly depressed and exhibit a spongy texture. Rays gradually increasing slightly in width distally and taper the end, lacking distinct ray tips.

Description: The test is moderately large, featuring a small central area and four long rays. The central area and the beginning of the rays are flattened, slightly depressed, and have a spongy appearance. Rays extend at approximately right angles, are equal in length, and lie perpendicular to the central area, sometimes showing slight inclination. They are cylindrical and subcircular in axial section, gradually increasing in width distally before narrowing rapidly near the tips. Rays contain longitudinal rows of subcircular pores and are slightly twisted sinistrally. Four to five longitudinal rows of pores are visible along one side of each ray, with nodes present at the vertices where the pores intersect.

Measurements (µm): Based on the nineteen specimens.

	HT	Min.	Max.	Mean
Diameter of central area	75	71	100	84.4
Maximum width of ray	63	45	63	54.8
Length of the longest ray	213	157	272	218.6

Remarks: This species can be distinguished from *Savaryella sinistra* O'DOGHERTY (1994, p. 371-372, Pl. 73, figs. 9-12) by its small, flattened and depressed central area and shorter rays without expanded tips. It also differs from *Savaryella guexi* JUD (1994, p. 103, Pl. 19, figs. 10-11) in that it has shorter rays with longitudinally arranged pores lacking the bulbous tips seen in the spongy rays of *S. guexi*.

Savaryella guexi JUD, 1994
Savaryella guexi guexi JUD, 1994

1994 *Savaryella guexi* JUD, p. 103, Pl. 19, figs. 10-11.

Locality and age: Fuime Bosso, Umbria-Marche, Italy; Early Cretaceous; middle Berriasian-early late Barremian.

Savaryella guexi breva TEKIN nov. subsp.

(Pl. 2, figs. V-AB)

Etymology: Derived from the Latin *breva*, meaning "short, small", in reference to its shorter rays compared to *Savaryella guexi guexi* JUD.

Types: Holotype: Sample Uy-10 (Pl. 2, fig. V; DN: HU.JMB.0178). Paratypes: Samples Uy-5 (Pl. 2, fig. W; DN: HU.JMB.0179), Uy-7 (Pl. 2, fig. X; DN: HU.JMB.0180), Uy-9 (Pl. 2, fig. Y; DN: HU.JMB.0181), Uy-10 (Pl. 2, fig. Z; DN: HU.JMB.0182), Uy-11 (Pl. 2, fig. AA; DN: HU.JMB.0183), Uy-11 (Pl. 2, fig. AB; DN: HU.JMB.0184).

Locality and age: Samples Uy-5, Uy-6, Uy-7, Uy-8, Uy-9, Uy-10, and Uy-11, Seyran Formation, Soğukçam Limestone Group, Haymana Basin, south of Ankara, central Türkiye; Early Cretaceous, early Barremian-early Aptian (Table 1).

Material: Over twenty specimens, with thirteen photographed and measured.

Diagnosis: Test with four equal rays. Central part consisting of a small lacuna. Rays rectangular in cross-section and spongy throughout, thin at the base, widening in the middle, and terminating with rounded tips.

Description: The test is typical of the genus with four equal, small rays arranged at right angles around a small central area featuring a slight depression. Rays are rectangular in cross-section and spongy, starting thin at the base and increasing in width toward the middle before terminating in bulbous tips.

Measurements (µm): Based on the thirteen specimens.

	HT	Min.	Max.	Mean
Diameter of central area	72	50	88	69.4
Maximum width of ray	72	63	100	80.6
Length of the longest ray	171	150	198	155.9

Remarks: *Savaryella guexi breva* TEKIN nov. subsp. differs from *Savaryella guexi guexi* JUD (1994, p. 103, Pl. 19, figs. 10-11) by its shorter rays, which widen at the middle rather than tapering toward a terminal expansion.

Subsuperfamily Patulibracchilae PESSAGNO, 1971
Family Angulobracchiidae BAUMGARTNER, 1980
Genus *Paronaella* PESSAGNO, 1971

Type species: *Paronaella solanoensis* PESSAGNO, 1971.

Paronaella ? *annemariae* JUD, 1994
Paronaella ? *annemariae annemariae* JUD, 1994

(Pl. 2, figs. AQ-AS)

1981 gen. et sp. indet. SCHAAF, Pl. 10, fig. 1a-b.
1988 gen. et sp. indet. THUROW, Pl. 10, fig. 16.
1994 *Paronaella* ? *annemariae* JUD, p. 90-91, Pl. 15, fig. 14
1995 *Paronaella* ? *annemariae* JUD, BAUMGARTNER *et al.*, p. 390, Pl. 5314, figs. 1-2.
1997 *Paronaella* ? *annemariae* JUD, DUMITRICA *et al.*, p. 29, Pl. 4, fig. 13.

Locality and age: Mid-Pacific Ocean; North Atlantic Ocean; Fuime Bosso, Umbria-Marche, Italy; Fayah Unit, Oman; Soğukçam Limestone Group, Haymana Basin, south of Ankara, central Türkiye; Early Cretaceous; middle Berriasian-early Aptian (Table 1).

Paronaella ? *annemariae oezgenerdemae* TEKIN nov. subsp.

(Pl. 2, figs. AT-AU)

Etymology: Named in honor of Prof. Dr. Nazire ÖZGEN-ERDEM (Sivas Cumhuriyet University, Sivas, Türkiye), recognizing her contributions to Cretaceous-Neogene foraminifera taxonomy.

Types: Holotype: Sample Uy-6 (Pl. 2, fig. AT; DN: HU.JMB.0185). Paratypes: Sample Uy-3 (Pl. 2, fig. AU; DN: HU.JMB.0186).

Locality and age: Samples Uy-3 and Uy-6, Seyran Formation, Soğukçam Limestone Group, Haymana Basin, south of Ankara, central Türkiye; Early Cretaceous, late Hauterivian-late Barremian (Table 1).

Material: Two specimens, photographed and measured.

Diagnosis: Test flat, triangular, with one convex and two concave sides. Surface of test spongy with large central nodes surrounded by 8-9 smaller, circular nodes. Two corners terminated with porous, tapering tubes and one corner terminating in two spines.

Description: The test is roughly flat and triangular, with one convex and two concave sides. Surface of the test is predominantly spongy featuring a large central tubercule surrounded by 8 to 9 slightly smaller and circular tubercules. Two corners of the test terminate in porous, tube-like contracting extensions, while a third corner has two unequal and bifurcated spines. The shorter spine is tricarinate with wide grooves and thin ridges, while the longer spine is needle-like, tapering distally.

Measurements (µm): Based on the two specimens.

	HT	Min.	Max.	Mean
Max. length of test	233	233	238	235.5
Length of tube	76	?	?	?
Length of tricarinate spine	67	67	69	68
Length of needle-like spine	76	76	87	81.5

Remarks: *Paronaella* ? *annemariae oezgenerdemae* TEKIN nov. subsp. is distinguished from *P.* ? *annemariae annemariae* JUD in possessing two tubular extensions at two corners and two spines at a third, rather than three tubular projections at each corner.

Family Patulibracchiidae PESSAGNO, 1971
Genus *Homoeparonaella* BAUMGARTNER, 1980

Type species: *Paronaella elegans* PESSAGNO, 1977a.

Homoeparonaella elegans (PESSAGNO, 1977a)
Homoeparonaella elegans elegans (PESSAGNO, 1977a)

1977a *Paronaella elegans* PESSAGNO, p. 70, Pl. 1, figs. 10-11.

1980 *Homoeparonaella elegans* (PESSAGNO), BAUMGARTNER, p. 289, Pl. 2, figs. 2-6; Pl. 11, fig. 6.

Locality and age: Worldwide; Middle to Late Jurassic, early Bajocian-early Kimmeridgian.

Homoeparonaella elegans bulbosa TEKIN nov. subsp.

(Pl. 3, figs. U-Y)

Etymology: Derived from the Latin *bulbosa*, meaning "bulbous", in reference to the enlarged ray tips.

Types: Holotype: Sample Uy-5 (Pl. 3, fig. U; DN: HU.JMB.0187). Paratypes: Samples Uy-4 (Pl. 3, fig. V; DN: HU.JMB.0188), Uy-5 (Pl. 3, fig. W; DN: HU.JMB.0189), Uy-5 (Pl. 3, fig. X; DN: HU.JMB.0190), Uy-5 (Pl. 3, fig. Y; DN: HU.JMB.0191).

Locality and age: Samples Uy-4 and Uy-5, Seyran Formation, Soğukçam Limestone Group, Haymana Basin, south of Ankara, central Türkiye; Early Cretaceous, early Barremian-early late Barremian (Table 1).

Material: Seven specimens, five of which are photographed and measured.

Diagnosis: Test with three slender, equal-length rays terminating in bulbous tips. Rays composed of 8-10 longitudinal beams, uniform in width, except of their ellipsoidal, expanded tips. Ray axis consisting of polygonal pore frames containing subcircular pores with central spines.

Description: The test has three long, ellipsoidal rays. Each ray consists of straight, longitudinal beams, with four to five beams visible along one side, creating rectangular pore frames and large, subcircular pores. The ray width remains uniform, expanding only at the tip, which are large, bulbous, ellipsoidal, and oriented perpendicular to the ray axis. These tips feature large polygonal pore frames containing circular to subcircular pores. The central spines are thin and elongated, tapering distally. They are tricarinate, featuring thin ridges and shallow grooves, and terminate in sharp points. No auxiliary spines are present on the tips.

Measurements (µm): Based on the five specimens.

	HT	Min.	Max.	Mean
Width of ray at the base	57	57	90	69.6
Width of ray at the tip	100	100	150	120
Length of the longest ray	257	200	320	256.4
Length of the longest spine	86	86	110	99

Remarks: *Homoeparonaella elegans bulbosa* TEKIN nov. subsp. can be distinguished from *Paronaella elegans* PESSAGNO (1977a, p. 70, Pl. 1, figs. 10-11) by its longer rays and significantly larger, ellipsoidal tips compared to the smaller, subcircular tips in the latter.

Homoeparonaella sp. A

(Pl. 3, fig. AD)

Locality and age: Sample Uy-7, Seyran Formation, Soğukçam Limestone Group, Haymana Basin, south of Ankara, central Türkiye; Early Cretaceous, late Barremian (Table 1).

Description: The test has a narrow central area and three very long, thin rays, which are equal in length and positioned at right angles. Rays are slender at the base and gradually widen towards the distal end. They consist of straight, thin longitudinal beams; five to six beams are visible at one side of each ray, forming rectangular pore frames with small, circular pores. Small, tricarinate central spines are present at the ray ends.

Remarks: This species differs from *Homoeparonaella peteri* Jud (1994, p. 80, Pl. 11, figs. 9-12) by having significantly longer, thinner rays that gradually widen distally and have small central spines, rather than the broader, uniform rays with bulbous tips and auxiliary spines.

Family Pseudoaulophacidae Riedel, 1967
Genus *Becus* Wu, 1986

Type species: *Becus gemmatus* Wu, 1986.

***Becus multispinosus* Tekin nov. sp.**

(Pl. 3, figs. AN-AR)

Etymology: Derived from the Latin *multispinosus*, meaning "many thorned", referring to the numerous spines on the cortical shell.

Types: Holotype: Sample Uy-5 (Pl. 3, fig. AN; DN: HU.JMB.0192). Paratypes: Samples Uy-7 (Pl. 3, fig. AO; DN: HU.JMB.0193), Uy-5 (Pl. 3, fig. AP: DN: HU.JMB.0194), Uy-6 (Pl. 3, fig. AQ; DN: HU.JMB.0195), Uy-5 (Pl. 3, fig. AR; DN: HU.JMB. 0196).

Locality and age: Samples Uy-5, Uy-6, and Uy-7, Seyran Formation, Soğukçam Limestone Group, Haymana Basin, south of Ankara, central Türkiye; Early Cretaceous, Barremian (Table 1).

Material: Eight specimens, five of which are photographed and measured.

Diagnosis: Test large and lenticular, with a circular to subcircular outline and numerous spines. Central area featuring a large central node surrounded by a ring of nodes. Area between the circle of nodes and the distal end covered by randomly dispersed small tubercules and pores. Outer rim exhibiting numerous tricarinate, needle-like spines.

Description: The test is large and lenticular, with an inflated central area that tapers gradually to a sharp distal end. The central part of the test contains a large, subspherical to slightly ellipsoidal node, surrounded by a single, subcircular to subellipsoidal ring of fourteen pores. The region between the circle of nodes and the distal end of the test includes numerous small, randomly dispersed tubercules and pores. The distal part of the test has twelve to seventeen primary spines of two types: shorter, needle-like spines that taper to pointed ends, and longer, tricarinate spines with thin ridges and broad grooves, also tapering to pointed ends. All spines are shorter than the diameter of the cortical shell.

Measurements (µm): Based on the five specimens.

	HT	Min.	Max.	Mean
Diameter of the cortical shell	205	170	225	207
Length of the longest ray	90	75	100	86.2

Remarks: This species can be distinguished from *Becus gemmatus* Wu (1986, p. 356, Pl. 1, figs. 13, 23-24, 26) by having a single large central node surrounded by a ring of fourteen strong nodes instead of three nodes, and by possessing a greater number (twelve to seventeen) of peripheral spines on the test.

Genus *Godia* Wu, 1986

Type species: *Godia floreusa* Wu, 1986.

***Godia* ? *orbicula* Tekin nov. sp.**

(Pl. 4, figs. I-K)

Etymology: Derived from the Latin *orbicula*, meaning "rounded", referring to the rounded outline of the test.

Types: Holotype: Sample Uy-2 (Pl. 4, fig. I; DN: HU.JMB.0197). Paratypes: Samples Uy-2 (Pl. 4, fig. J; DN: HU.JMB.0198), Uy-4 (Pl. 4, fig. K; DN: HU.JMB.0199).

Locality and age: Samples Uy-2 and Uy-4, Seyran Formation, Soğukçam Limestone Group, Haymana Basin, south of Ankara, central Türkiye; Early Cretaceous, Hauterivian-early Barremian (Table 1).

Material: Four specimens, all photographed and measured.

Diagnosis: Test lenticular, circular to subcircular in outline, with a central part that includes a large subcircular node surrounded by a raised circle. Small depression encircling this area, followed by a slight elevation at distal end. Test spongy, featuring numerous fine pores and lacking peripheral spines.

Description: The test is circular to subcircular, lenticular, and smooth along the distal edge with no peripheral spines. The central part of test is slightly elevated, with a single large node encircled by a raised ring. A slight depression is present toward the distal end, followed by a slightly elevated platform. The surface is spongy and populated with small, randomly dispersed, subcircular pores.

Measurements (µm): Based on the four specimens.

	HT	Min.	Max.	Mean
Diameter of the circle of nodes	100	90	117	105.3
Diameter of the test	250	230	271	254.5

Remarks: This species differs from *Godia nodocentrum* Dumitrica in Dumitrica *et al.* (1997, p. 24, Pl. 2, fig. 15) by its smaller size and central node encircled by a single raised ring rather than multiple (11-12) small nodes. This taxon is tenta-

tively assigned to the genus *Godia* Wu due to the presence of a single raised circle at the centre of test, contrasting with the multiple rings of nodes as defined by Wu (1986).

Family Veghicycliidae Kozur & Mostler, 1972
Subfamily Tetrapaurinellinae
Dumitrica & Tekin *in* Dumitrica *et al.*, 2013
Genus *Tetrapaurinella* Kozur & Mostler, 1994

Type species: *Tetrapaurinella discoidalis* Kozur & Mostler, 1994.

***Tetrapaurinella lepida* Tekin nov. sp.**

(Pl. 4, figs. R-W)

Etymology: Derived from the Latin *lepida*, meaning "pleasant, charming, neat", referring to the aesthetically pleasing appearance of the test.

Types: Holotype: Sample Uy-5 (Pl. 4, fig. R; DN: HU.JMB.0200). Paratypes: Samples Uy-1 (Pl. 4, fig. S; DN: HU.JMB.0201), Uy-5 (Pl. 4, fig. T; DN: HU.JMB.0202), Uy-6 (Pl. 4, fig. U; DN: HU.JMB.0203), Uy-6 (Pl. 4, fig. V; DN: HU.JMB.0204), Uy-10 (Pl. 4, fig. W; DN: HU.JMB.0205).

Locality and age: Samples Uy-1, Uy-5, Uy-6, and Uy-10, Seyran Formation, Soğukçam Limestone Group, Haymana Basin, south of Ankara, central Türkiye; Early Cretaceous, Hauterivian-early Aptian (Table 1).

Material: Eight specimens, six of which are photographed and measured.

Diagnosis: Test large, subspherical, and lenticular with an inflated central part covered with a spongy surface containing small and scattered pores. Four primary spines at each corner that taper to needle-like, pointed tips.

Description: The test is large and subspherical with four primary spines at each corner and has convex sides. It is lenticular in outline, slightly inflated at the center, and narrows distally to a pointed end. The surface is spongy, covered with a meshwork of small, randomly distributed, subcircular pores. The primary spines are slightly shorter than the test width and taper gradually to needle-like, pointed tips. No auxiliary spines are present along the rim.

Measurements (µm): Based on the six specimens.

	HT	Min.	Max.	Mean
Diameter of cortical shell	167	150	202	171.5
Length of the longest ray	150	110	150	127.5

Remarks: This species differs from *Tetrapaurinella staurus* Dumitrica in Dumitrica *et al.* (1997, p. 25, Pl. 3, figs. 1-2) by having a wider, subcircular test with convex sides rather than a square shape.

Superfamily Sponguracea Haeckel, 1862
Family Archaeospongoprunidae
Pessagno, 1973
Genus *Archaeospongoprunum*
Pessagno, 1973

Type species: *Archaeospongoprunum venadoensis* Pessagno, 1973.

Archaeospongoprunum ankaraense
Tekin nov. sp.

(Pl. 4, figs. Y-AB)

Etymology: Named after Ankara, the capital city of Türkiye.

Types: Holotype: Sample Uy-10 (Pl. 4, fig. Y; DN: HU.JMB.0206). Paratypes: Samples Uy-10 (Pl. 4, fig. Z; DN: HU.JMB.0207), Uy-6 (Pl. 4, fig. AA; DN: HU.JMB.0208), Uy-11 (Pl. 4, fig. AB; DN: HU.JMB.0209).

Locality and age: Samples Uy-6, Uy-10, and Uy-11, Seyran Formation, Soğukçam Limestone Group, Haymana Basin, south of Ankara, central Türkiye; Early Cretaceous, late Barremian-early Aptian (Table 1).

Material: Four specimens, all photographed and measured.

Diagnosis: Cortical shell large, drum-like, subspherical with flat surfaces and a central constriction. Surface meshwork consisting of polygonal pore frames with subspherical to ellipsoidal pores. Two polar spines straight, unequal, tricarinate with thin ridges and deep grooves.

Description: The cortical shell is large, subspherical, drum-like with a flat surface and a central constriction. The surface of cortical shell is covered by polygonal pore frames of varying sizes, containing subspherical to ellipsoidal pores. Two polar spines are unequal, straight, uniform in width from the medial to distal part, tapering to pointed ends. These spines are tricarinate with thin ridges and deep grooves.

Measurements (µm): Based on the four specimens.

	HT	Min.	Max.	Mean
Diameter of cortical shell	200	200	200	200
Length of shorter spine	142	120	150	134.5
Length of the longer spine	200	143	200	181

Remarks: This species can be distinguished from other *Archaeospongoprunum* Pessagno species by its medially constricted, drum-like cortical shell.

Archaeospongoprunum carrierensis
Pessagno, 1977a
***Archaeospongoprunum carrierensis carrierensis* Pessagno, 1977a**

(Pl. 4, fig. AC)

1977a *Archaeospongoprunum carrierensis* Pessagno, p. 29, Pl. 1, figs. 6-7, 9.
1993 *Archaeospongoprunum carrierensis* Pessagno, Ellis, Pl. 3, figs. 3-4.

Locality and age: Worldwide; Early Cretaceous, Aptian-Albian (Table 1).

Archaeospongoprunum carrierensis globosum Tekin nov. subsp.

(Pl. 4, figs. AD-AI)

Etymology: Derived from the Latin *globosum*, meaning "ball, sphere", referring to the spherical outline of the cortical shell.

Types: Holotype: Sample Uy-10 (Pl. 4, fig. AD; DN: HU.JMB.0210). Paratypes: Samples Uy-7 (Pl. 4, fig. AE; DN: HU.JMB.0211), Uy-11 (Pl. 4, fig. AF; DN: HU.JMB.0212), Uy-11 (Pl. 4, fig. AG; DN: HU.JMB.0213), Uy-11 (Pl. 4, fig. AH; DN: HU. JMB.0214), Uy-11 (Pl. 4, fig. AI; DN: HU.JMB. 0215).

Locality and age: Samples Uy-7, Uy-10, and Uy-11, Seyran Formation, Soğukçam Limestone Group, Haymana Basin, south of Ankara, central Türkiye; Early Cretaceous, late Barremian-early Aptian (Table 1).

Material: More than ten specimens, six photographed and measured.

Diagnosis: Cortical shell subspherical, globular, with polygonal pore frames. Two polar spines tricarinate and unequal, tapering distally to pointed ends: shorter spine straight and longer spine slightly sinistrally twisted.

Description: The cortical shell is subspherical, slightly widened perpendicular to the polar spines. The surface is composed of polygonal pore frames with pores in varying sizes and shapes. The two polar spines, featuring thick ridges and thin grooves, are tricarinate and unequal in length. The shorter one is thin, straight, and tapers distally to a point. In contrast, the longer spine is wider with a slight sinistral twist near the pointed end.

Measurements (µm): Based on the six specimens.

	HT	Min.	Max.	Mean
Diameter of cortical shell on the axis of polar spines	140	114	140	126.3
Diameter of cortical shell, perpendicular to polar spines	160	125	160	141.6
Length of shorter spine	145	113	162	134.3
Length of the longer spine	180	133	185	168.5

Remarks: This subspecies differs from the *Archaeospongoprunum carrierensis carrierensis* Pessagno by its larger, more globular cortical shell, and by having one longer and thinner, less-twisted polar spine compared to the ellipsoidal cortical shell with a strongly twisted polar spine.

Archaeospongoprunum obesum Tekin nov. sp.

(Pl. 4, figs. AJ-AM)

Etymology: Derived from the Latin *obesum*, meaning "fat, plump, coarse", referring to the large cortical shell.

Types: Holotype: Sample Uy-7 (Pl. 4, fig. AJ; DN: HU.JMB.0216). Paratypes: Samples Uy-5 (Pl. 4, fig. AK; DN: HU.JMB.0217), Uy-5 (Pl. 4, fig. AL; DN: HU.JMB.0218), Uy-6 (Pl. 4, fig. AM; DN: HU.JMB.0219).

Locality and age: Samples Uy-5, Uy-6, and Uy-7, Seyran Formation, Soğukçam Limestone Group, Haymana Basin, south of Ankara, central Türkiye; Early Cretaceous, Barremian (Table 1).

Material: Seven specimens, four of which are photographed and measured.

Diagnosis: Cortical shell large and lenticular with an inflated central region and a sharply tapered distal end. Shell surface covered with dispersed, mainly unequal pores within polygonal pore frames. Two polar spines unequal in length; the shorter spine straight and the longer one straight proximally, becoming slightly dextrally twisted distally. Both spines tricarinate, featuring wide grooves and small ridges, gradually narrowing towards the distal end.

Description: The cortical shell is lenticular, characterized by an inflated central region and a sharply pointed distal end. Some specimens are flattened, maintaining the sharply tapered form. The surface displays numerous dispersed pores of varying sizes, enclosed within polygonal pore frames. Two polar spines are unequal, tricarinate with wide, shallow grooves and thin ridges, terminating in a sharp point. The shorter polar spine is entirely straight, while the longer spine is straight from the proximal to medial parts, transitioning into a slight dextral twist distally.

Measurements (µm): Based on the four specimens.

	HT	Min.	Max.	Mean
Diameter of the cortical shell on the axis of polar spines	188	188	283	233.5
Diameter of cortical the shell, perpendicular to polar spines	188	188	316	248
Length of the shorter spine	100	63	100	82.5
Length of the longer spine	100	100	117	104.3

Remarks: This species can be distinguished from other species within *Archaeospongoprunum* Pessagno by its lenticular cortical shell and relatively short polar spines. It differs from the *Archaeospongoprunum* sp. A in this study by possessing a spherical shell instead of an ellipsoidal form, as well as shorter, thinner, and less pronounced polar spines.

Archaeospongoprunum tortilum TEKIN nov. sp.

(Pl. 4, figs. AN-AQ)

pars 1994 *Archaeospongoprunum patricki* JUD, p. 63-64, Pl. 4, fig. 3, **non** Pl. 4, fig. 2 (=*Archaeospongoprunum patricki* JUD), **non** Pl. 4, fig. 3 (=*Archaeospongoprunum* sp.)

Etymology: Derived from the Latin *tortilum*, meaning "twisted", in reference to twisted primary spines.

Types: Holotype: Sample Uy-5 (Pl. 4, fig. AN; DN: HU.JMB.0220). Paratypes: Samples Uy-10 (Pl. 4, fig. AO; DN: HU.JMB.0221), Uy-10 (Pl. 4, fig. AP; DN: HU.JMB.0222), Uy-11 (Pl. 4, fig. AQ; DN: HU.JMB.0223).

Locality and age: Ticino, Switzerland, and samples Uy-5, Uy-10, and Uy-11, Seyran Formation, Soğukçam Limestone Group, Haymana Basin, south of Ankara, central Türkiye; Early Cretaceous, early to early late Barremian-early Aptian (Table 1).

Material: Seven specimens, four of which are photographed and measured.

Diagnosis: Cortical shell medium in size, spherical to subspherical, and covered with numerous small, dispersed pores. Two polar spines unequal, tricarinate, with wide ridges and thin, deep grooves. Shorter spine very slightly dextrally twisted and longer one strongly sinistrally twisted.

Description: The cortical shell is medium-sized, spherical to subspherical in outline. It is composed of numerous small, subcircular pores arranged within polygonal (mainly trigonal) pore frames. Two polar spines are unequal and tricarinate, featuring wide ridges and deep, thin grooves. The shorter polar spine is slightly dextrally twisted while the longer spine is strongly sinistrally twisted. Both spines decrease slightly in width distally and terminate with in sharp ends.

Measurements (µm): Based on the five specimens.

	HT	Min.	Max.	Mean
Diameter of the cortical shell on the axis of polar spines	171	117	171	136.5
Diameter of the cortical shell, perpendicular to polar spines	143	117	143	127.5
Length of the shorter spine	143	117	188	144
Length of the longer spine	170	167	183	180

Remarks: *Archaeospongoprunum patricki* JUD, as erected by JUD (1994), includes three different morphotypes. The paratype illustrated by JUD (1994, Pl. 4, fig. 3) exhibits quite different characteristics and is included into this new species. *Archaeospongoprunum tortilum* TEKIN nov. sp. can be distinguished from the holotype of *Archaeospongoprunum patricki* JUD (1994, Pl. 4, fig. 2) by possessing a shorter cortical shell with much smaller pores and two twisted spines (the shorter one with slightly dextrally twisted, while the longer one is strongly sinistrally twisted) instead of a shorter spine is straight and a longer spine is dextrally twisted.

Archaeospongoprunum sp. A

(Pl. 4, figs. AR-AS)

Locality and age: Sample Uy-11, Seyran Formation, Soğukçam Limestone Group, Haymana Basin, south of Ankara, central Türkiye; Early Cretaceous, early Aptian (Table 1).

Description: The cortical shell is large, slightly ellipsoidal, and extended along the polar spines. It is covered by numerous small pores dispersed within the polygonal pore frames. The two polar spines are wide, short, unequal, straight, and taper slightly distally, terminating in pointed ends. They are tricarinate, with very wide, shallow grooves and thin ridges.

Remarks: This species was compared to *Archaeospongoprunum obesum* TEKIN nov. sp. in the previous discussion.

Family Pyramipongiidae KOZUR & MOSTLER, 1978

Genus *Pyramispongia* PESSAGNO, 1973

Type species: *Pyramispongia magnifica* PESSAGNO, 1973.

Pyramispongia sphaerica TEKIN nov. sp.

(Pl. 5, figs. C-F)

Etymology: Derived from the Latin *sphaerica*, meaning "ball, globe, sphere", in reference to the spherical outline of the cortical shell.

Types: Holotype: Sample Uy-7 (Pl. 5, fig. C; DN: HU.JMB.0224). Paratypes: Samples Uy-7 (Pl. 5, fig. D; DN: HU.JMB.0225), Uy-3 (Pl. 5, fig. E; DN: HU.JMB.0226), Uy-4 (Pl. 5, fig. F; DN: HU.JMB.0227).

Locality and age: Samples Uy-3, Uy-4, Uy-6, and Uy-7, Seyran Formation, Soğukçam Limestone Group, Haymana Basin, south of Ankara, central Türkiye; Early Cretaceous, late Hauterivian-Barremian (Table 1).

Material: Five specimens have been photographed and measured, with four illustrated.

Diagnosis: Tetrahedral cortical shell, subspherical to subpyramidal in shape, featuring four primary spines at each corner. Meshwork of the test including two different pore structures with large pentagonal and hexagonal pore frames, overlain by a spongy cover with dispersed pores in varying sizes. Four spines tricarinate, wide at the base, and tapering distally.

Description: The cortical shell is tetrahedral, subspherical to subpyramidal in shape with convex sides. The tetrahedral test includes four, prominent primary spines at each corner. The surface of cortical shell includes underlying large pentagonal and hexagonal pore frames covered by spongy pore frames with dispersed pores. Four primary spines tricarinate with very wide grooves and thin ridges. Their length is always shorter than

the diameter of the test and they are gradually, contracting distally and terminated with the pointed end.

Measurements (µm): Based on the five specimens.

	HT	Min.	Max.	Mean
Diameter of shell	176	118	176	148.8
Maximum length of spine	112	83	117	100.6
Maximum width of spine at the base	32	27	41	33.2

Remarks: This species can be distinguished from *Pyramispongia barmsteinensis* (STEIGER, 1992, p. 33, Pl. 4, figs. 9-14) by having a smooth surface without by-spines and tricarinate main spines instead of needle-like ones. It also differs from *Pyramispongia spinosa* TEKIN nov. sp. in this study by possessing a smooth surface on the test without needle-like by-spines.

***Pyramispongia spinosa* TEKIN nov. sp.**

(Pl. 5, figs. G-H)

Etymology: Derived from the Latin *spinosa*, meaning "thorny, prickly", in reference to the test with many spines.

Types: Holotype: Sample Uy-3 (Pl. 5, fig. G; DN: HU.JMB.0228). Paratype: Sample Uy-3 (Pl. 5, fig. H; DN: HU.JMB.0229).

Locality and age: Sample Uy-3, Seyran Formation, Soğukçam Limestone Group, Haymana Basin, south of Ankara, central Türkiye; Early Cretaceous, late Hauterivian (Table 1).

Material: Three specimens have been photographed and measured, with two illustrated.

Diagnosis: Tetrahedral cortical shell medium-sized, subspherical to subpyramidal with highly convex sides. Cortical shell including four primary spines and many by-spines. Needle-like by-spines on the surface of the test shorter than the primary spines and terminating in a sharp end. Primary spines tricarinate with wide grooves and relatively thin ridges, wide at the base and tapering distally.

Description: The cortical shell is tetrahedral with four primary spines at each corner and numerous by-spines on its surface. The subspherical to subpyramidal cortical shell has convex sides, and its surface consists of many subspherical pores within polygonal pore frames. The by-spines on the surface of the cortical shell are needle-like, solid, tapering distally, pointed, and always shorter than the primary spines. The primary spines are prominent, equal in size, and tricarinate, featuring wide grooves and relatively thin ridges. They are wide at the base, gradually tapering distally to terminate in a sharp end.

Measurements (µm): Based on the three specimens.

	HT	Min.	Max.	Mean
Diameter of the shell	138	120	150	136
Maximum length of the spine	100	100	113	107.6
Maximum width of the spine at the base	25	20	27	24

Remarks: This species was compared to *Pyramispongia sphaerica* TEKIN nov. sp. It differs from *Pyramispongia barmsteinensis* (STEIGER, 1992, p. 33, Pl. 4, figs. 9-14) by having tricarinate primary spines instead of needle-like ones.

***Pyramispongia* sp. A**

(Pl. 5, figs. I-J)

Locality and age: Sample Uy-6, Seyran Formation, Soğukçam Limestone Group, Haymana Basin, south of Ankara, central Türkiye; Early Cretaceous, late Barremian (Table 1).

Description: The tetrahedral cortical shell is large, slightly elongated in one direction, subspherical at the base and triangular at the apex, resembling a roughly elongated pyramid. The surface of the cortical shell is covered by small subspherical pores. Each corner of the test is terminated with shorter, tricarinate primary spines, which feature wide grooves and relatively thin ridges that taper distally to a sharp point.

Remarks: This species can be distinguished from other species of the genus *Pyramispongia* PESSAGNO by its unique elongated subpyramidal cortical shell.

Family Spongodiscidae HAECKEL, 1862
Genus *Haliodictya* HOJNOS, 1916

Type species: *Haliodictya loerentheyi* HOJNOS, 1916.

Remarks: Although the genus *Haliodictya* was assigned to "*Nomina dubia*" by O'DOGHERTY *et al.* (2009), and its original generic definition (skeleton square and latticed, with four elongated lattice-like prolongations at the corners) by HOJNOS (1916) was considered insufficient, the new species (*Haliodictya* ? *quadrata* TEKIN nov. sp.) and two taxa left in open nomenclature (*Haliodictya* ? sp. A and *Haliodictya* ? sp. B) are questionably included to this genus as they exhibit the main characteristics of *Haliodictya* HOJNOS.

***Haliodictya* ? *quadrata* TEKIN nov. sp.**

(Pl. 5, figs. N-R)

Etymology: Derived from the Latin *quadrata*, meaning "square", in reference to the square outline of the test.

Types: Holotype: Sample Uy-11 (Pl. 5, fig. N; DN: HU.JMB.0230). Paratypes: Samples Uy-10 (Pl. 5, fig. O; DN: HU.JMB.0231), Uy-10 (Pl. 5, fig. P; DN: HU.JMB.0232), Uy-10 (Pl. 5, fig. Q; DN: HU.JMB.0233), Uy-11 (Pl. 5, fig. R; DN: HU.JMB.0234).

Locality and age: Samples Uy-7, Uy-10, and Uy-11, Seyran Formation, Soğukçam Limestone Group, Haymana Basin, south of Ankara, central Türkiye; Early Cretaceous, late Barremian-early Aptian (Table 1).

Material: Eight specimens are photographed and measured, with five illustrated.

Diagnosis: Shell square in outline, featuring four strong primary spines at each corner. Primary spines thin, tricarinate with deep thin grooves and wide ridges, tapering distally.

Description: The cortical shell is square in shape with straight linear sides. The central part of the test is marked circular elevated region, while the test is medially depressed, and the rim of the test is slightly elevated. The surface is spongy and characterized by numerous, dispersed, and subcircular pores. Each corner of the test is terminated by four relatively thin primary spines that are equal in length and tricarinate, featuring very thin grooves and wide ridges.

Measurements (µm): Based on the eight specimens.

	HT	Min.	Max.	Mean
Minumum diameter of shell	200	178	238	199.1
Maximum diameter of shell, between two opposite spines	244	211	275	238.5
Maximum length of spine	111	78	111	95.8
Maximum width of spine at the base	33	23	38	31.4

Remarks: This species can be distinguished from *Haliodictya crucelliforma* DUMITRICA (in DUMITRICA *et al.*, 1997, p. 25, Pl. 3, fig. 4) by its straight linear sides instead of concave sides. It differs from *Haliodictya* ? sp. A in this study by possessing a medially depressed cortical shell with longer primary spines.

***Haliodictya* ? sp. A**

(Pl. 5, fig. S)

Locality and age: Sample Uy-1, Seyran Formation, Soğukçam Limestone Group, Haymana Basin, south of Ankara, central Türkiye; Early Cretaceous, early Hauterivian (Table 1).

Description: The test is perfectly square with straight sides and each corner is terminated by four very short primary spines. The central part of the test is elevated and marked by a circular feature, then tapers in thickness toward the rim. The spongy test surface is covered with numerous subcircular pores. The primary spines are very short, tricarinate, and feature wide grooves and relatively thin ridges.

Remarks: This taxon is compared to *Haliodictya* ? *quadrata* TEKIN nov. sp. with differences noted in previous descriptions.

***Haliodictya* ? sp. B**

(Pl. 5, figs. T-U)

Locality and age: Samples Uy-7 and Uy-11, Seyran Formation, Soğukçam Limestone Group, Haymana Basin, south of Ankara, central Türkiye; Early Cretaceous, late Barremian-early Aptian (Table 1).

Description: The test is approximately square with projections at each corner. The spongy test is covered with numerous small, dispersed subcircular pores. Four primary spines are positioned medially on each side. These spines are robust, straight, equal in size, and taper distally. They have a tricarinate structure with thin, deep grooves and relatively wide ridges.

Remarks: This species can be distinguished from *Haliodictya* ? *quadrata* TEKIN nov. sp. by the location of its primary spines, which are positioned medially on each side of the square test, rather than at the test corners.

Suborder Nasselariina EHRENBERG, 1875
Superfamily Archaeodictyomitraceae PESSAGNO, 1976
Family Archaeodictyomitridae PESSAGNO, 1976
Genus *Archaeodictyomitra* PESSAGNO, 1976

Type species: *Archaeodictyomitra squinaboli* PESSAGNO, 1976.

***Archaeodictyomitra mostleri* TEKIN nov. sp.**

(Pl. 6, figs. AB-AD)

Etymology: This species is dedicated to the late Prof. Dr. Helfried MOSTLER (Innsbruck University, Austria) in honor of his significant contributions to radiolarian biochronology.

Types: Holotype: Sample Uy-3 (Pl. 6, fig. AB; DN: HU.JMB.0235). Paratypes: Samples Uy-3 (Pl. 6, fig. AC; DN: HU.JMB.0236), Uy-3 (Pl. 6, fig. AD; DN: HU.JMB.0237).

Locality and age: Sample Uy-3, Seyran Formation, Soğukçam Limestone Group, Haymana Basin, south of Ankara, central Türkiye; Early Cretaceous, late Hauterivian (Table 1).

Material: Three photographed and measured specimens.

Diagnosis: Test large and roughly spindle-shaped, composed of ten segments. Cephalis dome-shaped, followed by a trapezoidal thorax, both mainly poreless or weakly costate. Lumbar and post-abdominal strictures less distinct, marked by constrictions and a row of pores. First inflated segment, the abdomen, including thin and continuous costae. First to third post-abdominal segments subtrapezoidal in outline, and last two segments inversely subtrapezoidal. Some specimens with a vertical row of pores visible between costae.

Description: The large, roughly spindle-shaped test has a smooth surface and lacks a horn. The dome-shaped cephalis and subtrapezoidal thorax are mainly poreless, though the thorax may be weakly costate. The lumbar stricture is generally indistinct, occasionally with a row of pores. The first inflated chamber, the abdominal segment, has thin costae that continue to the end of the test, with 11 to 12 costae visible on one side. The first to third post-abdominal segments are subtrapezoidal, while the fourth and fifth are inversely subtrapezoidal. The lumbar stricture and other post-abdominal strictures marked by shallow constrictions with a row of pores. A continuous row of pores is also visible between the costae. The pores on the test surface are circular to subcircular and vary in size.

Measurements (µm): Based on the three specimens.

	HT	Min.	Max.	Mean
Total length of the test	400	363	400	377.7
Maximum width of the test	167	150	180	165.6

Remarks: This species differs from *Archaeodictyomitra leptocostata* (WU & LI, 1982, Pl. 1, figs. 18-19) by having a spindle-shaped test with a smooth surface, rather than a conical test with distinct constrictions and a greater number of less distinct costae and constrictions.

Archaeodictyomitra sp. A

(Pl. 6, fig. AE)

Locality and age: Sample Uy-10, Seyran Formation, Soğukçam Limestone Group, Haymana Basin, south of Ankara, central Türkiye; Early Cretaceous, early Aptian (Table 1).

Description: The test is spindle-shaped with eight segment, increasing in width until the fourth post-abdominal segment then decreasing in width at the fifth post-abdominal segment, which is the last one. The cephalis is poreless and dome-shaped, lacking a horn, and the collar stricture is indistinct. The thorax is subtrapezoidal with weak costae. The abdomen, up to the fourth post-abdominal segment, is ring-like to subtrapezoidal in outline with distinct costae. 10 costae are visible on the test surface. The line of thin costae shifts at the constriction between the third and fourth post-abdominal segments. The lumbar stricture and other strictures between post-abdominal segments are distinctly marked by deep constrictions and a row of pores. The last post-abdominal segment is inversely subtrapezoidal in outline.

Remarks: This taxon can be distinguished from other species of *Archaeodictyomitra* PESSAGNO by the shifted costae on the surface between the third and fourth post-abdominal segments.

Family Eucyrtidinae TAKEMURA, 1986
Genus *Pseudoeucyrtis* PESSAGNO, 1977b

Type species: *Eucyrtis ? zhamoidai* FOREMAN, 1973.

Pseudoeucyrtis sp. A

(Pl. 7, fig. AR)

pars 1997 *Pseudoeucyrtis zhamoidai* (FOREMAN), DUMITRICA *et al.*, p. 65, figs. 6, 13, **non** fig. 2 (= *Pseudoeucyrtis zhamoidai* (FOREMAN)).

Locality and age: Maghilah Unit, Masirah Island, Oman; Sample Uy-3, Seyran Formation, Soğukçam Limestone Group, Haymana Basin, south of Ankara, central Türkiye; Early Cretaceous, late Hauterivian-Barremian (Table 1).

Description: The test is spindle-shaped with five segments and a long tube. The cephalis is dome-shaped and poreless, featuring a small, needle-like horn. The thorax is much broader and subtrapezoidal in outline. From the thorax to the second post-abdominal segment, the test displays small thorns or tubercules on its surface. The collar stricture is indistinct, while the lumbar stricture is more pronounced, marked by a relatively deep constriction. The abdomen is ring-like, and the stricture between the abdomen and the first post-abdominal segment is distinct characterized by a wide and deep constriction with numerous small, dispersed pores. The first post-abdominal segment is subtrapezoidal in outline, whereas the second post-abdominal segment is inversely subtrapezoidal in outline with small pores. This segment is followed by a long tube with many larger pores in varying shapes. The tube is gradually decreasing in width distally and terminating with a blunt end.

Remarks: This species can be distinguished from *Pseudoeucyrtis zhamoidai* (FOREMAN, 1973, p. 264, Pl. 10, figs. 9-10; Pl. 16, figs. 1-2) by its much wider proximal part and the presence of segments with tubercules on their surface.

Unnamed *pro* Stichocapsidae HAECKEL, 1881
Subfamily Favosyringiinae STEIGER, 1992, nom. corr. by O'DOGHERTY *et al.*, 2009
Genus *Spinosicapsa* OZVOLDOVA, 1975

Type species: *Spinosicapsa ceblienica* OZVOLDOVA, 1975.

Spinosicapsa producta TEKIN nov. sp.

(Pl. 8, figs. O-W)

Etymology: Derived from the Latin *producta*, meaning "lengthened, long", in reference to the elongated test.

Types: Holotype: Sample Uy-10 (Pl. 8, fig. O; DN: HU.JMB.0238). Paratypes: Samples Uy-10 (Pl. 8, fig. P; DN: HU.JMB.0239), Uy-10 (Pl. 8, fig. Q; DN: HU.JMB.0240), Uy-10 (Pl. 8, fig. R; DN: HU.JMB.0241), Uy-10 (Pl. 8, fig. S; DN: HU.JMB.0242), Uy-10 (Pl. 8, fig. T; DN: HU.JMB.0243), Uy-10 (Pl. 8, fig. U; DN: HU.JMB.0244), Uy-10 (Pl. 8, fig. V; DN: HU.JMB.0245), Uy-11 (Pl. 8, fig. W; DN: HU.JMB.0246).

Locality and age: Samples Uy-10 and Uy-11, Seyran Formation, Soğukçam Limestone Group, Haymana Basin, south of Ankara, central Türkiye; Early Cretaceous, early Aptian (Table 1).

Material: More than 20 specimens, with 15 photographed and measured; 9 are illustrated.

Diagnosis: Test of four segments and a long tube. Cephalis, thorax, and abdomen conical, with rare pores and a needle-like horn. Collar and lumbar strictures indistinct. Post-abdominal segment subspherical and inflated with fine pore frames. Eight needle-like spines present on the medial portion of the post-abdominal segment. Post-abdominal segment followed by a relatively long tube with much wider pores of various shapes.

Description: The test is composed of four segments and an elongated, porous tube. The proximal part (cephalis, thorax, and abdomen) is conical with a short, needle-like horn and is mostly poreless or with very few pores. Collar and lumbar strictures are indistinct, with no strictures or pores. The post-abdominal segment is subspherical and features fine, scattered pores. The medial part of the post-abdominal segment contains eight needle-like spines that are not aligned and gradually taper distally. A long tube follows, with rather larger, irregularly shaped pores. This tube gradually narrows distally, ending in a pointed tip.

Measurements (µm): Based on the fifteen specimens.

	HT	Min.	Max.	Mean
Total length of the test (including horn and tube)	400	328	428	399.5
Max. width of the test at first post-abdominal segment	142	114	157	132.6
Length of spine on the post-abdominal segment	57	33	57	41.9

Remarks: This species can be distinguished from *Spinosicapsa triacantha octaradiata* (STEIGER, 1992, p. 74, Pl. 20, figs. 6-7) by its bulbous, subspherical post-abdominal segment with finer pores and eight needle-like spines, in contrast to the ellipsoidal post-abdominal segment with eight tricarinate spines.

Plates

▶ **Plate 1:** Scanning electron micrographs of the Early Cretaceous (early Hauterivian- early Aptian) radiolarian microfauna from the Seyran Formation within the Soğukçam Limestone Group in the Uyuzhamamı section. **A-C**. *Hexapyramis precedis* JUD: A-B. Uy-5, C. Uy-7, scale bar = 200, 300 and 200 µm, respectively; **D-F**. *Cecrops septemporatus* (PARONA): D. Uy-1, E. Uy-3, F. Uy-4, scale bar for all specimens = 200 µm; **G**. *Cecrops* ? *sexaspina* JUD: Uy-3, scale bar = 150 µm; **H-J**. *Pantanellium* sp. aff. *P. cantuchapai* PESSAGNO & MACLEOD *sensu* JUD: H. Uy-6, I. Uy-10, J. Uy-11, scale bar for all specimens = 200 µm; **K**. *Pantanellium masirahense* DUMITRICA: Uy-7, scale bar = 180 µm; **L-N**. *Pantanellium squinaboli* (TAN SIN HOK): L. Uy-9, M. Uy-10, N. Uy-11, scale bar for all specimens = 150, 180, and 180 µm, respectively; **O**. *Pantanellium* sp. A: Uy-11, scale bar = 180 µm; **P-Q**. *Acaeniotyle helicta* FOREMAN: P. Uy-5, Q. Uy-7, scale bar for both specimens = 250 µm; **R-S**. *Acaeniotyle umbilicata* (RÜST): R. Uy-10, S. Uy-11, scale bar for both specimens = 300 µm; **T-V**. *Acastea diaphorogona* (FOREMAN): T. Uy-3, U. Uy-5, V. Uy-7, scale bar for all specimens = 250 µm; **W-X**. *Dicroa periosa* FOREMAN: both from Uy-3, scale bar for both specimens = 200 µm; **Y-Z-AA**. *Stylosphaera macroxiphus* (RÜST): Y. Uy-3, Z. Uy-5, AA. Uy-7, scale bar = 250, 250, and 330 µm, respectively; **AB-AD**. *Suna echiodes* (FOREMAN): AB. Uy-1, AC. Uy-3, AD-AE. Uy-10, scale bar for all specimens = 250 µm; **AF-AG**. *Suna hybum* (FOREMAN): Both from Uy-11, scale bar for both specimens = 70 µm; **AH-AJ**. *Triactoma haymanaense* TEKIN nov. sp.: AH. Holotype, Uy-10, AI-AJ. Paratypes both from Uy-7, scale bar = 230, 280, and 280 µm, respectively; **AK-AN**. *Triactoma merici* TEKIN nov. sp.: AK. Holotype, Uy-1, AL-AN. Paratypes, AL. Uy-1, AM. Uy-10, AN. Uy-6, scale bar = 260, 260, 200, and 200 µm, respectively; **AO**. *Triactoma tithonianum* RÜST: Uy-5, scale bar = 200 µm; **AP**. *Triactoma* sp. A: Uy-4, scale bar = 200 µm; **AQ-AS**. *Crucella angulata* YANG: AQ. Uy-1, AR-AS. Uy-3, scale bar = 370, 370, and 290 µm, respectively.

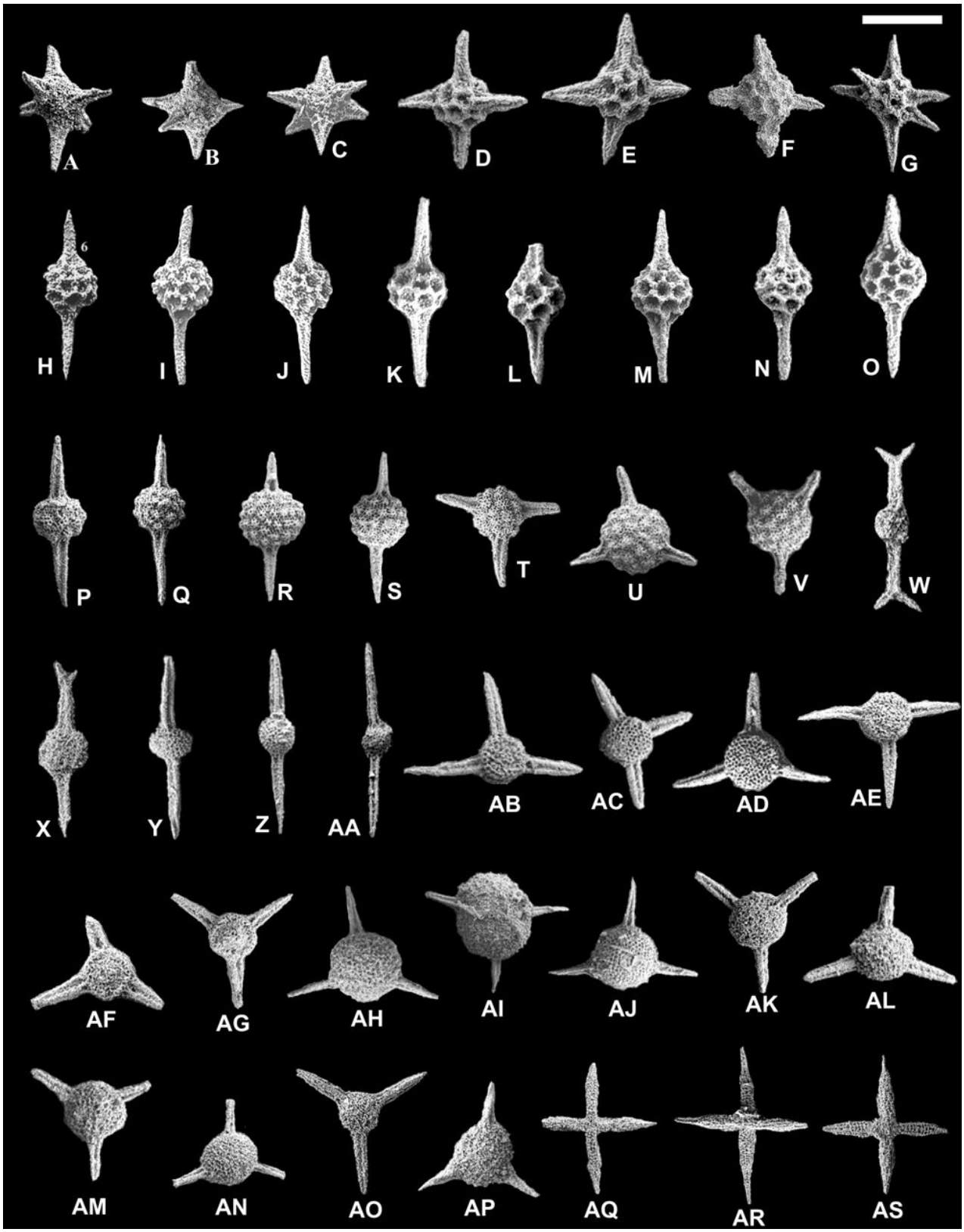
A
B
C
D
E
F
G
H
I
J
K
L
M
N
O
P
Q
R
S
T
U
V
W
X
Y
Z
AA
AB
AC
AD
AE
AF
AG
AH
AI
AJ
AK
AL
AM
AN
AO
AP
AQ
AR
AS

▶ **Plate 2:** Scanning electron micrographs of the Early Cretaceous (early Hauterivian- early Aptian) radiolarian microfauna from the Seyran Formation within the Soğukçam Limestone Group in the Uyuzhamamı section.**A-C**. *Crucella bossoensis* JUD: A. Uy-5, B. Uy-10, C. Uy-11, scale bar = 250, 250, and 150 µm, respectively; **D-F**. *Crucella collina* JUD: D. Uy-2, E. Uy-6, F. Uy-7, scale bar for all specimens = 200 µm; **G-I**. *Crucella gavalai* O'DOGHERTY: G-H. Uy-10, I. Uy-11, scale bar for all specimens = 250 µm; **J-L**. *Crucella* ? *inflexa* (RÜST): J-K. Uy-1, L. Uy-10, scale bar for all specimens = 350 µm; **M**. *Crucella remanei* JUD: Uy-6, scale bar = 330 µm; **N**. *Pseudocrucella* ? *elisabethae* (RÜST): Uy-6, scale bar = 300 µm; **O-U**. *Savaryella cruciforma* TEKIN nov. sp.: O. Holotype, Uy-10, P-U. Paratypes, P. Uy-6, Q. Uy-5, R. Uy-7, S. Uy-10, T-U. Uy-11, scale bar for all specimens = 280 µm; **V-AB**. *Savaryella guexi breva* TEKIN nov. subsp.: V. Holotype, Uy-11, W-AB. Paratypes, W. Uy-5, X. Uy-7, Y. Uy-9, Z. Uy-10, AA-AB. Uy-11, scale bar for all specimens = 240 µm; **AC-AE**. *Angulobracchia portmanni* s.l. BAUMGARTNER: AC. Uy-6, AD. Uy-7, AE. Uy-11, scale bar for all specimens = 250 µm; **AF-AH**. *Cyclastrum infundibuliforme* RÜST: AF. Uy-1, AG. Uy-7, AH. Uy-10, scale bar for all specimens = 330 µm; **AI-AJ**. *Cyclastrum* ? *planum* JUD: AI. Uy-5, AJ. Uy-11, scale bar for both specimens = 230 µm; **AK-AM**. *Cyclastrum* ? *trigonum* (RÜST): AK-AL. Uy-7, AM. Uy-10, scale bar for all specimens = 330 µm; **AN-AP**. *Deviatus diamphidius* (FOREMAN): AN. Uy-7, AO-AP. Uy-10, scale bar for all specimens = 220 µm; **AQ-AS**. *Paronaella* ? *annemariae annemariae* JUD: AQ. Uy-3, AR. Uy-5, AS. Uy10, scale bar = 180, 200, and 180 µm, respectively; **AT-AU**. *Paronaella* ? *annemariae oezgenerdemae* TEKIN nov. subsp.: AT: Holotype, Uy-6, AU. Paratype, Uy-3, scale bar for both specimens = 200 µm.

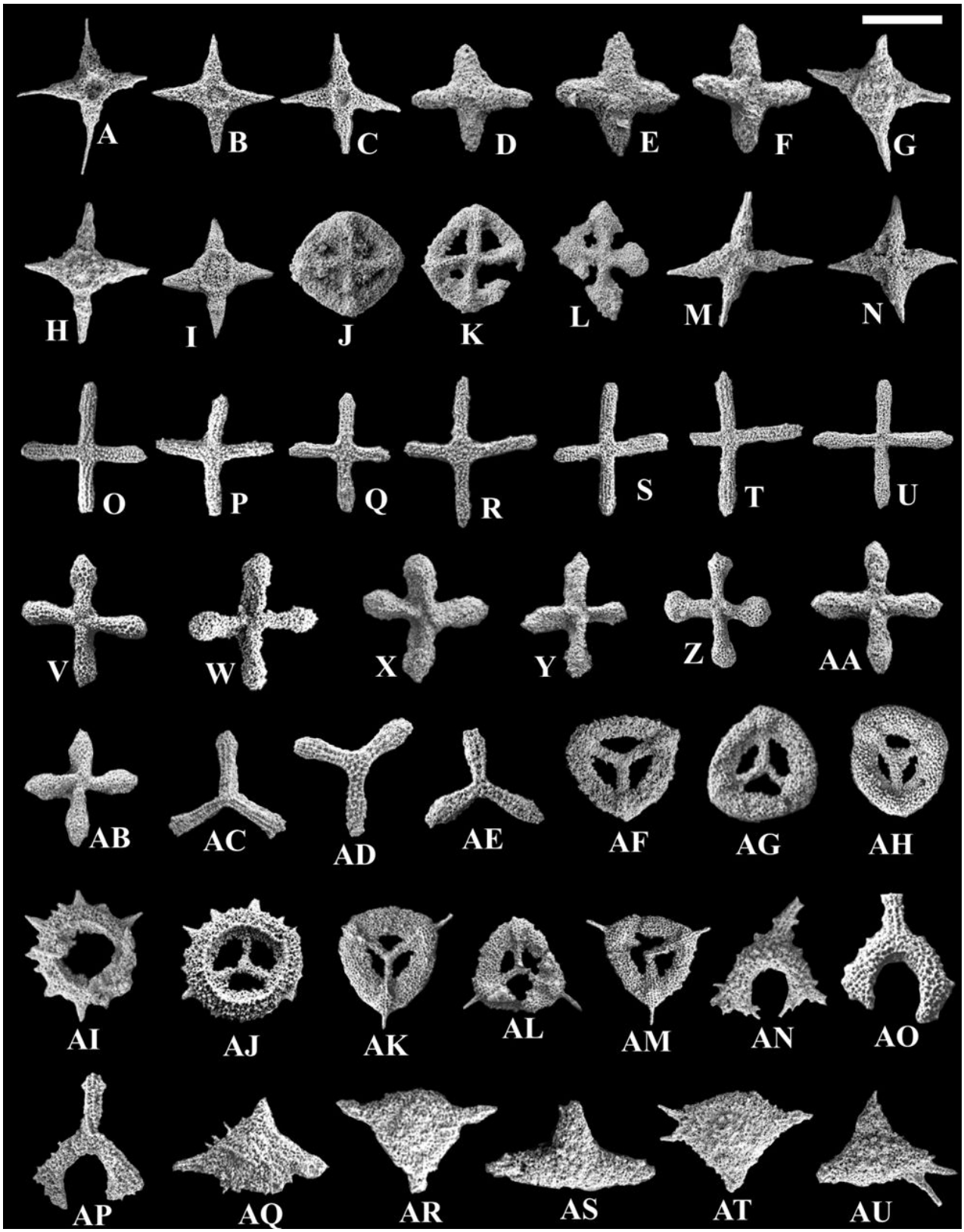
A
B
C
D
E
F
G
H
I
J
K
L
M
N
O
P
Q
R
S
T
U
V
W
X
Y
Z
AA
AB
AC
AD
AE
AF
AG
AH
AI
AJ
AK
AL
AM
AN
AO
AP
AQ
AR
AS
AT
AU

▶ **Plate 3:** Scanning electron micrographs of the Early Cretaceous (early Hauterivian-early Aptian) radiolarian microfauna from the Seyran Formation within the Soğukçam Limestone Group in the Uyuzhamamı section. **A**. *Paronaella grapevinensis* (PESSAGNO): Uy-11, scale bar = 240 µm; **B-D**. *Paronaella trifoliacea* OZVOLDOVA: B. Uy-4, C. Uy-5, D. Uy-6, scale bar = 190, 210, and 190 µm, respectively; **E-G**. *Paronaella* ? *tubulata* STEIGER: E. Uy-9, F-G. Uy-10, scale bar = 210, 160, and 160 µm, respectively; **H-J**. *Halesium biscutum* JUD: H. Uy-1, I. Uy-7, J. Uy-9, scale bar = 340, 280, and 340 µm, respectively; **K-M**. *Halesium crassum* (OZVOLDOVA): K. Uy-1, L. Uy-2, M. Uy-11, scale bar for all specimens = 300 µm; **N-P**. *Halesium* ? *lineatum* JUD: N. Uy-1, O. Uy-7, P. Uy-11, scale bar = 280, 240, and 280 µm, respectively; **Q-S**. *Halesium medium* (STEIGER): Q. Uy-3, R. Uy-7, S. Uy-10, scale bar = 240, 240, and 260 µm, respectively; **T**. *Halesium palmatum* DUMITRICA: Uy-1, scale bar = 210 µm; **U-Y**. *Homoeparonaella elegans bulbosa* TEKIN nov. subsp.: U. Holotype, Uy-5, V-Y. Paratypes, V. Uy-4, W-X-Y. Uy-5, scale bar = 300, 350, 330, 300, and 280 µm, respectively; **Z**. *Homoeparonaella irregularis* (SQUINABOL): Uy-3, scale bar = 300 µm; **AA-AC**. *Homoeparonaella peteri* JUD: AA. Uy-3, AB. Uy-5, AC. Uy-10, scale bar = 360, 300, and 360 µm, respectively; **AD**. *Homoeparonaella* sp. A: Uy-7, scale bar = 260 µm; **AE**. *Alievium* ? *fatuum* DUMITRICA: Uy-6, scale bar = 240 µm; **AF-AH**. *Alievium regulare* (WU & LI): AF. Uy-3, AG. Uy-5, AH. Uy-7, scale bar = 230, 200, and 200 µm, respectively; **AI-AK**. *Becus gemmatus* WU: AI. Uy-7, AJ. Uy-10, AK. Uy-11, scale bar for all specimens = 220 µm; **AL-AM**. *Becus helenae* (SCHAAF): AL. Uy-10, AM. Uy-11, scale bar = 220 and 180 µm, respectively; **AN-AR**. *Becus multispinosus* TEKIN nov. sp.: AN. Holotype, Uy-5, AO-AR. Paratypes, AO. Uy-7, AP. Uy-5, AQ. Uy-6, AR. Uy-5, scale bar = 230, 250, 250, 250, and 250 µm, respectively; **AS-AU**. *Godia concava* (LI & WU): AS. Uy-7, AT-AU. Uy-11, scale bar = 280, 260, and 260 µm, respectively.

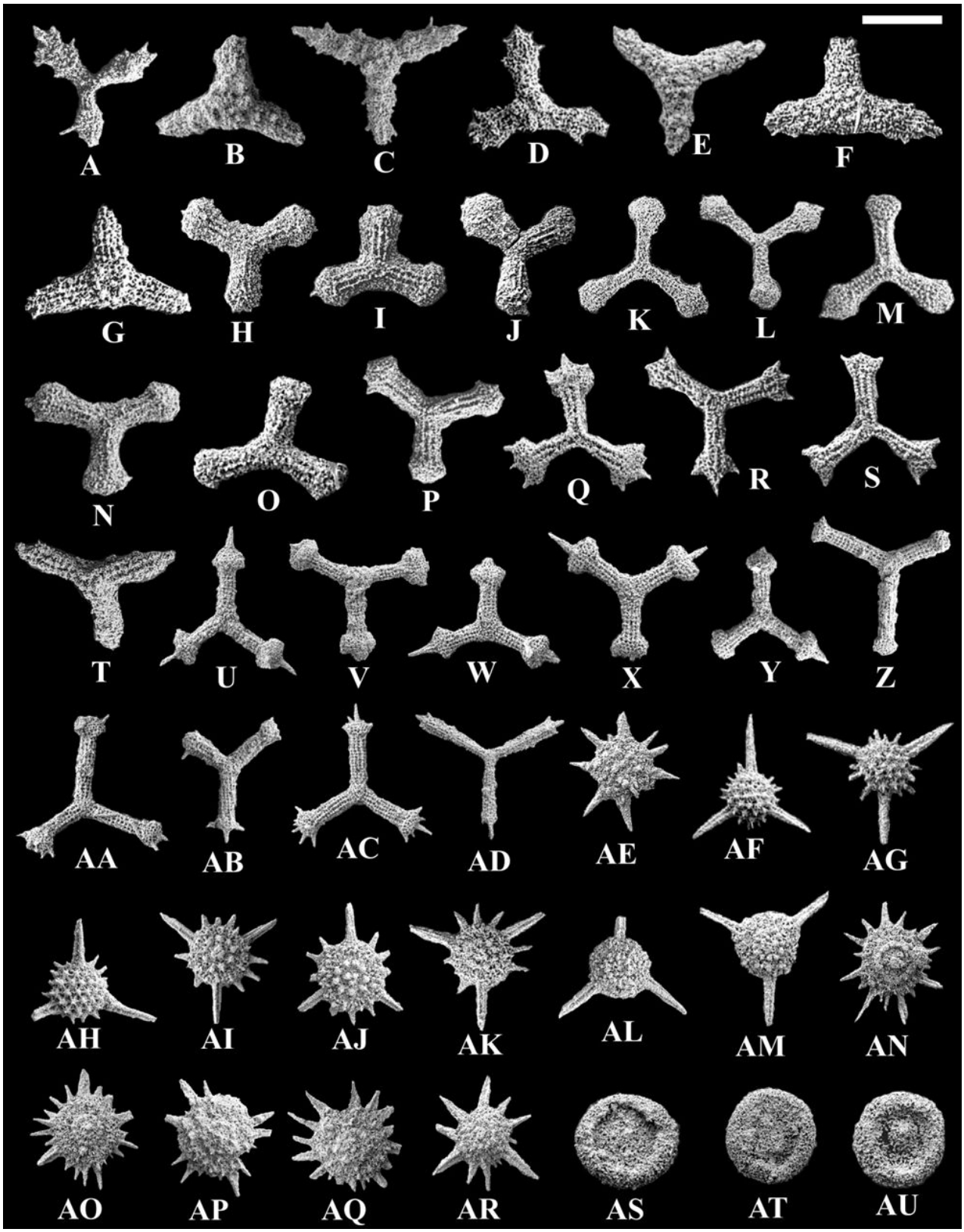
A
B
C
D
E
F
G
H
I
J
K
L
M
N
O
P
Q
R
S
T
U
V
W
X
Y
Z
AA
AB
AC
AD
AE
AF
AG
AH
AI
AJ
AK
AL
AM
AN
AO
AP
AQ
AR
AS
AT
AU

▶ **Plate 4:** Scanning electron micrographs of the Early Cretaceous (early Hauterivian-early Aptian) radiolarian microfauna from the Seyran Formation within the Soğukçam Limestone Group in the Uyuzhamamı section. **A-C**. *Godia coronata* (TUMANDA): A. Uy-1, B. Uy-4, C. Uy-7, scale bar = 260, 280, and 260 µm, respectively; **D-E**. *Godia florealis* (JUD): D. Uy-3, E. Uy-10, scale bar = 240 and 180 µm, respectively; **F-H**. *Godia lenticulata* JUD: F. Uy-3, G. Uy-10, H. Uy-11, scale bar = 260, 260, and 220 µm, respectively; **I-K**. *Godia* ? *orbicula* TEKIN nov. sp.: I. Holotype, Uy-2, J-K. Paratypes, J. Uy-2, K. Uy-4, scale bar = 180, 160, and 200 µm, respectively; **L-N**. *Godia* ? *satoi* (TUMANDA): L. Uy-5, M. Uy-6, N. Uy-10, scale bar = 310, 310, and 230 µm, respectively; **O-P**. *Archaeotritrabs gracilis* STEIGER: O. Uy-1, P. Uy-6, scale bar for both specimens = 290 µm; **Q**. *Tritrabs ewingi* s.l. (PESSAGNO): Uy-3, scale bar = 300 µm; **R-W**. *Tetrapaurinella lepida* TEKIN nov. sp.: R. Holotype, Uy-5, S-W. Paratypes, S. Uy-1, T. Uy-5, U-V. Uy-6, W. Uy-10, scale bar = 280, 240, 240, 260, 300, and 280 µm, respectively; **X**. *Tetrapaurinella staurus* DUMITRICA: Uy-1, scale bar = 220 µm; **Y-AB**. *Archaeospongoprunum ankaraense* TEKIN nov. sp.: Y. Holotype, Uy-10, Z-AB. Paratypes, Z. Uy-10, AA. Uy-6, AB. Uy-11, scale bar = 260, 240, 280, and 260 µm; **AC**. *Archaeospongoprunum carrierensis carrierensis* PESSAGNO: Uy-11, scale bar = 160 µm; **AD-AI**. *Archaeospongoprunum carrierensis globosum* TEKIN nov. subsp.: AD. Holotype, Uy-10, AE-AI. Paratypes, AE. Uy-7, AF. Uy-10, AG-AH-AI. Uy-11, scale bar = 200, 210, 220, 200, 180, and 210 µm, respectively; **AJ-AM**. *Archaeospongoprunum obesum* TEKIN nov. sp.: AJ. Holotype, Uy-7, AK-AM. Paratypes, AK. Uy-5, AL. Uy-6, AM. Uy-5, scale bar = 200, 240, 270, and 200 µm, respectively; **AN-AQ**. *Archaeospongoprunum tortilum* TEKIN nov. sp.: AN. Holotype, Uy-5, AO-AQ. Paratypes, AO-AP. Uy-10, AQ. Uy-11, scale bar = 180, 180, 160, and 200 µm, respectively; **AR-AS**. *Archaeospongoprunum* sp. A: both from sample Uy-11, scale bar for both specimens = 230 µm.

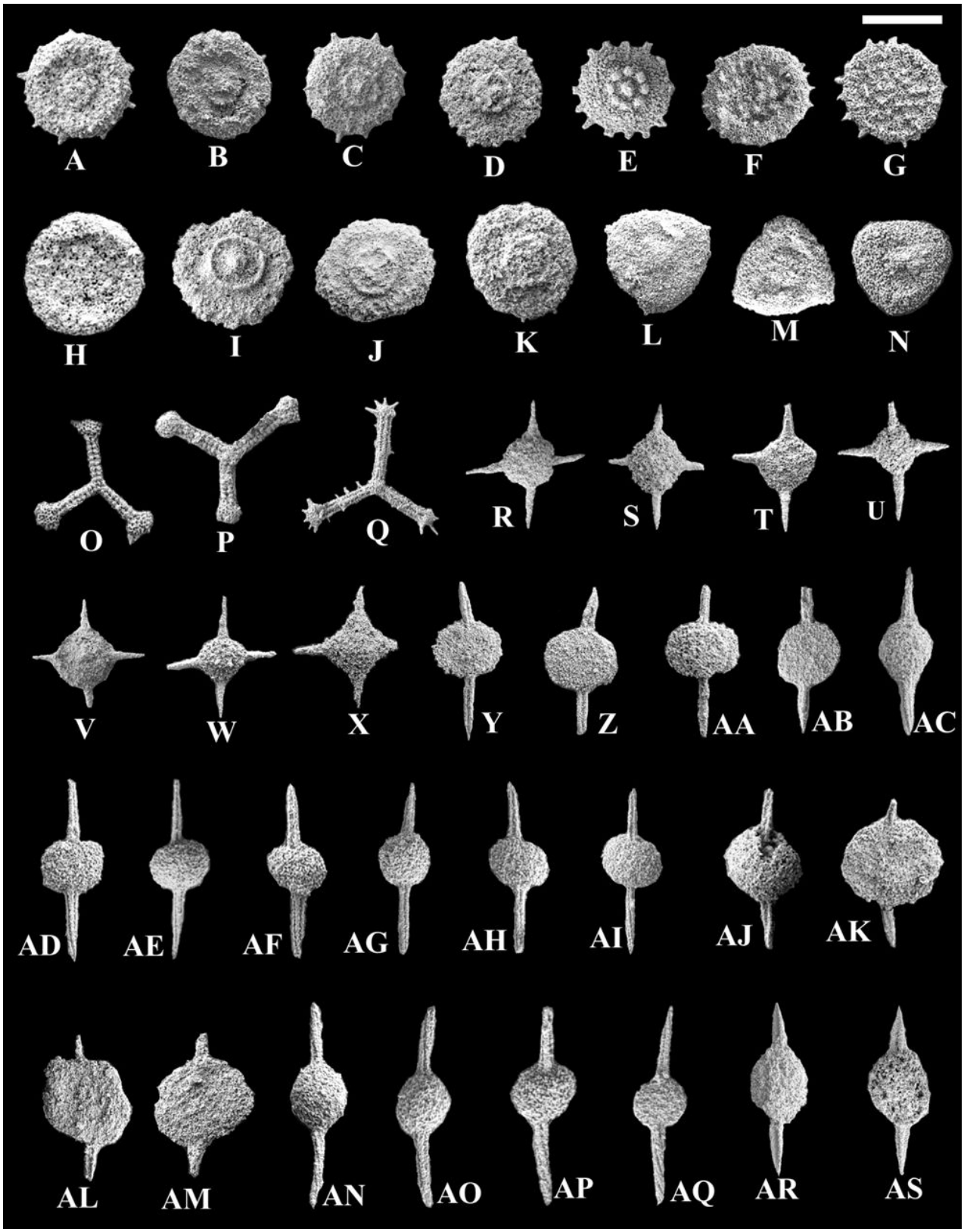
A
B
C
D
E
F
G
H
I
J
K
L
M
N
O
P
Q
R
S
T
U
V
W
X
Y
Z
AA
AB
AC
AD
AE
AF
AG
AH
AI
AJ
AK
AL
AM
AN
AO
AP
AQ
AR
AS

▶ **Plate 5:** Scanning electron micrographs of the Early Cretaceous (early Hauterivian- early Aptian) radiolarian microfauna from the Seyran Formation within the Soğukçam Limestone Group in the Uyuzhamamı section. **A**. *Bernoullius spelae* JUD: Uy-11, scale bar = 120 µm; **B**. *Pyramispongia barmsteinensis* (STEIGER): Uy-7, scale bar = 150 µm; **C-F**. *Pyramispongia sphaerica* TEKIN nov. sp.: C. Holotype, Uy-7, D-F. Paratypes, D. Uy-7, E. Uy-3, F.Uy-4, scale bar = 180, 130, 150, and 180 µm, respectively; **G-H**. *Pyramispongia spinosa* TEKIN nov. sp.: G. Holotype, Uy-3, H. Paratype, Uy-3, scale bar = 170 and 190 µm, respectively; **I-J**. *Pyramispongia* sp. A: both from Uy-6, scale bar for both specimens = 200 µm; **K-M**. *Haliodictya* ? *crucelliforma* DUMITRICA: K. Uy-3, L. Uy-5, M. Uy-7, scale bar for all specimens = 230 µm; **N-R**. *Haliodictya* ? *quadrata* TEKIN nov. sp.: N. Holotype, Uy-11, O-R. Paratypes, O-P-Q. Uy-10, R. Uy-11, scale bar = 210, 260, 250, 260, and 260 µm, respectively; **S**. *Haliodictya* ? sp. A: Uy-1, scale bar = 260 µm; **T-U**. *Haliodictya* ? sp. B: T. Uy-7, U. Uy-11, scale bar for both specimens = 250 µm; **V-X**. *Stylospongia* ? *titirez* JUD: V. Uy-3, W. Uy-5, X. Uy-7, scale bar for all specimens = 240 µm; **Y-AA**. *Dicerosaturnalis amissus* (SQUINABOL): Y. Uy-3, Z. Uy-5, AA. Uy-10, scale bar = 260, 330, and 360 µm, respectively; **AB**. *Dicerosaturnalis major* (SQUINABOL): Uy-2, scale bar = 220 µm; **AC-AE**. *Dicerosaturnalis trizonalis dicranacanthos* (SQUINABOL): AC. Uy-3, AD. Uy-5, AE. Uy-10, scale bar for all specimens = 350, 330, and 300 µm, respectively; **AF-AH**. *Acanthocircus horridus* SQUINABOL: AF. Uy-3, AG. Uy-5, AH. Uy-6, scale bar for all specimens = 300 µm; **AI-AK**. *Acanthocircus hueyi* (PESSAGNO): AI. Uy-3, AJ. Uy-5, AK. Uy-6, scale bar = 260, 280, and 260 µm, respectively; **AL-AM**. *Acanthocircus italicus* (SQUINABOL); AL. Uy-3, AM. Uy-5, scale bar for both specimens = 270 µm; **AN-AP**. *Acanthocircus levis* (DONOFRIO & MOSTLER): AN. Uy-3, AO-AP. Uy-7, scale bar for all specimens = 300, 260, and 280 µm; **AQ**. *Acanthocircus multidentatus* (SQUINABOL): Uy-3, scale bar = 310 µm.

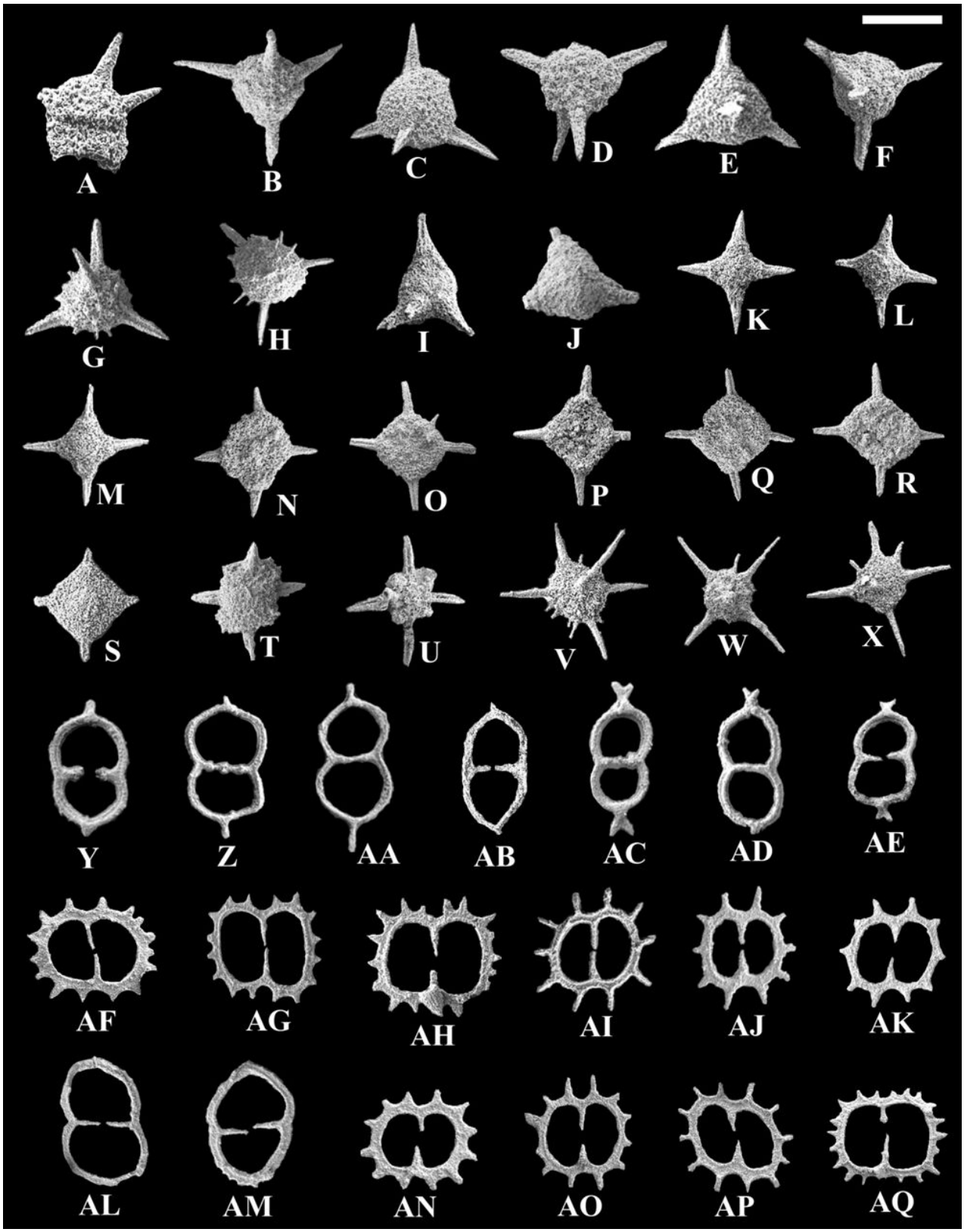
A
B
C
D
E
F
G
H
I
J
K
L
M
N
O
P
Q
R
S
T
U
V
W
X
Y
Z
AA
AB
AC
AD
AE
AF
AG
AH
AI
AJ
AK
AL
AM
AN
AO
AP
AQ

▶ **Plate 6:** Scanning electron micrographs of the Early Cretaceous (early Hauterivian-early Aptian) radiolarian microfauna from the Seyran Formation within the Soğukçam Limestone Group in the Uyuzhamamı section. **A-B**. *Acanthocircus multidentatus* (SQUINABOL): A. Uy-3, B. Uy-5, scale bar = 270 and 300 µm, respectively; **C-D**. *Acanthocircus simplex* (SQUINABOL): C. Uy-5, D. Uy-7, scale bar for both specimens = 300 µm; **E-G**. *Acanthocircus venetus* (SQUINABOL): E. Uy-3, F. Uy-5, G. Uy-11, scale bar 400, 400, and 320 µm, respectively; **H-J**. *Aurisaturnalis carinatus inconstans* DUMITRICA & DUMITRICA-JUD: all from Uy-3, scale bar for all specimens = 270 µm; **K**. *Aurisaturnalis carinatus carinatus* DUMITRICA & DUMITRICA-JUD: Uy-5, scale bar = 240 µm; **L**. *Aurisaturnalis carinatus perforatus* DUMITRICA & DUMITRICA-JUD: Uy-6, scale bar = 300 µm; **M**. *Eospongosaturninus breggiensis* DUMITRICA & HUNGERBÜHLER: Uy-3, scale bar = 230 µm; **N**. *Vitorfus campbelli* PESSAGNO: Uy-11, scale bar = 220 µm; **O**. *Archaeodictyomitra excellens* (TAN SIN HOK): Uy-7, scale bar = 180 µm; **P-R**. *Archaeodictyomitra lacrimula* (FOREMAN): P. Uy-1, Q. Uy-7, R. Uy-10, scale bar = 180, 140, and 130 µm, respectively; **S-U**. *Archaeodictyomitra leptocostata* (WU & LI): S. Uy-1, T. Uy-10, U. Uy-10, scale bar for all specimens = 180 µm; **V-X**. *Archaeodictyomitra longovata* DUMITRICA: V. Uy-7, W. Uy-9, X. Uy-10, scale bar for all specimens = 170 µm; **Y-AA**. *Archaeodictyomitra mitra* DUMITRICA: Y. Uy-1, Z-AA. Uy-3, scale bar = 160, 160, and 140 µm, respectively; **AB-AD**. *Archaeodictyomitra mostleri* TEKIN nov. sp.: AB. Holotype, Uy-3, AC-AD. Paratypes, all from Uy-3, scale bar = 210, 180, and 190 µm, respectively; **AE**. *Archaeodictyomitra* sp. A: Uy-10, scale bar = 170 µm; **AF-AG**. *Thanarla pacifica* NAKASEKO & NISHIMURA: AF. Uy-7, AG. Uy-11, scale bar for both specimens = 170 µm; **AH-AI**. *Thanarla pulchra* (SQUINABOL): AH. Uy-7, AI. Uy-10, scale bar for both specimens = 150 µm; **AJ**. *Amphipyndax mediocris* (TAN SIN HOK): Uy-11, scale bar = 150 µm; **AK-AM**. *Obeliscoites dorysphaeroides* (NEVIANI): AK-AL. Uy-10, AM. Uy-11, scale bar = 240, 230, and 270 µm, respectively; **AN-AP**. *Mirifusus chenodes* (RENZ): AN-AO. Uy-7, AP. Uy-10, scale bar = 220, 210, and 200 µm, respectively; **AQ-AS**. *Svinitzium pseudopuga* DUMITRICA: AQ. Uy-3, AR-AS. Uy-6, scale bar = 150, 160, and 170 µm, respectively.

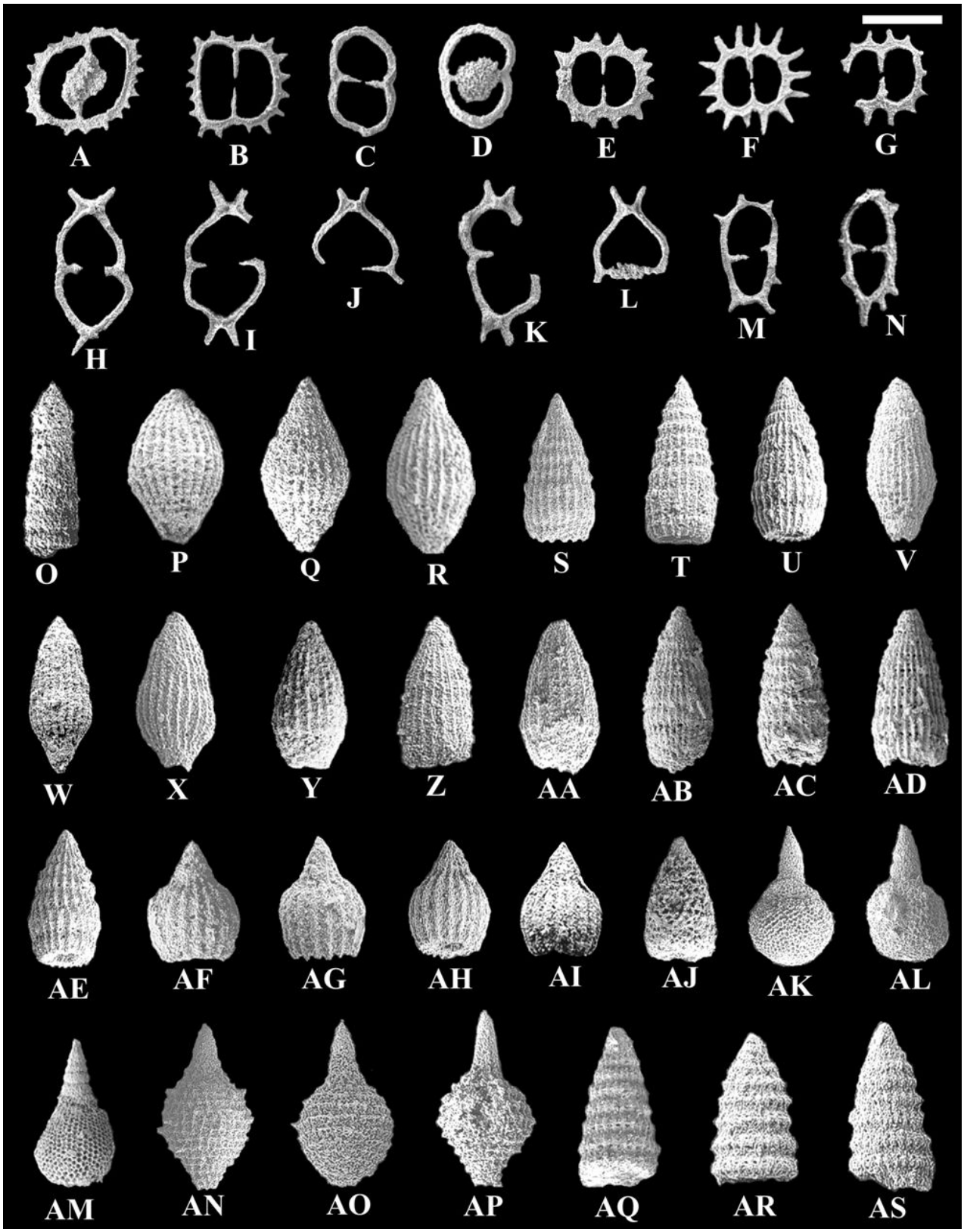
A
B
C
D
E
F
G
H
I
J
K
L
M
N
O
P
Q
R
S
T
U
V
W
X
Y
Z
AA
AB
AC
AD
AE
AF
AG
AH
AI
AJ
AK
AL
AM
AN
AO
AP
AQ
AR
AS

▶ **Plate 7:** Scanning electron micrographs of the Early Cretaceous (early Hauterivian-early Aptian) radiolarian microfauna from the Seyran Formation within the Soğukçam Limestone Group in the Uyuzhamamı section. **A-B**. *Tethysetta boesii* (PARONA): A. Uy-7, B. Uy-11, scale bar = 150 and 130 µm, respectively; **C-D**. *Tethysetta usotanensis* (TUMANDA): both from Uy-10, scale bar for both specimens = 140 µm; **E-G**. *Pseudocrolanium puga* (SCHAAF): E. Uy-6, F. Uy-9, G. Uy-10, scale bar = 140, 140, and 160 µm, respectively; **H-J**. *Loopus nudus* (SCHAAF): H. Uy-5, I. Uy-6, J. Uy-9, scale bar for all specimens =150 µm; **K**. *Pseudodictyomitra carpatica* (LOZYNIAK): Uy-6, scale bar = 160 µm; **L**. *Pseudodictyomitra matsuokai* DUMITRICA: Uy-3, scale bar = 160 µm; **M-O**. *Pseudodictyomitra nodocostata* DUMITRICA: M. Uy-9, N-O. Uy-11, scale bar for all specimens= 160 µm; **P**. *Pseudodictyomitra thurowi* DUMITRICA: Uy-6, scale bar = 140 µm; Q. *Clavaxitus clava* (PARONA): Uy-10, scale bar = 190 µm; **R-T**. *Praexitus alievi* (FOREMAN): R. Uy-5, S. Uy-7, T. Uy-11, scale bar = 200, 210, and 180 µm, respectively; **U**. *Pseudoxitus laguncula* DUMITRICA: Uy-6, scale bar = 160 µm; **V-W**. *Pseudoxitus seriola* DUMITRICA: V. Uy-7, W. Uy-11, scale bar for both specimens = 170 µm; **X-Z**. *Xitus normalis* (WU & LI): X. Uy-7, Y-Z. Uy-10, scale bar = 160, 170 and 210 µm, respectively; **AA**. *Xitus sandovali* JUD: UY-10, scale bar = 260 µm **AB-AD**. *Xitus vermiculatus* (RENZ): AB-AC. Uy-7, AD. Uy-10, scale bar = 170, 150, and 190 µm, respectively; **AE**. *Novixitus robustus* (WU): Uy-11, scale bar = 140 µm; **AF**. *Neorelumbra tippitae* KIESSLING: Uy-9, scale bar = 160 µm; **AG-AI**. *Crolanium bipodium* (PARONA): AG. Uy-5, AH-AI. Uy-10, scale bar = 180, 140, and 180 µm, respectively; **AJ**. *Rhopalosyringium fossile* (SQUINABOL): Uy-10, scale bar = 150 µm; **AK**. *Solenotryma ichikawai* MATSUOKA & YAO: Uy-5, scale bar = 170 µm; **AL**. *Pseudoeucyrtis corpulentus* DUMITRICA: Uy-11, scale bar = 160 µm; **AM-AN**. *Pseudoeucyrtis tenuis* (RÜST): AM. Uy-5, AN. Uy-7, scale bar for both specimens= 180 µm; **AO-AQ**. *Pseudoeucyrtis zhamoidai* (FOREMAN): AO. Uy-5, AP. Uy-6, AQ. Uy-11, scale bar = 210, 190, and 220 µm, respectively; **AR**. *Pseudoeucyrtis* sp. A: Uy-3, scale bar = 170 µm.

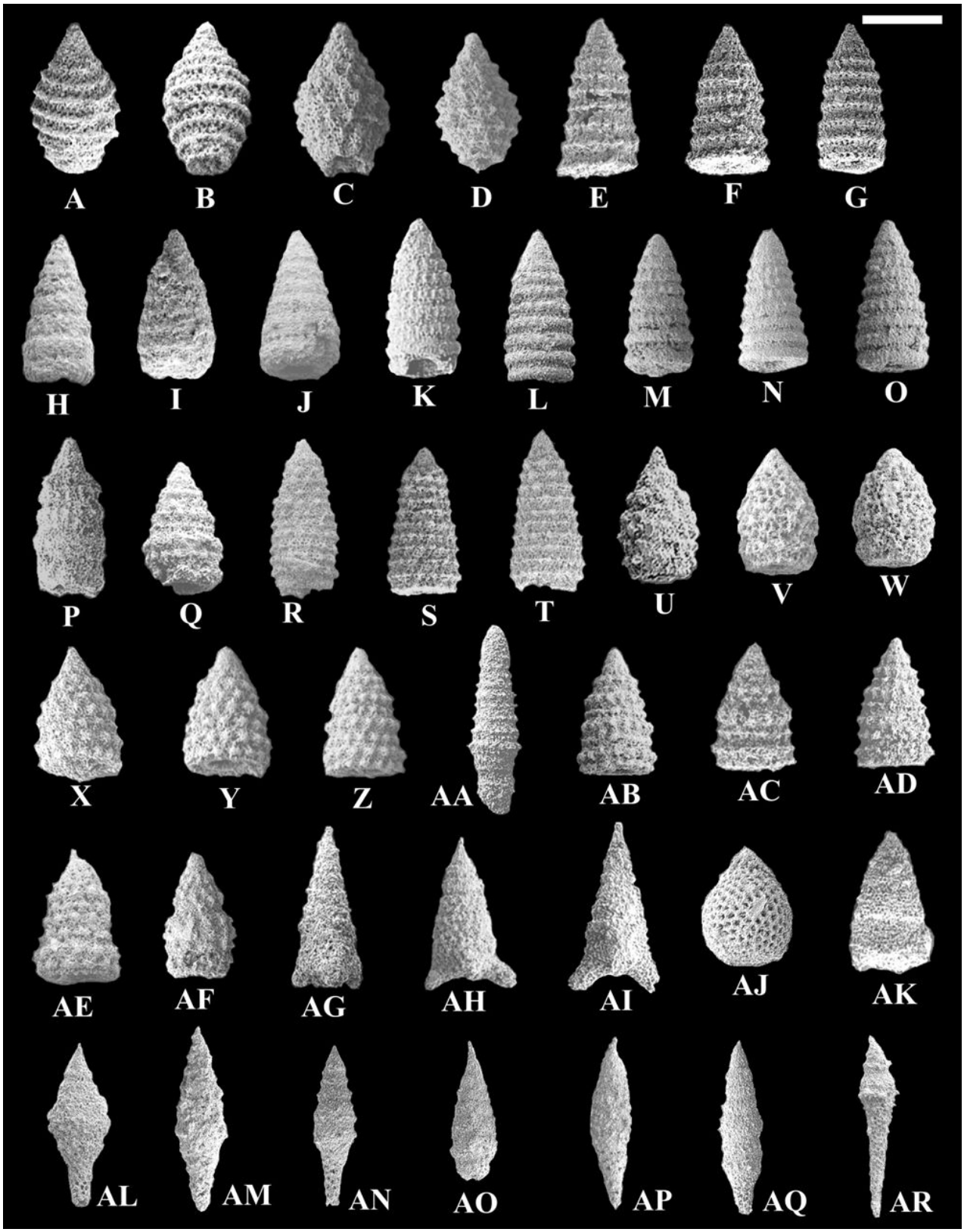
A
B
C
D
E
F
G
H
I
J
K
L
M
N
O
P
Q
R
S
T
U
V
W
X
Y
Z
AA
AB
AC
AD
AE
AF
AG
AH
AI
AJ
AK
AL
AM
AN
AO
AP
AQ
AR

▶ **Plate 8:** Scanning electron micrographs of the Early Cretaceous (early Hauterivian- early Aptian) radiolarian microfauna from the Seyran Formation within the Soğukçam Limestone Group in the Uyuzhamamı section. **A**. *Napora praespinifera* (PESSAGNO): Uy-7, scale bar = 260 µm; **B-D**. *Spongocapsula coronata* (SQUINABOL): B. Uy-7, C. Uy-9, D. Uy-10, scale bar = 180, 160, and 200 µm, repectively; **E-G**. *Spongocapsula obesa* JUD: E. Uy-3, F. Uy-7, G. Uy-9, scale bar = 200, 220, and 220 µm, respectively; **H-I**. *Spongostichomitra elatica* (ALIEV): H. Uy-10, I. Uy-11, scale bar = 150 and 170 µm, respectively; **J-L**. *Dibolachras tytthopora* FOREMAN: J. Uy-3, K. Uy-5, L. Uy-10, scale bar = 220, 260, and 210 µm, respectively; **M**. *Spinosicapsa agolarium* (FOREMAN): Uy-1, scale bar = 190 µm; **N**. *Spinosicapsa limatum* (FOREMAN): Uy-1, scale bar = 230 µm; **O-W**. *Spinosicapsa producta* TEKIN nov. sp.: O. Holotype, Uy-10, P-W. Paratypes, P-V. Uy-10, W. Uy-11, scale bar = 190, 180, 190, 180, 190, 190, 180, 180, and 190 µm, respectively; **X-Y**. *Spinosicapsa spinosa* (SQUINABOL): X. Uy-9, Y. Uy-10, scale bar for both specimens = 180 µm; **Z-AB**. *Spinosicapsa triacantha tetraradiata* (STEIGER): Z. Uy-1, AA. Uy-3, AB. Uy-11, scale bar = 290, 230, and 220 µm, respectively; **AC-AD**. *Arcanicapsa leiostraca* (FOREMAN): both from Uy-1, scale bar for both specimens = 220 µm; **AE-AF**. *Arcanicapsa trachyostraca* (FOREMAN): AE. Uy-1, AF. Uy-11, scale bar = 220 and 240 µm, respectively; **AG-AH**. *Crococapsa asseni* (TAN SIN HOK): Uy-11, scale bar = 150 and 130 µm, respectively; **AI**. *Crococapsa uterculus* (PARONA): Uy-11, scale bar = 130 µm; **AJ-AL**. *Crypthamporella clivosa* (ALIEV): AO. Uy-9, AP-AQ. Uy-11, scale bar for all specimens = 120 µm; **AM**. *Hemicryptocapsa capita* TAN SIN HOK: Uy-6, scale bar = 240 µm; **AN**. *Trimulus parmatus* O'DOGHERTY: Uy-10, scale bar = 130 µm.

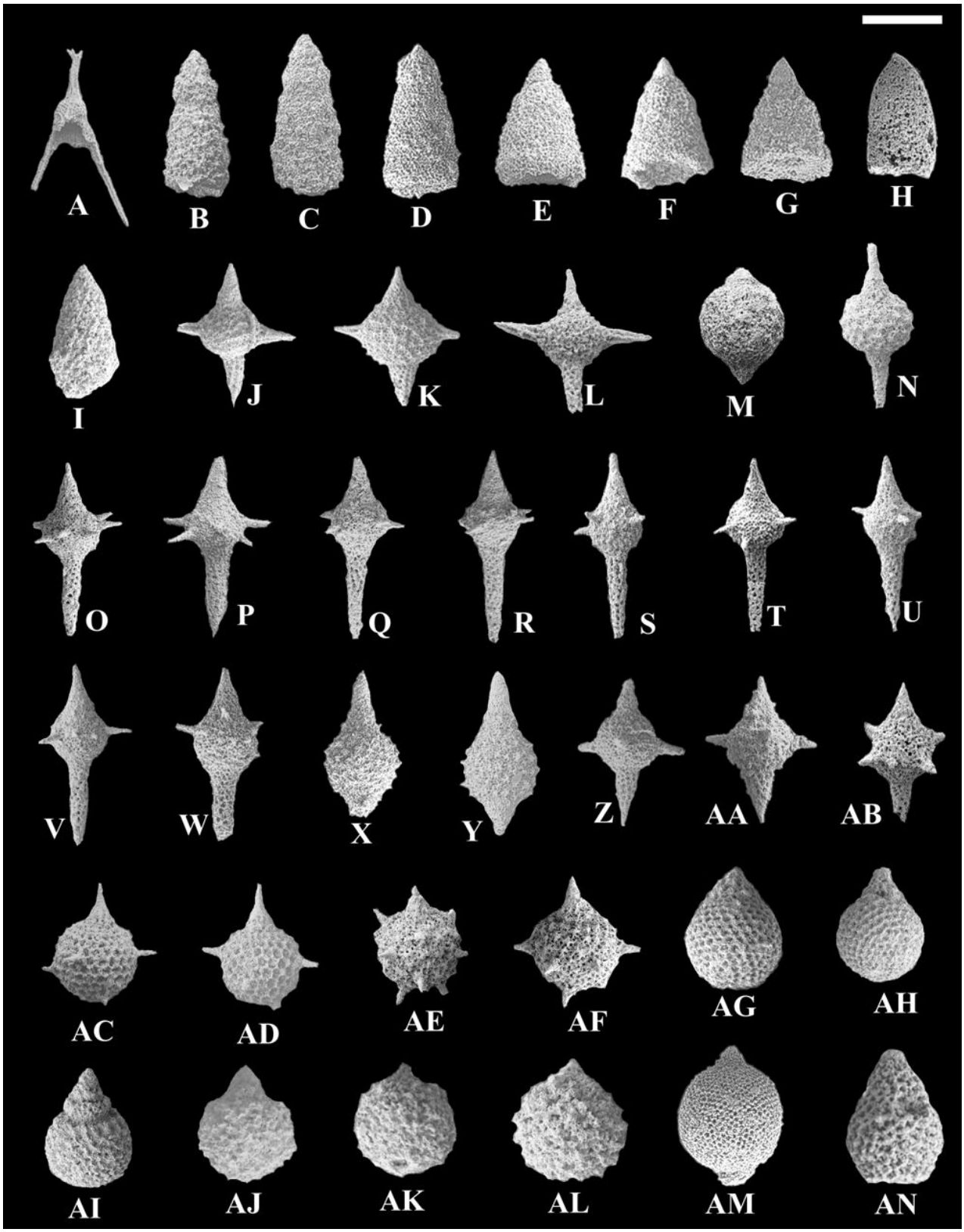
A
B
C
D
E
F
G
H
I
J
K
L
M
N
O
P
Q
R
S
T
U
V
W
X
Y
Z
AA
AB
AC
AD
AE
AF
AG
AH
AI
AJ
AK
AL
AM
AN

▶ **Plate 9:** Scanning electron micrographs of the late Middle Jurassic-earliest Cretaceous radiolarian microfauna from the pelagic blocks in the Elmadağ Olistostrome from the Yakacık and north of Alagöz regions in chronological order; **A-I**. Assemblage from sample Damla-6 of early Callovian-–early Kimmeridgian age from the Yakacık region **A**. *Emiluvia salensis* PESSAGNO; **B**. *Paronaella kotura* BAUMGARTNER; **C**. *Homoeparonaella argolidensis* BAUMGARTNER; **D**. *Tritrabs exotica* (PESSAGNO); **E**. *Haliodictya* ? *antiqua antiqua* (RÜST) *sensu* PESSAGNO; F. *Haliodictya* ? *hojnosi* RIEDEL & SANFILIPPO; **G**. *Perispyridium ordinarium* (PESSAGNO); **H**. *Cinguloturris carpatica* DUMITRICA; **I**. *Spinosicapsa triacantha tetraradiata* (STEIGER); scale bar for figures A to I = 240, 300, 420, 330, 310, 160, 190, 160, and 220 µm, respectively. **J-R**. Assemblage from Acı-3 in the Acısu section of Callovian-early Kimmeridgian age from the Yakacık region **J**. *Emiluvia pessagnoi* s.l. FOREMAN; **K**. *E. orea* s.l. BAUMGARTNER; **L**. *Tetratrabs zealis* (OZVOLDOVA); **M**. *Angulobracchia digitata* BAUMGARTNER; **N**. *Paronaella kotura* BAUMGARTNER; **O**. *Paronaella mulleri* PESSAGNO; **P**. *Perispyridium ordinarium* (PESSAGNO); **Q**. *Cinguloturris carpatica* DUMITRICA; **R**. *Praewilliriedellium convexum* (YAO); scale bar for figures J to R = 400, 340, 500, 230, 370, 180, 210, 170, and 210 µm, respectively. **S-Z**. Assemblage from the sample Acı-4 in the Acısu section of Callovian-early Tithonian age from the Yakacık region, **S**. *Homoeparonaella argolidensis* BAUMGARTNER; **T**. *Transhsuum* sp. aff*. T. maxwelli* (PESSAGNO); **U**. *Cinguloturris primorika* KEMKIN & TAKETANI; **V**. *Mirifusus* sp.; **W**. *Svinitzium mizutanii* DUMITRICA; **X**. *Palinandromeda* sp. aff. *P. podbielensis* (OZVOLDOVA); **Y**. *Spongocapsula palmerae* PESSAGNO; **Z**. Mould of juvenile ammonoid; scale bar for figures S to Z = 310, 180, 230, 280, 160, 210, 190, and 830 µm, respectively. **AA-AJ**. Assemblage from sample Güd-2 in the Güdük section of latest Valanginian-early late Hauterivian age from the north of Alagöz region **AA**. *Cecrops septemporatus* (PARONA); **AB**. *Cecrops* ? *sexaspina* JUD; **AC**. *Crucella angulata* YANG; **AD**. *Cyclastrum infundibuliforme* RÜST; **AE**. *Paronaella trifoliacea* OZVOLDOVA; **AF**. *Dicerosaturnalis trizonalis dicranacanthos* (SQUINABOL); **AG**. *Spongocapsula coronata* (SQUINABOL); **AH**. *Spinosicapsa agolarium* (FOREMAN); **AI**. *S.* sp. aff. *S. coronata* (STEIGER) *sensu* JUD; **AJ**. *Arcanicapsa leiostraca* (FOREMAN), scale bar for figures AA to AJ = 170, 170, 190, 350, 190, 350, 140, 180, 250, and 150 µm, respectively. **AK-AY**: Assemblage from the sample Damla-1 of Hauterivian age from the Yakacık region **AK**. *Cecrops septemporatus* (PARONA); **AL**. *Triactoma tithonianum* RÜST; **AM**. *Crucella angulata* YANG; **AN**. *C. collina* JUD; **AO**. *Paronaella* ? *annemariae* JUD; **AP**. *Paronaella* ? *tubulata* STEIGER; **AQ**. *Godia florealis* (JUD); **AR**. *Halesium crassum* (OZVOLDOVA); **AS**. *Haliodictya* ? *crucelliforma* DUMITRICA; **AT**. *Archaeodictyomitra mitra* DUMITRICA; **AU**. *Mirifusus* sp.; **AV**. *Xitus elegans* (SQUINABOL); **AW**. *X. normalis* (WU & LI); **AX**. *Obesacapsula verbana* (PARONA); **AY**. *Arcanicapsa leiostraca* (FOREMAN); scale bar for figures AK to AY = 190, 200, 430, 240, 330, 220, 190, 260, 230, 160, 280, 190, 230, 320, and 200 µm, respectively.

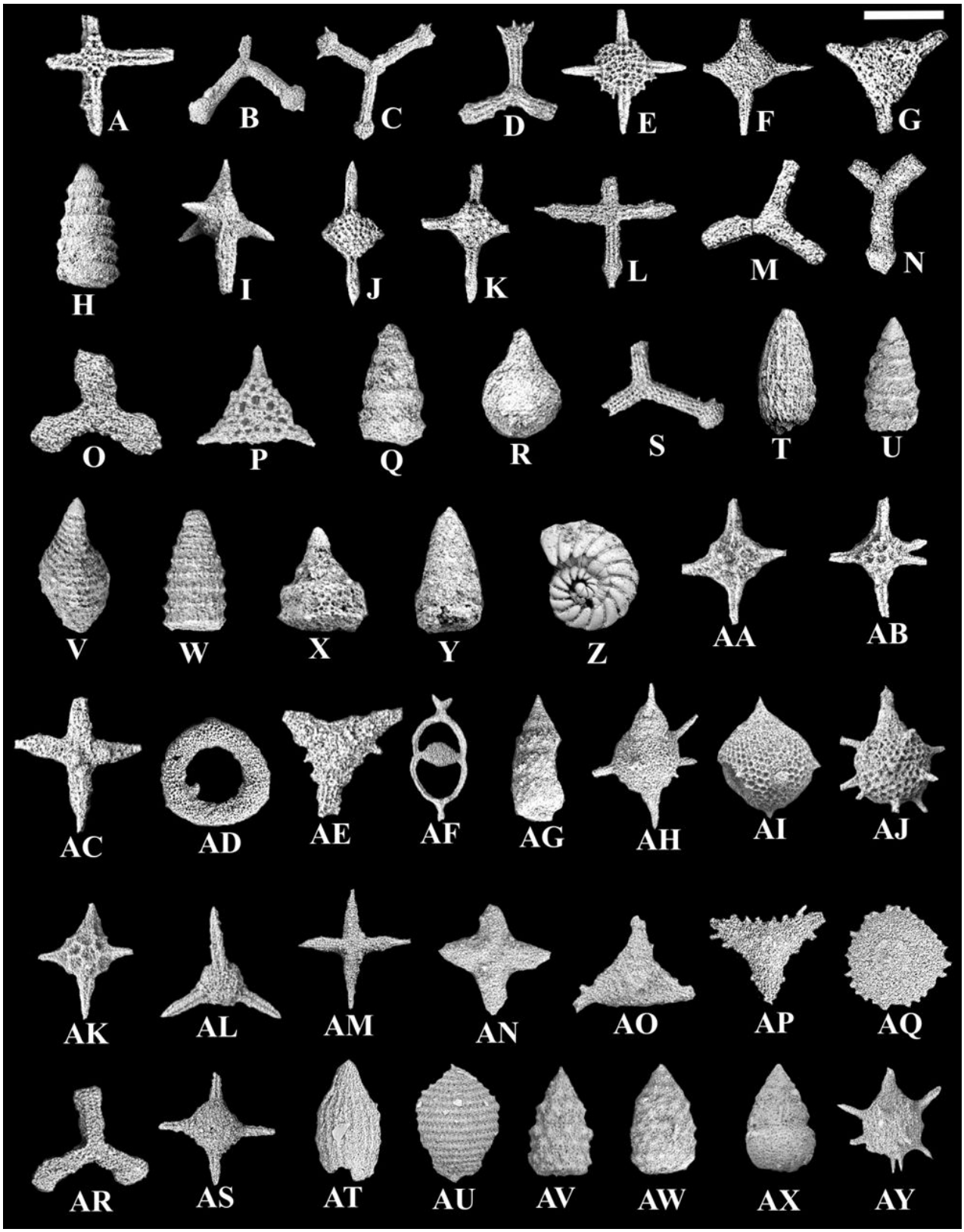
A
B
C
D
E
F
G
H
I
J
K
L
M
N
O
P
Q
R
S
T
U
V
W
X
Y
Z
AA
AB
AC
AD
AE
AF
AG
AH
AI
AJ
AK
AL
AM
AN
AO
AP
AQ
AR
AS
AT
AU
AV
AW
AX
AY

Nomenclatural note:
Life Sciences Identifier (LSID)
https://zoobank.org/References/8C18D2FB-AF9F-4AB5-A300-3FA05753B403

Species Group

- *Archaeodictyomitra mostleri* Tekin *in* Tekin *et al.*, 2024
https://zoobank.org/NomenclaturalActs/CE16055F-FF97-4B39-B9CB-792A4081D03F
- *Archaeospongoprunum ankaraense* Tekin *in* Tekin *et al.*, 2024
https://zoobank.org/NomenclaturalActs/440967FC-7BB7-4A8A-AFDB-C96A37A2B00C
- *Archaeospongoprunum obesum* Tekin *in* Tekin *et al.*, 2024
https://zoobank.org/NomenclaturalActs/BCC610C9-4D85-4CA0-A92A-AB876CCD8EF6
- *Archaeospongoprunum tortilum* Tekin *in* Tekin *et al.*, 2024
https://zoobank.org/NomenclaturalActs/F3886955-2545-41E2-9CEB-D73FA0DC030E
- *Becus multispinosus* Tekin *in* Tekin *et al.*, 2024
https://zoobank.org/NomenclaturalActs/7C9003AF-7500-46FF-BA74-E043DF11441D
- *Godia* ? *orbicula* Tekin *in* Tekin *et al.*, 2024
https://zoobank.org/NomenclaturalActs/D824997C-1610-4C78-B2D8-31F27763DAD4
- *Haliodictya* ? *quadrata* Tekin *in* Tekin *et al.*, 2024
https://zoobank.org/NomenclaturalActs/3FDBA1F1-867B-446C-880C-DA8205C3F2DA
- *Pyramispongia sphaerica* Tekin *in* Tekin *et al.*, 2024
https://zoobank.org/NomenclaturalActs/47E68077-BABB-489B-A2DC-95580374823A
- *Pyramispongia spinosa* Tekin *in* Tekin *et al.*, 2024
https://zoobank.org/NomenclaturalActs/7C4C6965-F3F5-41AF-8AFF-81FE36CC6255
- *Savaryella cruciforma* Tekin *in* Tekin *et al.*, 2024
https://zoobank.org/NomenclaturalActs/E83F6B60-B313-48FB-9E48-EA30CAFA5AFC
- *Spinosicapsa producta* Tekin *in* Tekin *et al.*, 2024
https://zoobank.org/NomenclaturalActs/7843A913-3B9D-4194-A127-C76453B6C461
- *Tetrapaurinella lepida* Tekin *in* Tekin *et al.*, 2024
https://zoobank.org/NomenclaturalActs/8BEC9DAE-98FC-4B66-9C07-3FBF045F96C1
- *Triactoma haymanaense* Tekin *in* Tekin *et al.*, 2024
https://zoobank.org/NomenclaturalActs/0D922088-0C8B-4B87-AE6F-56DE014467A4
- *Triactoma merici* Tekin *in* Tekin *et al.*, 2024
https://zoobank.org/NomenclaturalActs/D3046097-8EDD-4372-A569-32FC32AA2E71

Subspecies Group

- *Archaeospongoprunum carrierensis globosum* Tekin *in* Tekin *et al.*, 2024
https://zoobank.org/NomenclaturalActs/5A9197E7-8352-4FB9-8FCE-8D185144E7FA
- *Homoeparonaella elegans bulbosa* Tekin *in* Tekin *et al.*, 2024
https://zoobank.org/NomenclaturalActs/3928FF28-FAC4-4866-BFC7-D7BC31EECDCF
- *Paronaella* ? *annemariae oezgenerdemae* Tekin *in* Tekin *et al.*, 2024
https://zoobank.org/NomenclaturalActs/38E95BE1-2715-4D1C-9BBA-1FD084BB609F
- *Savaryella pseudoguexi breva* Tekin *in* Tekin *et al.*, 2024
https://zoobank.org/NomenclaturalActs/37DE1415-2F10-4D37-AA3D-2AD7A58A2C91